

**Molecular Composition and Function of Apical Ciliary Tuft
in Sea Urchin Embryos**

October 2013

Yinhua JIN

**Molecular Composition and Function of Apical Ciliary Tuft
in Sea Urchin Embryos**

A Dissertation Submitted to
the Graduate School of Life and Environmental Sciences,
the University of Tsukuba
in Partial Fulfillment of the Requirements
for the Degree of Doctor of Philosophy in Science

Yinhua JIN

Table of Contents

Abbreviations	iii
Abstract	1
Introduction	3
Materials and Methods	7
Results	14
1. Identification GSTT as specific component of apical tuft	14
1.1 <i>GSTT is a major apical tuft-specific protein in sea urchin embryos</i>	14
1.2 <i>GSTT is expressed in the animal plate of the normal embryo</i>	16
2. Functional analysis of GSTT: its role in amplitude of apical tuft and behavior in sea urchin embryo	19
2.1 <i>Inhibition of GSTT increases ciliary bending in the apical tuft</i>	19
2.2 <i>Embryos treated with BSP show normal negative geotactic behavior</i>	19
2.3 <i>BSP-treated embryos exhibit less escaping responses against a mechanical barrier</i>	20
3. Proteomic profiling of the apical tuft cilia in the sea urchin embryo	22
3.1 <i>LC-MS/MS detects more proteins specific to apical tuft</i>	22

3.2 Apical tuft cilia have a set of motile axonemal components	24
Discussion	25
Acknowledgement.....	30
References	31
Tables	42
Figures	78

Abbreviations

ASW, artificial seawater

BSA, bovine serum albumin

BSP, bromosulfalein(bromosulfophthalein)

CBB, Coomassie Brilliant Blue

DID1, dillapiol isoxazoline derivative 1

FSW, filtered natural seawater

GST, glutathione S-transferase

GSTT, glutathione S-transferase theta

LC-MS/MS, liquid chromatography-tandem mass spectrometry

MALDI-TOF, matrix assisted laser desorption ionization-time of flight

MOPS, 3-(N-morpholino)propanesulfonic acid

MS, mass spectrometry

SDS, sodium dodecyl sulfate

SDS-PAGE, SDS-polyacrylamide gel electrophoresis

TRP, transient receptor potential

2DE, two-dimensional electrophoresis

Abstract

Apical tuft, observed in a wide range of embryos/larvae of marine invertebrates, is composed of long and less motile cilia. Although apical tuft has been thought to function as a sensory organ, its molecular composition is poorly understood. To elucidate the function of apical tuft, I examined the structure, and molecular composition of apical tuft in sea urchin embryo and analyzed the function of apical tuft-specific molecule.

First, I compared the components of apical tuft and lateral motile cilia in the sea urchin *Hemicentrotus pulcherrimus*. Sea urchin embryos treated with Zn²⁺ become animalized. Thereby, apical tuft region is extended, and sufficient amount of apical tufts are collected for biochemical studies. Here, I isolated cilia from normal embryos and Zn-treated animalized embryos and identified protein components of cilia by mass spectrometric analysis using MALDI-TOF/MS. By comparison of protein components in both cilia, I identified glutathione S-transferase theta (GSTT) as an abundant and apical tuft-specific protein.

Secondly, I examined the role of GSTT in the motility of apical tuft and the locomotion of embryos, by using an inhibitor of GST. I found that GSTT in the apical tuft appears to play an important role in the mechanical reception for the motility regulation of lateral motile cilia in sea urchin embryos.

Finally, I extensively identified and compared the protein components between apical tuft and lateral motile cilia by the analysis with LC-MS/MS. Apical tuft was found to possess almost all the axonemal components like lateral motile cilia, suggesting that the apical tuft is motile cilia. Several redox-related proteins as well as GSTT and the proteins found in sensory cilia were found in the apical tuft. A serotonin receptor was identified as a protein specific to the lateral motile cilia, implying a signaling pathway from apical tuft to the lateral motile cilia through serotonergic neurons.

In this thesis, I made clear the molecular features of the structure and the function of apical tuft in sea urchin embryos. This study provides the molecular information for understanding the function of apical tuft and should shed new lights on the regulation of ciliary movements of embryos in marine invertebrates.

Introduction

Cilia and flagella are microtubule-based structures that are well conserved among eukaryotes from protozoan to human. Both structures are basically the same and conventionally distinguished by the length, the number per cell, or pattern of motion, such as “flagella” in *Chlamydomonas*, “cilia” in *Paramecium*, “flagella” in sperm, and “cilia” in epithelia. Motile cilia and flagella are centered by 9+2 microtubule structures called the axonemes (Fig. 1). Axonemal dyneins are observed as “arms” attached to nine outer doublet microtubules and are classified by anchoring positions into outer and inner arm dyneins. Sliding of outer doublet microtubules caused by dyneins is the driving force for oscillatory bending. The central apparatus is composed of radial spokes and central pair microtubules. These structures are thought to be involved in producing planar waveforms by regulating the dynein activity (reviewed in Gibbons, 1981; King, 2000; Porter and Sale, 2000; Inaba, 2003; Mitchell, 2004; Smith and Yang, 2004; Inaba, 2007, 2011).

Cilia become diverse through the evolution of multicellular organisms. Primary cilia are immotile monocilia with mostly 9+0 structures found on most vertebrate cell types (Marshall and Nonaka, 2006; Singla and Reiter, 2006). They function as sensors to perceive chemical or mechanical stimuli and transduce them into intracellular signaling pathways as typified by morphogenesis through Wnt/PCP pathway. Motile

9+0 cilia found on the node of early embryos in mammals are involved in the breaking of right-left symmetry. On the other hand, cilia on sensory organs are immotile and play roles in perception of several stimuli. For example, olfactory cilia are protruded from the olfactory receptor cells and cover the surface of the olfactory epithelium. A type of G protein-coupled receptor is known to be accumulated on the surface of the cilia. All of these cilia work as the center of signaling reception, and therefore the dysfunction of these cilia by the deficiencies in axonemal or intraflagellar transport components causes diverse ranges of disease, including respiratory defect, male sterility, polycystic kidney, defects in sensory reception, and randomization of right-left asymmetry (Ibanez-Tallon et al., 2003; Sharma et al., 2008; Sedmak and Wolfrum, 2011).

Diversification of ciliary structures and functions is observed even in lower invertebrates (e.g. Konno et al., 2010). Before metamorphosis, many of the marine invertebrates larvae undergo plankton stage and swim with motile cilia. Besides motile cilia at the lateral side, larvae develop longer and less motile cilia, called apical ciliary tuft. The apical tuft was first described quite a long time ago, but little is known about their functions. A number of phyla in marine invertebrates, including echinoids, bryozoans, polychaetes, mollusks, and cnidarians, possess apical tuft in the embryos or larvae (Hadfield, 2000). The apical tuft in Cnidaria, often called with their peripheral region as “apical organ”, is considered be involved in the regulation of swimming direction and metamorphosis (Chia and Loss, 1979).

Ciliogenesis occurs during sea urchin embryo development immediately prior to hatching into a swimming blastula and it ensures embryo motility up to the feeding

pluteic larval stage (Prulière et al., 2011). Before hatching, a series of rapid cleavages gives rise to a blastoderm consisting of several hundred cells arranged as a spherical monolayer of epithelial cells surrounding the blastocoel (Fig. 2). At this stage, each blastomere protrudes one single motile cilium during interphase. Each blastomere retracts and disassembles its axonemes, builds a mitotic spindle with the centrioles as spindle poles in mitosis, and then returns its centriole pair to the apical cell surface to grow a new cilium during interphase (Masuda and Sato, 1984; Dawe et, al., 2007; Stephens, 2008). After hatching, the blastomeres grow short motile cilia, which then show a metachronal beating along the animal-vegetal axis and provide directional motility to the blastula (Stephens, 1995). On the animal pole, a small group of longer and less motile cilia are formed. These cilia are called apical tuft. (Fig. 2 I). The polarity of the embryo and the difference in cilia become more evident during following mesenchyme blastula and gastrula (Fig. 2 I-K).

Apical tuft, together with apical ganglions, are considered to function as a sensory organ called apical organ and to be involved in the regulation of larval swimming and settlement at metamorphosis in sea urchins(Burke, 1978; Nakajima et al., 2004). To date, it is suggested that the different combination of transcription factors is used in apical tuft formation between sea urchin and gastropod (Dunn et al., 2007), and FoxQ2-Nk2.1-AnkAT-1 is reported as the molecular pathway to form apical tuft in the sea urchin embryo at the neurogenic ectoderm region (Yaguchi et al, 2010). However, more detailed studies on the molecular composition of apical tuft or molecular differences between apical tuft and the lateral motile cilia are necessary to elucidate all

characters of apical tuft.

In this thesis, I compared the protein components between apical tuft and lateral motile cilia in the sea urchin embryos by a proteomic approach. To carry out the analysis, I prepared the animalized embryos by Zinc treatment to obtain sufficient amount of apical tuft cilia. Both normal and Zn-treated embryos are deciliated by a high salt solution. Proteins are separated by SDS-polyacrylamide gel electrophoresis (SDS-PAGE) or two-dimensional PAGE (2DE) and subjected to matrix-assisted laser desorption/ionization mass spectrometry (MALDI-TOF/MS). An isoform of glutathione S-transferase theta (GSTT) was identified as an abundant and specific component of apical tuft. From the experiment using an inhibitor for GST, I revealed that GSTT plays essential roles in mechanical reception to regulate the motility of lateral cilia and the locomotion of embryos. I further carried out an extensive and comparative proteomics of apical tuft and lateral motile cilia by liquid chromatography-tandem mass spectrometry (LC-MS/MS), and found several intriguing proteins specific to either apical tuft or lateral motile cilia. The proteomic features of both cilia suggest that apical tuft functions as sensory center to regulate the lateral motile cilia and embryonic locomotion.

Materials and Methods

Chemicals, reagents and solutions

Immobilized pH gradient (IPG) strips and buffers were purchased from GE Healthcare (Buckinghamshire, UK). Ammonium bicarbonate and Triton X-100 were purchased from Sigma-Aldrich (St. Louis, MO). Trypsin was purchased from Promega (Madison, WI). Molecular weight standards for SDS-PAGE and 2DE were purchased from Bio-Rad (Hercules, CA). Dillapiol isoxazoline derivative 1 was kindly provided by Dr. Victor Semenov, Zelinsky Institute of Organic Chemistry, Russian Academy of Sciences, Moscow, Russia. The artificial seawater (ASW) was comprised of 423.0 mM NaCl, 9.0 mM KCl, 9.27 mM CaCl₂, 22.94 mM MgCl₂, 25.5 mM MgSO₄, and 2.14 mM NaHCO₃ (MBL seawater). Bromosulfalein (bromosulfophthalein, BSP) was purchased from Sigma-Aldrich. All other reagents were purchased from Wako Pure Chemical (Osaka, Japan) or Nacalai Tesque (Kyoto, Japan).

Handling of sea urchin embryos

Japanese sea urchins, *Hemicentrotus pulcherrimus*, were collected from around the Shimoda Marine Research Center, University of Tsukuba, Research Center for Marine Biology, Tohoku University, and the Marine and Coastal Research Center, Ochanomizu University. The gametes were collected by an intra-blastocoelar injection of 0.5 M KCl.

After insemination in filtered natural seawater (FSW) containing 3-amino-1,2,4-triazole (Sigma), eggs were transferred to FSW or FSW containing 0.5 mM ZnSO₄ (Showman RM et al., 1979). Embryos were cultured by standard methods with FSW at 15°C. Cilia were isolated from embryos by treatment with 2 × ASW to double the salt concentration (Auclair and Siegel, 1966; Fig. 3). Embryos were first removed by a swing-type of centrifuge (TOMY LC122, TOMY, Tokyo) at 1,800 rpm for 1 min, and the supernatant was further centrifuged at 2,500 rpm for 10 min to remove embryonic debris. Cilia were collected by centrifugation of the resulting supernatant at 10,000 g for 10 min. Successive extraction of ciliary protein was carried out according to Inaba et al. (1988). For isolation of apical tuft from normal embryos, 26-hr embryos were treated with 4 µM dillapiol isoxazoline derivative 1 (Semenova et al, 2008) for 3 hrs on ice. After collection of detached cilia, which contained both lateral motile cilia and a part of apical tuft, by centrifugation, the embryos were treated with 2 × ASW to collect apical tuft.

Proteomics

Ciliary proteins from normal and Zn-treated embryos were separated by 2DE. Protein spots stained by SYPRO RUBY were cut out, digested by trypsin and subjected to peptide mass finger printing (PMF) with MALDI-TOF/MS (Bruker Daltonics), as described (Nakachi et al., 2011). For LC-MS/MS, ciliary proteins were separated by SDS-PAGE with 10% polyacrylamide in the separating gel. Proteins were visualized by Coomassie Brilliant Blue R-250 and excised to 16 pieces per lane. Each piece of the gel

was digested with trypsin for LC/MS/MS analysis as described previously (Yamada et al., 2009). The digested peptides were analyzed using a LC (Ultima3000; DIONEX) -MS/MS (LTQ-XL, Thermo Scientific, Japan). Raw spectra data were processed using SEQUEST software to extract peak lists. The obtained peak lists were analyzed using MASCOT program against *S. purpuratus* protein database extracted from SpBase (<http://www.spbase.org/SpBase/>). Proteins with the peptide counts of more than 2 in either normal or Zn-treated embryo were treated as identified in this study.

Isolation of cDNA for GSTT in *H. pulcherrimus*

Protein-coding region of GSTT cDNA was amplified from *H. pulcherrimus* mesenchyme blastula cDNA library by PCR using following primers: GSTT-F1, ATGACAATCCAGCTGTACGTT; GSTT-R1, CTACTTCGCAAGCGAATCTCT. The 5'- and 3'-UTRs were amplified by RACE. The sequence of the full length cDNA was deposited to DDBJ/EMBL/NCBI (Accession number, AB762295).

Whole-mount *in situ* hybridization

Whole-mount *in situ* hybridization was performed as described previously (Minokawa et al., 2004; Yaguchi et al., 2010). cDNA containing the protein coding region was reverse transcribed by T7 polymerase (Takara Bio Inc., Japan) with NTP containing digoxigenin-labeled UTP. Embryos were fixed with 4% paraformaldehyde in FSW at 4°C overnight. After exhaustive washing with a MOPS buffer (0.1 M MOPS, pH 7.0, 0.5 M NaCl, 0.1% Tween-20), embryos were further washed with a

hybridization buffer (70% formamide, 0.1 M MOPS, pH 7.0, 0.5 M NaCl, 1.0 mg/ml bovine serum albumin, 0.1% Tween 20). Prehybridization and hybridization with probes was carried out at 50°C for 3 hrs and 1 week, respectively.

Antibodies

The protein-coding region of GSTT was sub-cloned into pET32a vector and transfected into *Escherichia coli* AD494. Protein expression was induced by 1.0 mM iso-propoly-β-D-thiogalactoside. The purification of fusion proteins and the preparation of polyclonal antibodies in mouse were carried out as described (Padma et al., 2003; Mizuno et al., 2009).

Analysis of ciliary motility and embryonic behavior

The ciliary movements were observed and analyzed as described (Shiba et al., 2002; Yaguchi et al., 2010). The embryos were observed under a phase contrast microscope (BX51; Olympus, Tokyo) equipped with a high-speed camera (200 frames per seconds, HAS-220; Ditect Co. Ltd, Tokyo, Japan). The embryos at 24~30-h post-fertilization were immobilized between a slide glass and a coverslip separated by 58-μm-thick mending tape (3M Scotch). Cilia of the apical tuft and those in the lateral region of embryos were observed and analyzed. Individual images of ciliary movements were analyzed with Bohboh software (Bohboh Soft, Tokyo). The angles of apical tuft cilia were defined as that between the animal-vegetal axis of the embryo and the straight line from the base to the tip of the cilium. The shear angle was estimated as the angle of

the tangent to the ciliary shaft measured with respect to the direction of the axis of the ciliary base.

Swimming behavior of sea urchin embryos was recorded with a stereomicroscope (MZ12.5; Leica, Tokyo) equipped with a digital camera (HDR-CX700; Sony, Tokyo). The embryos at 24~30 h post-fertilization were kept in seawater in a chamber by a glass slide (1% BSA-coated) and coverslip sandwiched with a 1-mm-thick silicon spacer. The swimming behaviors of embryos in the chamber were observed at room temperature. For the analysis of geotactic behavior and escaping behavior, a chamber or a micro-maze similarly made of silicon spacers as described above was vertically placed. Embryos were inserted by a pipette at a small entrance opened at the base of the spacer. Swimming velocities and rotational direction were analyzed with Bohboh software. The images of embryonic distribution in a chamber were taken from the movie and processed by Photoshop and Bohboh software.

Electron microscopy

Embryos were fixed in a solution (0.45 M sucrose, 2.5% glutaraldehyde, 0.1 M sodium cacodylate; pH 7.4) at 4°C for 2 h. After three washes with 0.45 M sucrose buffered with 0.1 M sodium cacodylate (pH 7.4), the embryos were postfixed with 1% OsO₄ buffered with 0.1 M sodium cacodylate (pH 7.4) on ice for 2 h. They were then washed with 0.1 M sodium cacodylate (pH 7.4) at 4°C for 10 min, dehydrated through an ethanol series, and embedded in Quetol 812 (Nissrin EM Co., Tokyo). The resin was solidified sequentially at 37°C overnight, 45°C for 12 h, and 60°C for 48 h and

thin-sectioned with an average thickness of 70 nm. Sections were stained with uranyl acetate and observed under a transmission electron microscope (JEM 1200EX; JEOL, Tokyo).

Computational Analysis

Protein identification from mass spectrum was done using Mascot (Matrix Science Inc., Yokohama, Japan). Translation of DNA sequence into amino acid sequence, calculation of molecular mass, design of PCR primers, and estimation of isoelectric points were done by GENETYX software. BLASTP program was used to search for homologous proteins. Multiple sequences alignment and drawing of phylogenetic trees were carried out by Neighbor-Joining method using MEGA5 (Tamura et al., 2011). The accession numbers for GSTs in human, mouse and rat are as follows: human alpha1 (NP665683); human mu1 (AAH24005); human pi1 (AAH10915); human omega1 (AAH00127); human kappa1 (AAH50715); human theta1 (NP000844); human theta2 (NP000845); human zeta1 (NP665877); mouse alpha1 (NP032207); mouse mu1 (NP034488); mouse pi1 (NP038569); mouse omega1 (NP034492); mouse kappa1 (NP083831); mouse theta1 (NP032211); mouse theta2 (NP034491); mouse theta3 (NP598755); mouse theta4 (NP083748); rat alpha1 (NP058709); rat mu1 (NP058710); rat pi1 (AAH58440); rat omega1 (NP001007603); rat kappa1 (NP852036); rat theta1 (NP445745); rat theta2 (NP036928); rat theta3 (NP00113115); human sigma (EAX06052); mouse sigma (NP_062328); rat sigma (NP_113832). Protein sequences of

S. purpuratus GSTs are obtained from SpBase (<http://www.spbase.org/SpBase/>) and indicated as SPU numbers.

Results

1. Identification of GSTT as a specific component of apical tuft in sea urchin embryo

1.1 *GSTT is a major apical tuft-specific protein in sea urchin embryos.*

Since the apical tuft is located at the neurogenic animal plate in the sea urchin embryo, the cilia represent only a small number in each embryo. To enrich for apical tuft cilia, I used zinc treatment of embryos for animalization (Lallier, 1955, 1975). Zn-treatment expands the animal plate region, based on the observation of specific gene expression patterns (Poustka et al., 2007). The Zn-treated embryos bore a large number of long and less motile cilia, apparently representing those of an apical tuft (Fig. 4). I treated both normal and Zn-treated embryos with 2× concentrated artificial seawater (ASW) to collect cilia (Auclair and Siegel, 1966). Observation by differential interference microscopy showed a significant difference in the length of isolated cilia between normal and Zn-treated embryos (Fig. 5). The ciliary lengths of the apical tuft region determined by ankAT-1 expression (Yaguchi et al., 2010) ranged from 35 to 90 μm in the normal embryos (Fig. 6). From these measurements, the percentages of apical tuft cilia among total cilia in the normal and Zn-treated embryos were estimated as 6.3% and 37%, respectively (Fig. 6). Transmission electron microscopic observation showed that major axonemal components, such as outer and inner arms, radial spokes

and central apparatus, were present in both cilia from normal and Zn-treated embryos (Fig. 7).

I next compared protein components between cilia from normal and Zn-treated embryos. SDS-polyacrylamide gel electrophoresis (SDS-PAGE) apparently showed a similar protein pattern between the two samples, except that a 25-kDa protein that was specifically and abundantly contained in Zn-treated embryos (Fig. 8A). During successive extraction of isolated cilia, this protein was extracted with 0.1% Triton X-100 (Fig. 8B), indicating that it was a membrane-bound or cytosolic component. Two-dimensional gel electrophoresis (2DE) also showed a similar protein pattern in major proteins of cilia from normal and Zn-treated embryos, but clear differences were observed mainly in three spots with molecular masses of 25 kDa over broad pI ranges (Fig. 8C, D). The most basic 25 kDa spot was also detected in normal embryos in a lesser amount. I also observed differences in other protein spots, including an approx. 100-kDa protein (pI 5.0), a ~50-kDa protein (pI 5.0), a ~40-kDa protein (pI 4.5) and a ~30-kDa protein (pI 4.0).

To identify the 25-kDa proteins showing the most significant differences, I cut out the protein band and spots from SDS- and 2DE-gels, and had them digested by trypsin and subjected to matrix-assisted laser desorption ionization mass spectrometry (MALDI-TOF/MS). Because the genomic information of the sea urchin *H. pulcherrimus* is not yet available, I used the information from *Strongylocentrotus purpuratus* as the reference database for the mass spectrometry (Sea urchin genome sequencing consortium et al, 2006, SpBases: <http://www.spbase.org/SpBase/>). Although

the proteins were derived from Japanese sea urchin species, more than 70% of the proteins of randomly selected major 2D spots were identified using the *S. purpuratus* database (data not shown). It turned out that the ~25-kDa band in SDS-PAGE and all corresponding spots in 2DE showed a significant hit to the gene product SPU_016269 (Fig. 9, 10). A BLASTP search showed that SPU_016269 encodes a protein similar to *H. sapiens* glutathione transferase theta 1 (or glutathione S-transferase theta 1; GSTT) (E value = 2e-29). I found four gene models for GSTT in the genome of *S. purpuratus*, but they turned out to be identical genes with differently assigned IDs (also see Table 1 and 2).

Cytoplasmic GST is divided into eight classes in mammals; alpha, kappa, mu, omega, pi, sigma (also known as prostaglandin D synthase), theta and zeta (Board et al., 1997; 2000). Each class has several isotypes. This search for GST genes against the *S. purpuratus* database revealed four gene classes with sequence similarities to GST alpha (SPU_010192), omega (SPU_028633), theta (SPU_016269) and sigma (SPU_023664). A molecular phylogenetic analysis showed that the Sp sequences corresponding to the 25-kDa *H. pulcherrimus* proteins abundantly found in Zn-treated embryos are apparently grouped into GST theta (GSTT) (Fig. 11).

1.2 GSTT is expressed in the animal plate of the normal embryo

To investigate the functions of the apical tuft, I further focused on GSTT, which was abundantly and specifically found in the apical tuft cilia. Because I used Zn-treated embryos to identify apical tuft-specific proteins, it was possible that GSTT was not an

intrinsic apical tuft component but was artificially induced by the treatment. To exclude this possibility, I examined the expression pattern of *GSTT* in normal sea urchin embryos. I isolated and sequenced a 1,327-bp cDNA clone for GSTT from *Hemicentrotus pulcherrimus* (termed Hp-GSTT) with an open reading frame encoding 219 amino acids, predicting a molecular mass of 25.256 Da and pI 5.84 (Fig. 9). The molecular mass and pI well matched those that could be estimated by SDS-PAGE and 2DE (Fig. 8). By using the cDNA as a template, I prepared digoxigenin-labeled RNA probes and performed *in situ* hybridization. GSTT mRNA was faintly and evenly present until the hatched blastula stage but became increased and restricted to the animal plate of the mesenchyme blastula, gastrula and prism larva. In pluteus larva, the signal became strong at the ciliary band as well (Fig. 12). Embryos animalized by either Zn-treatment or Δcadherin injection (Logan et al., 1999) showed strong expression of *GSTT* throughout the entire region of the thickened ectoderm region (Fig. 13).

I prepared a fusion protein and immunized mice to obtain a polyclonal antibody against GSTT. Western blotting against the isolated cilia detected 25-kDa GSTT whose signal was weak in normal embryos but intense in Zn-treated embryos (Fig. 14). I next tried to isolate apical tuft from normal embryos using dillapiol isoxazoline derivative 1 (DID1) (Semenova et al, 2008). Although a part of apical tuft was detached, treatment of embryos with DID1 caused selective loss of lateral motile cilia (Fig. 15A). Following treatment of the embryos with 2× ASW resulted in the isolation of the rest of apical tuft without contamination of lateral motile cilia. Western blotting showed that GSTT was concentrated in apical tuft in the normal embryos (Fig. 15B). The result also

showed that GSTT was significantly increased in the cilia from Zn-treated embryos (Fig. 14B).

2. Functional analysis of GSTT: its role in the motility regulation of apical tuft and behavior of sea urchin embryo

2.1 Inhibition of GSTT increases ciliary bending in the apical tuft

To investigate the functions of GSTT in the apical tuft, I examined the effects of a potent GST inhibitor, bromosulfalein (BSP) (Kolobe et al., 2004), on sea urchin embryos. Treatment of 24 to 28 -hr embryos (mesenchyme blastula to early gastrula) with BSP induced remarkable bending of the apical tuft (Fig. 16). The angle of the apical tuft relative to the anterior-posterior axis was greatly increased by the treatment (Fig. 17). The shear angle showed a more than two-fold increase along the entire length of the cilium (Fig. 18). The maximum increase in the shear angle was achieved at 1 μM . The BSP treatment did not significantly affect the beat frequency of lateral motile cilia (Fig. 19).

Ciliary beating is the driving force for larval swimming. To identify the role of GSTT in the control of embryonic swimming behavior, I traced embryonic swimming in a chamber on a glass slide under a stereomicroscope. Both the normal and BSP-treated embryos swam at almost the same speed, with no significant differences in the trajectories (Fig. 20, 21).

2.2 Embryos treated with BSP show normal negative geotactic behavior

Sea urchin embryos/larvae show negative geotactic behavior at the stages from blastula to pluteus (Mogami et al., 1988). To determine whether GSTT in the apical tuft

is involved in the negative geotactic behavior of embryos, I examined the effect of BSP treatment on the embryonic behavior against gravity. A glass slide with a chamber (~1-mm-thick) was placed vertically, and early blastula embryos were inserted from an entrance at the bottom (Fig. 22). Normal embryos started to move toward the top of the chamber, and nearly 90% of the embryos reached the upper part of the chamber in 2 min. BSP-treated embryos were not significantly negative geotaxis from the normal embryos (Fig. 23).

2.3 BSP-treated embryos exhibit less escaping responses against a mechanical barrier

Next I carefully observed the escaping behavior of sea urchin embryos after they collided with the wall of the chamber. The normal embryos efficiently changed their body orientation and swimming direction after collisions with the wall, resulting in an escape from the wall (Fig. 24, top). More than 70% of the normal embryos escaped from the wall and changed direction to freely swim within 4 s (Fig. 25). In contrast, the BSP-treated embryos could not efficiently escape (Fig. 24, bottom). They stayed longer on the wall than the normal embryos, without changing their orientation. More than half of the embryos were trapped at the chamber wall (Fig. 25).

To further investigate the function of the apical tuft on the comprehensive response of the embryos to gravity and collision, I made a simple micro-maze to observe the embryonic swimming behavior (Fig. 26). Embryos were loaded to one side at the bottom of the micro-maze on a glass slide, which was then vertically placed.

Nearly 60% of the normal embryos reached the top compartment within 2.5 min (Fig. 27). Careful observation confirmed that the normal embryos efficiently escaped from the ceilings after collisions so that they could achieve negatively geotactic movement toward the top wall. In contrast, the BSP-treated embryos often were trapped at either of the two ceilings along on the way to the top of the maze, showing significantly lower efficiency in reaching the top compartment compared to the normal embryos (Fig. 26, 27).

3. Proteomic profiling of the apical tuft cilia in the sea urchin embryo

3.1 LC-MS/MS detects more proteins specific to apical tuft

To know in more detail the molecular differences between apical tuft and lateral motile cilia, I carried out LC-MS/MS. Cilia isolated from normal and Zn-treated embryos were separated by SDS-PAGE. After staining by Coomassie Brilliant Blue R-250 (CBB), one PAGE lane gel was excised into 16 pieces, each of which was subjected to LC-MS/MS. Proteins with the peptide counts of more than 2 in either normal or Zn-treated embryo were listed in Table 1. Totally 1,046 proteins were identified. The quantities (peptide count) of the proteins identified by LC-MS/MS were compared between cilia from normal and Zn-treated embryos. Intriguingly the most abundant apical tuft-specific protein was vitellogenin (apolipoprotein B). In addition, apical tuft contained several proteins with sequence similarities to histone species (Table 2).

GSTT was confirmed to be apical tuft-specific, although a small amount was detected in cilia from normal embryos, probably due to apical tuft at the animal plate (Table 2). Multiple gene IDs (SPU_016269, SPU_021662, SPU_016270, SPU_006495) showed sequence similarity to GSTT as described above. In addition to GSTT, several redox-related proteins were found to be more abundant in apical tuft, containing thioredoxin family Trp26 (SPU_020730), thioredoxin peroxidase (SPU_022529), and thioredoxin reductase 3 (SPU_004780). A protein named AnkAT-1 was previously reported as a factor regulating the length of apical tuft (Yaguchi et al., 2010). The

present proteomics identified this protein as an apical tuft-specific protein (SPU_024961). Usherin is a protein defective in the patient of Usher syndrome, the most frequent cause for hereditary deaf-blindness in human (Weston et al., 2000). This protein was also found to be apical tuft-specific (Table 1). I also found several proteins that potentially bind to extracellular matrix proteins: syndecan-binding protein (syntenin) (SPU_009549), fibrocystin (SPU_023486), and several proteins containing fibronectin- or PDZ domains (Table 1 and 2). Two tubulin isotypes, beta 2C and alpha 1C, also showed specific to apical tuft (Table 2).

On the other hand, I found several proteins specific to normal embryos (Table 3). Aminotransferase class V-1 was exclusively found in cilia from normal embryos, not in those from Zn-treated embryos. Another type of GST isoform, omega, was shown to be specific in cilia from normal embryos. It was notable that several cytoskeletons or their associated proteins were found specifically in cilia of normal embryos. For example, coronin (SPU_000974), an actin- and microtubule-binding protein, a 77 kDa echinoderm microtubule-associated protein (SPU_006911), and several isoforms of ankyrins were found specific to lateral motile cilia (Table 3). Intraflagellar transport protein (IFT144) and cytoplasmic dynein 2, both of which are involved in ciliogenesis, were seen more abundantly in normal embryos than Zn-treated embryos, as well as other IFT-relate proteins. Serotonin is known to regulate ciliary motility in mussels (Schor, 1965; Paparo et al., 1976; Stephens and Prior, 1992) and sea urchins (Gustafson et al., 1972; Wada et al., 1997; Yaguchi and Katow, 2003; Katow et al., 2007). Intriguingly, a protein similar to serotonin/octopamine receptor family protein 7 was

specifically found only in cilia from normal embryos (Table 1).

3.2 Apical tuft cilia have a set of motile axonemal components

To obtain information on the motile machinery axonemes, I listed axonemal proteins and their related proteins that were identified by LC-MS/MS in cilia of normal and Zn-treated embryos (Table 4). Major axonemal proteins, including those in outer and inner dynein arms, radial spokes, central apparatus and other axonemal proteins, were detected in similar quantity between normal and Zn-treated embryos, suggesting that apical tuft cilia are potentially motile. Intriguingly, the peptide counts of proteins for intraflagellar transport were significantly lower in Zn-treated embryos (Table 3).

Discussion

To obtain an adequate amount of apical tuft to perform a proteomic analysis, I treated sea urchin embryos with zinc. Several studies demonstrated that Zn-treated embryos are animalized and bear long and less motile cilia, similar to the apical tuft (Lallier, 1955, 1975; Poustka et al., 2007). In the present study, the Zn-treated embryos had expanded and thickened ectoderms with characteristics of the animal plate of normal embryos. It was possible that the long-immotile cilia specific components identified in this study were not present in the apical tuft of normal embryos but were artificially induced by the Zn treatment. The present *in situ* hybridization and immunoblot analyses clearly showed that at least GSTT was expressed and localized specifically at the animal plate region, suggesting that the cilia isolated from Zn-treated embryos are equivalent to the apical tuft of normal embryos. However specificity of all the other ciliary proteins identified in Zn-treated embryos is still to be confirmed by other methods.

I found that GSTT was abundantly present in the apical tuft but only present in trace amounts in the lateral motile cilia. Another type of GST, GST omega, was found in the lateral motile cilia, although the amount was not as high as that of GSTT in the apical tuft. Among the multiple types of GST, GSTT is evolutionarily distinct from the other types of GSTs and is conserved among non-mammalian species including plants (Sheehan et al., 2001; Dixon et al., 2009). GSTT has unique enzymatic properties,

including weak binding to a standard GST substrate CDNB, the bioactivation of dihaloalkanes (Sherratt et al., 1998), and hydroperoxide-reducing glutathione peroxidase activity (Landi, 2000). In mouse lung, GSTT is localized at the Clara cells and ciliated cells, and is suggested to be involved in the detoxification of several carcinogens (Mainwaring et al., 1996).

It should be noted that the sea urchin apical tuft contains abundant amounts of other redox-related enzymes, such as thioredoxin peroxidase (Table 2) and thioredoxin reductase (Table 1). It is possible that GSTT is involved in the redox-sensitive regulation of apical tuft function together with those proteins.

I observed a significant effect of an inhibitor of GST, BSP, in apical tufts but not significantly in the lateral motile cilia. BSP induced the bending of the apical tufts (Fig. 16-21), suggesting that GSTT regulates the microtubule-sliding of apical tuft cilia. The bending of the apical tufts seemed to cause less efficiency of escaping behavior when the embryos collided with an object. These results suggest that the apical tuft is involved in the mechanical reception and transduction to regulate lateral motile cilia. I could not exclude the possibility that BSP could affect on other enzymes or other types of GSTs, although BSP did not change the beat frequency of lateral cilia nor the swimming velocity or trajectory of the embryos. Specific knock down of GSTT in the embryos by morpholino antisense oligonucleotides should further clarify the function of GSTT in the control of apical tuft.

Sea urchin embryos show negative geotactic behavior at the stages from blastula to pluteus, which is thought necessary for vertical positioning for feeding (Mogami et

al., 1988). Factors regulating geotactic behavior, which has been widely studied in ciliated protozoa, include uniform density, different drag, and uneven locomotion within a cell (Bean, 1984). Gravireceptors and rheoreceptors have been posited as possible mechanisms underlying the geotaxis of sea urchin larvae (Gustafson et al., 1972; Strathmann et al., 1972; Mogami et al., 1988), and the apical tuft was one of the candidates. My data shown in this paper suggest that GSTT in the apical tuft is not involved in the negative geotaxis, but is involved in the mechanical response to escape from collisions (Fig. 22-24). The experiments using a micro-maze clearly showed the role of apical tuft GSTT in the behavior of sea urchin embryos (Fig. 26, 27). It is worth noticing that transient receptor potential (TRP) 11 is localized in flagella and essential for mechanoreception in the avoiding behavior of the unicellular algae *Chlamydomonas* (Fujii et al., 2011). It is possible that similar TRP channel is involved in the mechaoreception and avoiding response in multicellular organisms, such as sea urchin embryos. On the other hand, surface scattering of both mammalian sperm and *Chlamydomonas* is primarily governed by direct ciliary contact interaction (Kantsler et al., 2013). GSTT may participate in the maintenance of mechano-elastic properties of apical tuft. It is still unclear how GSTT is involved in the regulation of apical tuft bending, mechanoreception and control of the motility of lateral cilia. To identify the mechanisms of signal transduction from the apical tuft to lateral motile cilia during an escape after a collision, it is necessary to analyze the detailed changes in the waveforms of apical tuft and lateral cilia before and after collisions.

Since the ciliary motility of the apical tuft is much less than that of the lateral

motile cilia, I expected the axonemal components for motility to be different between the apical tuft and the lateral motile cilia. However most of the major components of motile axonemes, including those of outer and inner arms, radial spokes and central pair, were identified in both preparations (Fig. 1, Table 4). Therefore it appears that apical tuft cilia are potentially motile and that their reduced motility is the result of regulations inhibitory to the axonemes in apical tuft. I show that GSTT and other redox-related proteins are abundantly present in apical tuft. In *Chlamydomonas* flagella, outer arm dynein is regulated by redox poise (Wakabayashi et al., 2006). Such a regulation is clearly seen in the changes in flagellar motility when *Chlamydomonas* respond to light stimulation (Wakabayashi et al., 2011). Furthermore, reactive oxygen species regulates flagellar motility of human sperm (de Lamirande and Gagnon, 1997; de Lamirande et al., 2003). Taken together, it is possible that the motility of apical tuft is suppressed by redox poise through the action of GSTT. The physiological reason for less motility of apical tuft, however, is still unknown.

I found other proteins specifically present in either lateral motile cilia or apical tuft. Proteins specifically found in apical tuft include GSTT and other redox-related proteins, as well as those suggested to be related to primary cilia and sensory cilia such as fibrocystin (Wang et al., 2007; Harris and Torres, 2009) and usherin (Bhattacharya et al., 2002; Pearsall et al., 2002; Liu et al., 2007). These features strongly suggest that apical tuft functions as primary cilia or sensory cilia to transmit extracellular signals to the lateral motile cilia. Although the present study suggests that apical tuft GSTT is involved in the mechanical reception and the regulation of lateral motile cilia, it is not

clear how the mechanical signal at apical tuft is transmitted to the lateral motile cilia to regulate the motility and alter the behavior of embryos. To elucidate the molecular mechanism of the motility of apical tuft, signal transduction from apical tuft to the lateral cilia, and regulation of embryonic behavior, further works should be carried out, including knockdown of the expression of apical tuft-specific proteins, isolation of dynein and direct measurement of microtubule-sliding, physiological and biochemical characterization of a mechanical receptor of apical tuft, and detailed analysis of the motility of lateral cilia during embryonic escaping behavior.

Acknowledgement

I would like to express my cordial gratitude to Professor Kazuo Inaba, Shimoda Marine Research Center, University of Tsukuba, for his generous support, invaluable advice, and encouragement throughout the course of this study.

I am grateful to Dr. Shunsuke Yaguchi, Shimoda Marine Research Center, University of Tsukuba, for his guidance for this study, and to Dr. Kogiku Shiba, Shimoda Marine Research Center, University of Tsukuba, for her guidance for microscopic analysis and helpful suggestions for this study. I also thank Junko Yaguchi and other members of Shimoda Marine Resarch Center, University of Tsukuba for their valuable experimental suggestions and supports during the course of my study.

I thank professor Hitoshi Sawada and Dr. Lixy Yamada, Sugashima Marine Biological Laboratory, Nagoya University for their help in LC MS/MS analysis. Thanks are also due to the staff of Ochanomizu University Marine and Coastal Research Center and Asamushi Marine Biological Center, Tohoku University, for supplying *Hemicentrotus pulcherrimus*.

References

- Auclair, W. and Siegel, B.W.** (1966) Cilia regeneration in the sea urchin embryo: evidence for a pool of ciliary proteins. *Science*. **154**, 913-5
- Bean, B.** (1984). Microbial reotaxis. In *Membranes and Sensory Transduction* (ed. G. Colombetti and F. Lenci), pp. 163-198. New York, London, Plenum Press.
- Bhattacharya, G., Miller, C., Kimberling, W.J., Jablonski, M.M. and Cosgrove, D.** (2002) Localization and expression of usherin: a novel basement membrane protein defective in people with Usher's syndrome type IIa. *Hear. Res.* **163**, 1–11
- Board, P.G., Baker, R.T., Chelvanayagam, G. and Jermiin, L.S.** (1997) Zeta, a novel class of glutathione transferases in a range of species from plants to humans. *Biochem. J.* **328**, 929-935
- Board, P.G., Coggan, M., Chelvanayagam, G., Easteal, S., Jermiin, L.S., Schulte, G.K., Danley, D.E., Hoth, L.R., Griffor, M.C. and Kamath, A.V.** (2000) Identification, characterization and crystal structure of the Omega class glutathione transferases. *J. Biol. Chem.* **275**, 24798-24806
- Burke, R.D.** (1978) The structure of the nervous system of the pluteus larva of *Strongylocentrotus purpuratus*. *Cell Tissue Res.* **191**, 233-247

Chia, F.S. and Koss, R. (1979) Fine structural studies of the nervous system and the apical organ in the planula larva of the sea anemone *Anthopleura elegantissima*. *J Morphol.* **160**, 275-297

Dawe H.R., Shaw M.K., Farr H., Gull K. (2007) The hydrocephalus inducing gene product, Hydin, positions axonemal central pair microtubules. *BMC Biol.* **7**, 5-33

Dixon, D.P., Hawkins, T., Hussey, P.J. and Edwards, R. (2009) Enzyme activities and subcellular localization of members of the *Arabidopsis* glutathione transferase superfamily. *J Exp Bot.* **60**, 1207-1218

Dunn, E.F., Moy, V.N., Angerer, L.M., Angerer, R.C., Morris, R.L. and Peterson, K.J. (2007) Molecular paleoecology: using gene regulatory analysis to address the origins of complex life cycles in the late Precambrian. *Evol. Dev.* **9**, 10–24

de Lamirande, E., Jiang H., Zini A., Kodama, H. and Gagnon, C. (1997) Reactive oxygen species and sperm physiology. *Rev Reprod.* **2**, 48-54

de Lamirande, E. and Gagnon, C. (2003) Redox control of changes in protein sulphhydryl levels during human sperm capacitation. *Free Radic Biol Med.* **35**, 1271-1285

Gibbons, I.R. (1981) Cilia and flagella of eukaryotes. *J. Cell Biol. J Cell Biol.* **91**, 107s-124s

Fujiu, K., Nakayama, Y., Iida, H., Sokabe, M. and Yoshimura, K. (2011) Mechanoreception in motile flagella of *Chlamydomonas*. *Nat Cell Biol.* **13**, 630-632.

Gustafson, T., Lundgren, B. and Treufeldt, R. (1972) Serotonin and contractile activity in the echinopluteus. A study of the cellular basis of larval behaviour. *Exp Cell Res.* **72**, 115-139

Hadfield, M.G. (2000) Biofilms and marine invertebrate larvae: what bacteria produce that larvae use to choose settlement sites. *Ann. Rev. Mar. Sci.* **3**, 453-470

Harris, P.C. and Torres, V.E. (2009) Polycystic kidney disease. *Annu Rev Med.* **60**, 321-337

Ibanez-Tallon, I., Heintz, N. and Omran, H. (2003) To beat or not to beat: roles of cilia in development and disease. *Hum. Mol. Genet.* **12**, R27–R35

Inaba, K. (2003) Molecular architecture of sperm flagella: molecules for motility and signaling. *Zool. Sci.* **20**, 1043-1036

Inaba, K. (2007) Molecular basis of sperm flagellar axonemes: structural and evolutionary aspects. *Ann N Y Acad Sci.* **1101**, 506-526

Inaba, K. (2011) Sperm flagella: comparative and phylogenetic perspectives of protein components. *Mol Hum Reprod.* **17**, 524-538

Inaba, K., Mohri, T. and Mohri, H. (1988) B-band protein in sea urchin sperm flagella. *Cell Motil. Cytoskeleton.* **10**, 506-517

Kantsler, V., Dunkel, J., Polin, M. and Goldstein, R.E. (2013) Ciliary contact interactions dominate surface scattering of swimming eukaryotes. *Proc Natl Acad Sci USA.* **110**, 1187-1192

- Katow, H., Yaguchi, S. and Kyozuka K.** (2007) Serotonin stimulates $[Ca^{2+}]_i$ elevation in ciliary ectodermal cells of echinoplutei through a serotonin receptor cell network in the blastocoel. *J Exp Biol.* **210**, 403-412
- King, S.M.** (2000) The dynein microtubule motor. *Biochim Biophys Acta.* **1496**, 60-75
- Konno, A., Kaizu, M., Hotta, K., Horie, T., Sasakura, Y., Ikeo, K. and Inaba K.** (2010) Distribution and structural diversity of cilia in tadpole larvae of the ascidian *Cionax intestinalis*. *Dev Biol. Dev Biol.* **337**, 42-62
- Kolobe D., Sayed Y., Dirr H.W.** (2004) Characterization of bromosulphophthalein binding to human glutathione S-transferase A1-1: thermodynamics and inhibition kinetics. *Biochem J.* **382**, 703-709
- Lallier, R.** (1955) Effets des ions zinc et cadmium sur le dvelloppement de l'oursin *Paracentrotus lividus*. *Arch. Biol.* **66**, 75-102
- Lallier, R.** (1975) Animalization and vegetalization. In “the sea Urchin Embryo” (G.Czihak, ed.), 473-509
- Landi, S.** (2000) Mammalian class theta GST and differential susceptibility to carcinogens: a review. *Mutat Res.* **463**, 247-283
- Liu, X., Bulgakov, O.V., Darrow, K.N., Pawlyk, B., Adamian, M., Liberman, M.C. and Li, T.** (2007) Usherin is required for maintenance of retinal photoreceptors and normal development of cochlear hair cells. *Proc Natl Acad Sci U S A.* **104**, 4413-4418
- Logan, C.Y., Miller, J.R., Ferkowicz, M.J. and McClay, D.R.** (1999) Nuclear beta-catenin is required to specify vegetal cell fates in the sea urchin embryo. *Development.* **126**, 345-357

Mainwaring, G.W., Williams, S.M., Foster, J.R., Tugwood, J. and Green, T. (1996)

The distribution of theta-class glutathione S-transferases in the liver and lung of mouse, rat and human. *Biochem J.* **318**, 297-303

Marshall, W.F. and Nonaka, S. (2006) Cilia: tuning in to the cell's antenna. *Curr Biol.* **16**, R604-R614

Masuda, M., Sato, H. (1984) Reversible resorption of cilia and the centriole cycle in dividing cells of sea urchin blastulae. *Zool Sci.* **1**, 445-462

Minokawa, T., Rast, J.P., Arenas-Mena, C., Franco, C.B., Davidson, E.H. (2004) Expression patterns of four different regulatory genes that function during sea urchin development. *Gene Expr. Patterns* **4**, 449–456

Mitchell, D.R. (2004) Speculations on the evolution of 9+2 organelles and the role of central pair microtubules. *Biol Cell.* **96**, 691-696

Mizuno, K., Padma, P., Konno, A., Satouh, Y., Ogawa, K. and Inaba, K. (2009) A novel neuronal calcium sensor family protein, calaxin, is a potential Ca(2+)-dependent regulator for the outer arm dynein of metazoan cilia and flagella. *Biol Cell.* **101**, 91-103

Mogami, Y., Oobayashi, C., Yamaguchi, T., Ogiso, Y., and Baba, S.A. (1988) Negative geotaxis in sea urchin larvae: possible role of mechanoreception in the late stages of development. *J. Exp. Biol.* **137**, 141-156.

Nakachi, M., Nakajima, A., Nomura, M., Yonezawa, K., Ueno, K., Endo, T. and Inaba, K. (2011) Proteomic profiling reveals compartment-specific, novel functions of ascidian sperm proteins. *Mol Reprod Dev.* **78**, 529-549

Nakajima, Y., Kaneko, H., Murray, G. and Burke, R.D. (2004) Divergent patterns of neural development in larval echinoids and asteroids. *Evol Dev.* **6**, 95-104

Padma, P., Satouh, Y., Wakabayashi, K., Hozumi, A., Ushimaru, Y., Kamiya, R. and Inaba, K. (2003) Identification of a novel leucine-rich repeat protein as a component of flagellar radial spoke in the Ascidian *Ciona intestinalis*. *Mol Biol Cell.* **14**, 774-785

Paparo, A.A., Hamburg, M.D. and Morris, E. (1976) Pharmacological modification of unit activity of the cerebral ganglion of the mussel, *Mytilus edulis* and the control of ciliary movement. *Comp Biochem Physiol C.* **54**, 81-87

Pearsall, N., Bhattacharya, G., Wisecarver, J., Adams, J., Cosgrove, D. and Kimberling, W. (2002) Usherin expression is highly conserved in mouse and human tissues. *Hear Res.* **174**, 55-63

Porter, M.E. and Sale, W.S. (2000) The 9+2 axoneme anchors multiple inner arm dyneins and a network of kinases and phosphatases that controls motility. *J Cell Biol. J Cell Biol.* **151**, F37-F42

Poustka, A.J., Kühn, A., Groth, D., Weise, V., Yaguchi, S., Burke, R.D., Herwig, R., Lehrach, H. and Panopoulou, G. (2007) A global view of gene expression in lithium and zinc treated sea urchin embryos: new components of gene regulatory networks. *Genome Biol.* **8**, R85.

Prulière, G., Cosson, J., Chevalier, S., Sardet, C. and Chenevert, J. (2011) Atypical protein kinase C controls sea urchin ciliogenesis. *Mol Biol Cell.* **22**, 2042-2053

Sea Urchin Genome Sequencing Consortium, Sodergren E., Weinstock G.M., Davidson E.H., Cameron R.A., Gibbs R.A., Angerer R.C., Angerer L.M., Arnone M.I., Burgess D.R., Burke R.D., Coffman J.A., Dean M., Elphick M.R., Ettensohn C.A., Foltz K.R., Hamdoun A., Hynes R.O., Klein W.H., Marzluff W., McClay D.R., Morris R.L., Mushegian A., Rast J.P., Smith L.C., Thorndyke M.C., Vacquier V.D., Wessel G.M., Wray G., Zhang L., Elsik C.G., Ermolaeva O., Hlavina W., Hofmann G., Kitts P., Landrum M.J., Mackey A.J., Maglott D., Panopoulou G., Poustka A.J., Pruitt K., Sapochnikov V., Song X., Souvorov A., Solovyev V., Wei Z., Whittaker C.A., Worley K., Durbin K.J., Shen Y., Fedrigo O., Garfield D., Haygood R., Primus A., Satija R., Severson T., Gonzalez-Garay M.L., Jackson A.R., Milosavljevic A., Tong M., Killian C.E., Livingston B.T., Wilt F.H., Adams N., Bellé R., Carboneau S., Cheung R., Cormier P., Cosson B., Croce J., Fernandez-Guerra A., Genevière A.M., Goel M., Kelkar H., Morales J., Mulner-Lorillon O., Robertson A.J., Goldstone J.V., Cole B., Epel D., Gold B., Hahn M.E., Howard-Ashby M., Scally M., Stegeman J.J., Allgood E.L., Cool J., Judkins K.M., McCafferty S.S., Musante A.M., Obar R.A., Rawson A.P., Rossetti B.J., Gibbons I.R., Hoffman M.P., Leone A., Istrail S., Materna S.C., Samanta M.P., Stolc V., Tongprasit W., Tu Q., Bergeron K.F., Brandhorst B.P., Whittle J., Berney K., Bottjer D.J., Calestani C., Peterson K., Chow E., Yuan Q.A., Elhaik E., Graur D., Reese J.T., Bosdet I., Heesun S., Marra M.A., Schein J., Anderson M.K., Brockton V., Buckley K.M., Cohen A.H., Fugmann S.D., Hibino T., Loza-Coll M., Majeske A.J., Messier C., Nair S.V., Pancer Z., Terwilliger D.P., Agca C.,

Arboleda E., Chen N., Churcher A.M., Hallböök F., Humphrey G.W., Idris M.M., Kiyama T., Liang S., Mellott D., Mu X., Murray G., Olinski R.P., Raible F., Rowe M., Taylor J.S., Tessmar-Raible K., Wang D., Wilson K.H., Yaguchi S., Gaasterland T., Galindo B.E., Gunaratne H.J., Juliano C., Kinukawa M., Moy GW., Neill A.T., Nomura M., Raisch M., Reade A., Roux M.M., Song J.L., Su Y.H., Townley I.K., Voronina E., Wong J.L., Amore G., Branno M., Brown E.R., Cavalieri V., Duboc V., Duloquin L., Flytzanis C., Gache C., Lapraz F., Lepage T., Locascio A., Martinez P., Matassi G., Matranga V., Range R., Rizzo F., Röttinger E., Beane W., Bradham C., Byrum C., Glenn T., Hussain S., Manning G., Miranda E., Thomason R., Walton K., Wikramanayake A., Wu S.Y., Xu R., Brown C.T., Chen L., Gray R.F., Lee P.Y., Nam J., Oliveri P., Smith J., Muzny D., Bell S., Chacko J., Cree A., Curry S., Davis C., Dinh H., Dugan-Rocha S., Fowler J., Gill R., Hamilton C., Hernandez J., Hines S., Hume J., Jackson L., Jolivet A., Kovar C., Lee S., Lewis L., Miner G., Morgan M., Nazareth L.V., Okwuonu G., Parker D., Pu L.L., Thorn R., Wright R. (2006) The genome of the sea urchin *Strongylocentrotus purpuratus*. *Science*. **314**, 941-952

Semenova, M.N., Tsyganov, D.V., Yakubov, A.P., Kiselynov, A.S. and Semenov, V.V. (2008) A synthetic derivative of plant allylpolyalkoxybenzenes induces selective loss of motile cilia in sea urchin embryos. *ACS. Chem. Biol.* **3**, 95-100.

Schor, S.L. (1965) Serotonin and adenosine triphosphate: Synergistic effect on the beat frequency of cilia of mussel gills. *Science*. **148**, 500-501

- Sedmak, T. and Wolfrum, U.** (2011) Intraflagellar transport proteins in ciliogenesis of photoreceptor cells. *Biol Cell*. **103**, 449-466
- Sharma, N., Berbari, N.F. and Yoder, B.K.** (2008) Ciliary dysfunction in developmental abnormalities and diseases. *Curr. Top. Dev. Biol* **85**, 371–427
- Sheehan, D., Meade, G., Foley, V.M. and Dowd, C.A.** (2001) Structure, function and evolution of glutathione transferases: implications for classification of non-mammalian members of an ancient enzyme superfamily. *Biochem J*. **360**, 1-16
- Sherratt, P.J., Manson, M.M., Thomson, A.M., Hissink, E.A., Neal, G.E., van Bladeren, P.J., Green, T. and Hayes, J.D.** (1998) Increased bioactivation of dihaloalkanes in rat liver due to induction of class theta glutathione S-transferase T1-1. *Biochem J*. **335**, 619-630
- Shiba, K., Mogami Y., and Baba, S.A.** (2002) Ciliary movement of sea-urchin embryos. *Nat. Sci. Rep. Ochanomizu Univ.*, **53**, 49-54.
- Showman R.M., Foerder C.A.** (1979) Removal of the fertilization membrane of sea urchin embryo employing aminotriazole. *Exp Cell Res*. **120**, 253-255
- Singla, V. and Reiter, J.F.** (2006) The primary cilium as the cell's antenna: signaling at a sensory organelle. *Science*. **313**, 629-633
- Smith, E.F. and Yang, P.** (2004) The radial spokes and central apparatus: mechano-chemical transducers that regulate flagellar motility. *Cell Motil Cytoskeleton*. **57**, 8-17

Stephens, R.E. and Prior, G. (1992) Dynein from serotonin-activated cilia and flagella: extraction characteristics and distinct sites for cAMP-dependent protein phosphorylation. *J Cell Sci.* **103**, 999-1012

Stephens, R.E. (1995) Ciliogenesis in sea urchin embryos – a subroutine in the program of development. *Bioessays* **17**, 331-340

Stephens R.E. (2008) Ciliogenesis, ciliary function, and selective isolation. *ACS Chem Biol.* **3**, 84-86

Strathmann, R. R., Jahn, T. L., and Fonseca, J. R. C. (1972) Suspension feeding by marine invertebrate larvae: clearance of particles by ciliated bands of a rotifer, pluteus, and trochophore. *Biol. Bull.* **142**, 505–519

Tamura, K., Peterson, D., Peterson, N., Stecher, G., Nei, M., and Kumar, S. (2011) MEGA5: Molecular evolutionary genetics analysis using maximum likelihood, evolutionary distance, and aaximum parsimony methods. *Mol. Biol. Evol.* **28**, 2731-2739

Wada, Y., Mogami, Y. and Baba, S. (1997) Modification of ciliary beating in sea urchin larvae induced by neurotransmitters: beat-plane rotation and control of frequency fluctuation. *J Exp Biol.* **200**, 9-18

Wakabayashi, K. and King, S.M. (2006) Modulation of Chlamydomonas reinhardtii flagellar motility by redox poise. *J Cell Biol.* **173**, 743-754

Wakabayashi, K., Misawa, Y., Mochiji, S. and Kamiya, R. (2011) Reduction-oxidation poise regulates the sign of phototaxis in Chlamydomonas reinhardtii. *Proc Natl Acad Sci U S A.* **108**, 11280-11284

- Wang, S., Zhang, J., Nauli, S.M., Li, X., Starremans, P.G., Luo, Y., Roberts, K.A. and Zhou, J.** (2007) Fibrocystin/polyductin, found in the same protein complex with polycystin-2, regulates calcium responses in kidney epithelia. *Mol Cell Biol.* **27**, 3241-3252
- Weston, M.D., Eudy, J.D., Fujita, S., Yao, S., Usami, S., Cremers, C., Greenberg, J., Ramesar, R., Martini, A., Moller, C., Smith, R.J., Sumegi, J. and Kimberling, W.J.** (2000) Genomic structure and identification of novel mutations in usherin, the gene responsible for Usher syndrome type IIa. *Am J Hum Genet.* **66**, 1199-1210
- Yaguchi, S. and Katow, H.** (2003) Expression of tryptophan 5-hydroxylase gene during sea urchin neurogenesis and role of serotonergic nervous system in larval behavior. *J Comp Neurol.* **466**, 219-229
- Yaguchi, S., Yaguchi, J., Wei, Z., Shiba, K., Angerer, L.M. and Inaba, K.** (2010) ankAT-1 is a novel gene mediating the apical tuft formation in the sea urchin embryo. *Dev Biol.* **348**, 67-75
- Yamada, L., Saito, T., Taniguchi, H., Sawada, H. and Harada, Y.** (2009) Comprehensive egg coat proteome of the ascidian *Ciona intestinalis* reveals gamete recognition molecules involved in self-sterility. *J Biol Chem.* **284**, 9402-9410

Table 1. Proteins identified in this study.

ID	Description	N count	Z count	Z/N	N/Z
SPU_019990	alpha tubulin 5	4468	7200	1.611459266	0.620555556
SPU_013273	beta tubulin 4	2760	4039	1.463405797	0.68333746
SPU_000062	beta tubulin 3	1181	1695	1.435224386	0.696755162
SPU_007424	beta tubulin	1003	1602	1.597208375	0.626092385
SPU_007425	beta tubulin 6	755	1247	1.651655629	0.605453087
SPU_030230	DNAH9, axonemal dynein beta heavy chain, ODA-beta, Tubulin C, TUBB2A	1082	1131	1.045286506	0.956675508
SPU_014285		472	761	1.612288136	0.620236531
SPU_016746	alpha tubulin 3	378	720	1.904761905	0.525
SPU_030224	DNAH2, DHC5C, IDA1-beta, axonemal dynein	586	718	1.225255973	0.816155989
SPU_003660	dynein, axonemal, heavy polypeptide 5 - part II	570	698	1.224561404	0.816618911
SPU_012679	alpha tubulin 13	333	662	1.987987988	0.503021148
SPU_030228	DNAH7, DHC7A, axonemal dynein	561	622	1.108734403	0.90192926
SPU_030231	DNAH10, DHC4, IDA1-alpha, Sp-DNAH10, axonemal dynein	465	467	1.004301075	0.995717345
SPU_030226	DNAH5, DHC3B, axonemal dynein	459	465	1.013071895	0.987096774
SPU_030234	DNAH15, DHC3A, ODA-gamma, axonemal dynein	366	409	1.117486339	0.894865526
SPU_004619	PARK2 co-regulated [Homo sapiens]	264	383	1.450757576	0.689295039
SPU_004622	dynein, axonemal, heavy polypeptide 3	320	371	1.159375	0.862533693
SPU_004121	armadillo repeat containing 4	317	368	1.160883281	0.861413043
SPU_009481	Actin, cytoskeletal 1A	247	368	1.489878543	0.671195652
SPU_021429	EF-hand domain (C-terminal) containing 1	279	325	1.164874552	0.858461538
SPU_030227	DNAH6, DHC5A, axonemal dynein	316	320	1.012658228	0.9875
SPU_005442	radial spoke head 9	161	305	1.894409938	0.527868852
SPU_009439	EF-hand domain-containing family member C2	189	302	1.597883598	0.625827815
SPU_011000	transcription factor 2B	169	292	1.727810651	0.578767123
SPU_004880	hypothetical protein	299	288	0.963210702	1.038194444
SPU_030223	DNAH1, DHC6, Sp-DNAH1, axonemal dynein	266	286	1.07518797	0.93006993
SPU_006756	tubulin alpha-1A	174	286	1.643678161	0.608391608
SPU_025787	sperm-associated antigen 6	177	277	1.564971751	0.63898917
SPU_003123	WD repeat domain 16	322	269	0.835403727	1.197026022
SPU_003564	axonemal dynein heavy chain 7 - part II	243	267	1.098765432	0.91011236
SPU_023618	tektin-3	213	266	1.248826291	0.80075188
SPU_000013	dynein, axonemal, heavy polypeptide 1 - part II	226	254	1.123893805	0.88976378
SPU_004143	Alpha tubulin 2	150	241	1.606666667	0.622406639

SPU_022006	Nucleoside diphosphate kinase 7 (NDK 7) (NDP kinase 7) (nm23-H7)	102	240	2.352941176	0.425
XP_001176159.1	similar to arginine kinase	262	238	0.908396947	1.100840336
SPU_008777	tektin-4	228	235	1.030701754	0.970212766
SPU_022182	EF-hand calcium binding domain 6-2	259	233	0.8996139	1.111587983
SPU_010131	WD repeat domain 65	224	228	1.017857143	0.98245614
SPU_020728	tektin-2	249	225	0.903614458	1.106666667
SPU_020634	kinesin-like protein KIF1A	148	223	1.506756757	0.66367713
SPU_000061	tubulin beta-2C	205	214	1.043902439	0.957943925
SPU_015323	Creatine kinase B-type (Creatine kinase, B chain) (B-CK)	184	213	1.157608696	0.863849765
SPU_027786	arginine kinase	189	207	1.095238095	0.913043478
SPU_013841	tektin-1	192	200	1.041666667	0.96
SPU_019506	DYI2 dynein intermediate chain 2	221	186	0.841628959	1.188172043
SPU_027784	kinesin family member 1B [Homo sapiens]	190	185	0.973684211	1.027027027
SPU_014801	Radial spokehead-like 3	146	185	1.267123288	0.789189189
SPU_010764	Putative adenylate kinase 7	162	182	1.12345679	0.89010989
SPU_025936	coiled-coil domain containing 151	218	165	0.756880734	1.321212121
SPU_015625	dynein outer arm binding protein (Ap58)	215	165	0.76744186	1.303030303
SPU_030232	DNAH12, DHC7C, Sp-DNAH12, axonemal dynein	139	161	1.158273381	0.863354037
SPU_003919	EF-hand calcium binding domain 5	100	161	1.61	0.621118012
SPU_006699	Dynein intermediate chain 3, IA1-IC140	148	158	1.067567568	0.936708861
SPU_026705	heat shock protein 40 [Ciona intestinalis]	106	138	1.301886792	0.768115942
SPU_014186	similar to shippo 1 (ODF3)	92	130	1.413043478	0.707692308
SPU_021668	alpha tubulin 10	67	130	1.940298507	0.515384615
SPU_018537	human chromosome 20 open reading frame 26-like; flagellar associated protein-like	97	128	1.319587629	0.7578125
SPU_003263	sperm-associated antigen 16	110	124	1.127272727	0.887096774
SPU_024615	alpha tubulin 6	80	123	1.5375	0.650406504
SPU_021670	alpha tubulin 11	80	121	1.5125	0.661157025
SPU_014810	leucine rich repeat containing 23	111	116	1.045045045	0.956896552
SPU_010725	similar to LOC496017 protein	71	115	1.61971831	0.617391304
SPU_024605	catenin	117	111	0.948717949	1.054054054
SPU_004762	ODA-DC2, Outer Dynein Arm Docking Complex 2, Mr 70,000	130	111	0.853846154	1.171171171
SPU_015320	axonemal dynein light chain p33	106	109	1.028301887	0.972477064
SPU_019553	adenylate kinase	88	107	1.215909091	0.822429907
SPU_026533	Dynein intermediate chain 3	115	106	0.92173913	1.08490566
SPU_025942	radial spoke head 1	94	105	1.117021277	0.895238095

SPU_007092	Dynein Intermediate Chain 1 (NM23-H8)	99	105	1.060606061	0.942857143
SPU_002110	dynein, axonemal, heavy chain 8	97	102	1.051546392	0.950980392
SPU_012262	tetratricopeptide repeat domain 18	95	101	1.063157895	0.940594059
SPU_015272	EF-hand calcium binding domain 6; AP-binding protein complex interacting protein 1	128	99	0.7734375	1.292929293
SPU_027352	coiled-coil domain containing 147; flagellar associated protein (<i>Chlamydomonas reinhardtii</i>)	130	98	0.753846154	1.326530612
XP_780230.2	radial spoke head protein 9	39	95	2.435897436	0.410526316
SPU_028683	vitellogenin		94	-	-
SPU_028903	alpha tubulin 7	61	94	1.540983607	0.64893617
SPU_013875	human chromosome 6 open reading frame 165-like	77	93	1.207792208	0.827956989
SPU_010728	coiled-coil domain containing 11	65	91	1.4	0.714285714
SPU_022360	human chromosome 11 open reading frame 66-like	95	88	0.926315789	1.079545455
SPU_010767	adenylate kinase	82	88	1.073170732	0.931818182
SPU_002151	WD repeat domain 65	109	85	0.779816514	1.282352941
SPU_007140	WD repeat domain 66	80	85	1.0625	0.941176471
SPU_025272	dynein light chain 2, cytoplasmic	55	83	1.509090909	0.662650602
SPU_012677	Malate dehydrogenase, cytoplasmic	48	82	1.708333333	0.585365854
SPU_016563	human chromosome X open reading frame 22-like	61	81	1.327868852	0.75308642
SPU_009640	translin-associated factor X (Tsnax)-interacting protein 1	71	81	1.14084507	0.87654321
SPU_027932	Proteosome alpha-type 2	27	80	2.962962963	0.3375
SPU_024529	dynein, axonemal, heavy polypeptide 5 - part I	84	80	0.952380952	1.05
SPU_008700	serine/threonine protein phosphatase I, catalytic subunit; PPP1-like; PP-1-like	45	80	1.777777778	0.5625
SPU_009896	EF-hand domain (C-terminal) containing 2-1	60	77	1.283333333	0.779220779
SPU_019415	valosin-containing protein	33	77	2.333333333	0.428571429
SPU_001045	beta-tubulin 2-1	95	76	0.8	1.25
SPU_022852	EF-hand calcium binding domain 6-like-2	81	74	0.913580247	1.094594595
SPU_020625	human chromosome 6 open reading frame 224-like	66	73	1.106060606	0.904109589
SPU_006598	leucine rich repeat containing 48	80	71	0.8875	1.126760563
SPU_003865	PF2, Dynein Regulatory Complex Protein	72	71	0.986111111	1.014084507
SPU_002788	dynein light chain 2, cytoplasmic		70	-	-
SPU_021664	coiled-coil domain containing 81	85	69	0.811764706	1.231884058
SPU_000735	sperm autoantigenic protein 17	65	68	1.046153846	0.955882353
SPU_002966	solute carrier family 25, member 42-like	41	68	1.658536585	0.602941176
SPU_019556	human chromosome 6 open reading frame 199-like	70	65	0.928571429	1.076923077
SPU_012521	Nucleoside diphosphate kinase homolog 5 (NDK-H 5) (NDP kinase homolog 5) (nm23-H5)	44	64	1.454545455	0.6875
SPU_007254	coiled-coil domain containing 40	80	62	0.775	1.290322581

SPU_006495	glutathioneS-transferase theta 1	5	62	12.4	0.080645161
SPU_005191	rhabdoid tumor deletion region gene 1-like	28	62	2.214285714	0.451612903
SPU_012115	EF-hand domain family, member B	53	61	1.150943396	0.868852459
SPU_024395	calcium/calmodulin-dependent protein kinase IV, CaMK4, calspermin	38	61	1.605263158	0.62295082
SPU_007671	enkurin	74	60	0.810810811	1.233333333
SPU_023486	fibrocystin	8	59	7.375	0.13559322
SPU_002424	coiled-coil domain containing 105	71	58	0.816901408	1.224137931
SPU_019525	hydrocephalus-inducing protein-2	73	58	0.794520548	1.25862069
SPU_023583	NIM4, never in mitosis	57	57	1	1
SPU_002525	SPRY domain containing 3	63	56	0.888888889	1.125
SPU_005973	ODA-IC1, Outer Dynein Arm Intermediate Chain 1	62	56	0.903225806	1.107142857
SPU_025497	ropporin 1-like	19	56	2.947368421	0.339285714
SPU_020526	coiled-coil domain containing 39	58	54	0.931034483	1.074074074
SPU_006796	hypothetical protein-1682	85	54	0.635294118	1.574074074
SPU_028221	tubulin alpha-1A	40	54	1.35	0.740740741
SPU_024498	dynein light chain 2, cytoplasmic	38	54	1.421052632	0.703703704
SPU_005061	Flotillin 2	70	53	0.757142857	1.320754717
SPU_019989	tubulin, alpha 2	42	53	1.261904762	0.79245283
XP_790262.2	tubulin alpha chain	31	53	1.709677419	0.58490566
SPU_001344	PP2A regulatory subunit A, isoform alpha; alpha isoform of regulatory subunit A, protein phosphatase 2	28	52	1.857142857	0.538461538
SPU_016007	beta tubulin 8	44	51	1.159090909	0.862745098
SPU_014155	hypothetical protein-2134	28	51	1.821428571	0.549019608
SPU_001584	Multifunctional protein ADE2	44	50	1.136363636	0.88
SPU_030235	DYNC2H1, DHC1B, IFT-dynein, Beethoven	60	50	0.833333333	1.2
SPU_022298	Erythrocyte band 7 integral membrane protein (Stomatin) (Protein 7.2b)	29	50	1.724137931	0.58
SPU_012809	dynein intermediate chains IA1-IC140	58	50	0.862068966	1.16
SPU_018597	proteasome 26S subunit, non-ATPase, 6; 26S proteasome non-ATPase regulatory subunit 6	43	49	1.139534884	0.87755102
SPU_021669	alpha tubulin 2	47	49	1.042553191	0.959183673
SPU_026143	peptidylprolyl isomerase, rotamase, cyclophilin	47	49	1.042553191	0.959183673
SPU_016269	glutathione S-transferase theta 1	0	49	-	-
SPU_028896	peptidylprolyl isomerase, rotamase, cyclophilin	40	49	1.225	0.816326531
SPU_014490	proteasome beta 5	32	48	1.5	0.666666667
XP_001187749.1	hypothetical protein	36	47	1.305555556	0.765957447
SPU_009433	actin	31	46	1.483870968	0.673913043
SPU_009641	hypothetical protein-1863; human chromosome 7 open reading frame 31-like	26	46	1.769230769	0.565217391

SPU_017044	hypothetical protein-858	55	46	0.836363636	1.195652174
SPU_028322	EF-hand calcium binding domain 6-1	33	45	1.363636364	0.733333333
SPU_008348	hypothetical protein-1780	21	45	2.142857143	0.466666667
SPU_014568	Erythrocyte band 7 integral membrane protein (Stomatin) (Protein7.2b)	13	44	3.384615385	0.295454545
SPU_007633	Dynein Light Chain Type 3	26	43	1.653846154	0.604651163
SPU_018854	DLC2	24	43	1.791666667	0.558139535
SPU_009165	HSC70	39	43	1.102564103	0.906976744
SPU_026340	5-aminoimidazole-4-carboxamide ribonucleotide formyltransferase/IMP cyclohydrolase	67	43	0.641791045	1.558139535
SPU_013301	Vitellogenin	0	43	-	-
SPU_001242	hypothetical protein-1317	37	43	1.162162162	0.860465116
SPU_023638	ATP-binding cassette sub-family A member 3 (ATP-binding cassette transporter 3)	25	42	1.68	0.595238095
SPU_022570	Cancer Susceptibility Gene 1	34	42	1.235294118	0.80952381
SPU_021662	similar to glutathione S-transferase theta 1	0	42	-	-
SPU_003825	14-3-3 epsilon	35	41	1.171428571	0.853658537
SPU_008427	proteasome beta 7 subunit	14	41	2.928571429	0.341463415
SPU_024245	dynein beta-heavy chain 9 isoform 2	38	40	1.052631579	0.95
SPU_025528	zinc finger, MYND-type containing 12	28	40	1.428571429	0.7
SPU_007071	coiled-coil domain containing 65	38	40	1.052631579	0.95
SPU_004471	human chromosome 3 open reading frame 15	26	40	1.538461538	0.65
SPU_002299	proteasome (prosome, macropain) alpha 5 subunit	35	39	1.114285714	0.897435897
SPU_009670	tetratricopeptide repeat domain 18	26	39	1.5	0.666666667
SPU_002620	tetratricopeptide repeat domain 21B-2; intraflagellar transport protein 139	39	39	1	1
SPU_019829	proteasome beta 3 subunit	21	39	1.857142857	0.538461538
SPU_022224	hypothetical protein	15	39	2.6	0.384615385
SPU_024086	human chromosome 6 open reading frame 97-like	53	39	0.735849057	1.358974359
SPU_016486	Aldolase a, fructose-bisphosphate	31	38	1.225806452	0.815789474
SPU_015928	malate dehydrogenase 1B, NAD (soluble)	38	38	1	1
SPU_019148	EF-hand calcium binding domain 6-like	21	38	1.80952381	0.552631579
SPU_013097	proteasome (prosome, macropain) subunit, alpha type 6	29	37	1.275862069	0.783783784
SPU_019691	flotillin 1	48	37	0.770833333	1.297297297
SPU_022385	hypothetical protein	28	37	1.321428571	0.756756757
SPU_022198	hypothetical protein-2603	37	37	1	1
SPU_007252	tetratricopeptide repeat domain 29	37	36	0.972972973	1.027777778
SPU_011179	WD repeat domain 52-2	49	36	0.734693878	1.361111111
SPU_003742	arachidonate 5-lipoxygenase	16	36	2.25	0.444444444

SPU_024379	6-phosphogluconate dehydrogenase, decarboxylating	49	36	0.734693878	1.361111111
SPU_023286	proteasome (prosome, macropain) subunit, alpha type 1	27	36	1.333333333	0.75
SPU_026078	actin 5 [Aedes aegypti]	27	36	1.333333333	0.75
SPU_022074	proteasome (prosome, macropain) subunit, beta type, 6	15	35	2.333333333	0.428571429
SPU_003496	ADP-Ribosylation Factor 4/5	22	35	1.590909091	0.628571429
SPU_017013	WD repeat domain 52	49	35	0.714285714	1.4
SPU_021918	IFT140, Intraflagellar Transport Protein 140	24	35	1.458333333	0.685714286
SPU_014969	26S proteasome non-ATPase regulatory subunit 8	30	35	1.166666667	0.857142857
XP_001195160.1	hypothetical protein	39	35	0.897435897	1.114285714
SPU_000763	coiled-coil domain containing 135-2	31	34	1.096774194	0.911764706
SPU_005728	similar to shippo 1 (ODF3)	26	34	1.307692308	0.764705882
SPU_007670	Proteasome 26S subunit ATPase 5, Sug1	23	33	1.434782609	0.696969697
SPU_028659	proteasome (prosome, macropain) 26S subunit, non-ATPase, 11	23	33	1.434782609	0.696969697
SPU_024768	hypothetical protein	30	33	1.1	0.909090909
SPU_018895	similar to CG15429-PA	29	33	1.137931034	0.878787879
SPU_019494	Cell Division Cycle 42	21	33	1.571428571	0.636363636
SPU_006844	t-complex-associated-testis-expressed 1	21	33	1.571428571	0.636363636
SPU_006826	ADP-Ribosylation Factor-Like 3	21	32	1.523809524	0.65625
SPU_026986	hypothetical protein	30	32	1.066666667	0.9375
SPU_010081	Kinesin Family 9 isoform 3 [Homo sapiens]	37	32	0.864864865	1.15625
SPU_025914	NACHT and LRR containing protein	34	32	0.941176471	1.0625
SPU_024225	Nucleoside diphosphate kinase homolog 5 (NDK-H 5) (NDP kinase homolog 5) (nm23-H5)	30	32	1.066666667	0.9375
SPU_015013	proteasome 26S subunit, non-ATPase, 2; 26S proteasome non-ATPase regulatory subunit 2	26	32	1.230769231	0.8125
SPU_015389	similar to CG15429-PA	13	32	2.461538462	0.40625
SPU_015692	testis, prostate and placenta-expressed protein	20	32	1.6	0.625
SPU_027934	meiosis-specific nuclear structural 1	21	32	1.523809524	0.65625
SPU_012045	radial spoke 3 homolog	33	31	0.939393939	1.064516129
SPU_019087	RAS-Related Protein RAB-7	29	31	1.068965517	0.935483871
SPU_003404	dynein, axonemal, heavy chain 9	39	31	0.794871795	1.258064516
SPU_012895	coiled-coil domain containing 108	17	31	1.823529412	0.548387097
SPU_018971	leucine rich repeat containing 34	29	31	1.068965517	0.935483871
XP_001193173.1	hypothetical protein	14	31	2.214285714	0.451612903
SPU_016738	similar to LOC496031 protein	29	31	1.068965517	0.935483871
SPU_004036	proteasome (prosome, macropain) subunit, alpha type 4	28	30	1.071428571	0.933333333
SPU_003048	WD repeat domain 19	48	30	0.625	1.6

SPU_012850	spermatogenesis-associated 4; testis and spermatogenesis cell related protein 2	16	30	1.875	0.533333333
SPU_012236	hypothetical protein	21	29	1.380952381	0.724137931
SPU_018566	hypothetical protein-917	21	29	1.380952381	0.724137931
SPU_018986	coiled-coil domain containing 42	30	29	0.966666667	1.034482759
SPU_016758	Nucleoside diphosphate kinase B (NDK B) (NDP kinase B) (nm23-M2)(P18)	26	29	1.115384615	0.896551724
XP_001197604.1	hypothetical protein	0	29	-	-
SPU_026899	DYRK2; dual specificity tyrosine phosphorylation regulated kinase 2	14	29	2.071428571	0.482758621
SPU_004377	DLC4	8	29	3.625	0.275862069
SPU_019130	hypothetical protein-147; zonadhesin-like	25	29	1.16	0.862068966
SPU_013660	Puromycin-sensitive aminopeptidase (PSA)	28	28	1	1
SPU_011158	ankyrin repeat domain 45	32	28	0.875	1.142857143
SPU_019458	RAS-Related Protein RAB-2, Sp-RAB2A	16	28	1.75	0.571428571
SPU_027313	hypothetical protein-265; orofacial cleft 1 candidate 1-like; MRDS1 protein-like	27	28	1.037037037	0.964285714
SPU_009484	hypothetical protein	30	28	0.933333333	1.071428571
SPU_002316	Rab10 Like, RAS-Related Protein RAB-10-LIKE	8	27	3.375	0.296296296
XP_001182587.1	similar to LOC495941 protein	18	27	1.5	0.666666667
SPU_000632	human chromosome 10 open reading frame 134-like; enolase	32	27	0.84375	1.185185185
SPU_014364	Rsb-66 protein-like	18	27	1.5	0.666666667
SPU_006214	SOD	15	27	1.8	0.555555556
SPU_023508	RAB, RAS Family-LIKE 5	25	27	1.08	0.925925926
SPU_009378	vitellogenin	23	27	1.173913043	0.851851852
SPU_019734	similar to FLJ46082 protein	15	27	1.8	0.555555556
SPU_002433	armadillo repeat containing 3	22	27	1.227272727	0.814814815
SPU_005867	von Willebrand factor A domain-containing protein 3B	24	27	1.125	0.888888889
SPU_003379	hypothetical protein-1448; WD domain-containing protein	14	27	1.928571429	0.518518519
SPU_025182	Serine/threonine protein phosphatase 2A, catalytic subunit, alpha isoform (PP2A-alpha)	20	27	1.35	0.740740741
SPU_013200	Homo sapiens Tctex1 domain containing 1, TCTEX1D1	20	27	1.35	0.740740741
SPU_016270	glutathione S-transferase theta 1	1	27	27	0.037037037
SPU_024357	centrin-2-like	16	26	1.625	0.615384615
SPU_007125	CAP-binding protein complex interacting protein	30	26	0.866666667	1.153846154
SPU_018419	protein kinase, cAMP dependent regulatory, type II	23	26	1.130434783	0.884615385
SPU_026663	telomerase-associated protein 1-like-6	23	26	1.130434783	0.884615385
XP_793854.2	ropporin-1-like protein	8	26	3.25	0.307692308
SPU_003985	CG1106_PB	35	26	0.742857143	1.346153846
SPU_002535	leucine-rich repeats and guanylate kinase domain containing	31	26	0.838709677	1.192307692

SPU_021701	ubiquitin-activating enzyme E1; ubiquitin-like modifier-activating enzyme 1	34	26	0.764705882	1.307692308
SPU_013103	sperm associated antigen 17	30	26	0.866666667	1.153846154
SPU_028386	intermediate filament tail domain containing 1-like	34	26	0.764705882	1.307692308
SPU_010316	Ci-MORN40/meichroacidin	21	26	1.238095238	0.807692308
SPU_014594	14-3-3 proteins	32	25	0.78125	1.28
SPU_021825	similar to F-box protein 36	7	25	3.571428571	0.28
SPU_005017	phospholipid scramblase 1 - duplicate	11	25	2.272727273	0.44
SPU_018567	dynein light chain 1, cytoplasmic	29	25	0.862068966	1.16
SPU_019125	tetratricopeptide repeat domain 30B	33	25	0.757575758	1.32
SPU_008305	peptidylprolyl isomerase, rotamase, cyclophilin	11	25	2.272727273	0.44
SPU_024911	proteasome (prosome, macropain) 26S subunit, non-ATPase 1-1	12	24	2	0.5
SPU_021793	solute carrier family 8 (sodium/calcium exchanger), member 2	12	24	2	0.5
SPU_008699	ODA-LC7	16	24	1.5	0.666666667
SPU_009071	sperm flagellar 2	27	24	0.888888889	1.125
SPU_004721	Ribosomal protein S27a	12	24	2	0.5
SPU_011663	coiled-coil domain-containing protein 147	23	24	1.043478261	0.958333333
SPU_015172	human chromosome 7 open reading frame 63-1	14	24	1.714285714	0.583333333
SPU_005929	hypothetical protein-1618	19	24	1.263157895	0.791666667
XP_001193466.1	hypothetical protein	16	24	1.5	0.666666667
SPU_028374	hypothetical protein	12	24	2	0.5
SPU_013295	IQ motif containing with AAA domain 1	25	24	0.96	1.041666667
SPU_020389	dynein, axonemal, heavy chain 17	6	24	4	0.25
SPU_018404	calcineurin A	28	24	0.857142857	1.166666667
SPU_023159	tetratricopeptide repeat domain 18-1	44	24	0.545454545	1.833333333
SPU_013368	peroxiredoxin 6; glutathione peroxidase	34	24	0.705882353	1.416666667
NP_999761.1	radial spokehead [Strongylocentrotus purpuratus]	19	23	1.210526316	0.826086957
SPU_027236	Voltage-dependent anion-selective channel protein 2 (VDAC-2)		23	-	-
SPU_019962	telomerase-associated protein 1-like-8	10	23	2.3	0.434782609
SPU_019304	coiled-coil domain containing 146	23	23	1	1
SPU_002234	proteasome 26S ATPase subunit 6, prosome	28	23	0.821428571	1.217391304
XP_001197462.1	hypothetical protein	11	23	2.090909091	0.47826087
SPU_012417	dynein heavy chain domain 3	17	23	1.352941176	0.739130435
SPU_020863	DPY30 domain containing 1	15	23	1.533333333	0.652173913
SPU_010762	RAS-Related Protein RAB-1, RAB1A	22	22	1	1
SPU_000595	elongation factor 1A	4	22	5.5	0.181818182

XP_001197294.1	beta tubulin	20	22	1.1	0.909090909
SPU_006391	human chromosome 20 open reading frame 85-like	21	22	1.047619048	0.954545455
SPU_020748	IQ motif and ubiquitin domain containing	12	22	1.833333333	0.545454545
SPU_022982	Kinesin family member 3B [Homo sapiens]	27	22	0.814814815	1.227272727
SPU_024874	human chromosome 2 open reading frame 39-like	15	22	1.466666667	0.681818182
SPU_006956	serine/threonine protein phosphatase I, catalytic subunit;PP-1; PPP1; PP-1	15	22	1.466666667	0.681818182
SPU_028652	proteasome beta 5 subunit	8	21	2.625	0.380952381
SPU_014398	Carbonyl reductase [NADPH] 1 (NADPH-dependent carbonyl reductase 1)	15	21	1.4	0.714285714
SPU_018139	proteasome (prosome, macropain) subunit, beta type 1; component C5 of proteasome	12	21	1.75	0.571428571
SPU_001153	hypothetical protein	15	21	1.4	0.714285714
SPU_001752	PGP, MDR, PGY	7	21	3	0.333333333
SPU_009164	HSC70	29	21	0.724137931	1.380952381
SPU_023217	Ras-like protein, member RAS oncogene family	19	21	1.105263158	0.904761905
SPU_000191	UMP-CMP (Uridine monophosphate/cytidine monophosphate) kinase;	14	21	1.5	0.666666667
SPU_026491	similar to dpy-30-like protein	20	21	1.05	0.952380952
SPU_008162	hypothetical protein-1769; kinesin-like	12	21	1.75	0.571428571
SPU_023123	Glutamine synthetase (Glutamate--ammonia ligase) (GS)	10	20	2	0.5
SPU_026365	sorcin; grancalcin	24	20	0.833333333	1.2
SPU_010239	hypothetical protein	19	20	1.052631579	0.95
SPU_002850	human chromosome 10 open reading frame 79-like	39	20	0.512820513	1.95
XP_001177916.1	similar to Rtdr1-prov protein	16	20	1.25	0.8
XP_001176624.1	similar to EF-hand calcium binding domain 5	24	20	0.833333333	1.2
SPU_011786	testicular haploid gene product-like	17	20	1.176470588	0.85
SPU_011092	A kinase (PRKA) anchor protein 14	11	20	1.818181818	0.55
SPU_000034	forkhead-associated (FHA) phosphopeptide binding domain 1	30	20	0.666666667	1.5
XP_001190137.1	proteasome-like protein	2	19	9.5	0.105263158
SPU_014431	hypothetical protein	11	19	1.727272727	0.578947368
SPU_022035	dual specificity tyrosine phosphorylation regulated kinase 4	11	19	1.727272727	0.578947368
SPU_024140	proteasome (prosome, macropain) 26S subunit, non-ATPase, 7 (Mov34 homolog)	6	19	3.166666667	0.315789474
SPU_013919	fibronectin type III and ankyrin repeat domains 1	2	19	9.5	0.105263158
SPU_005272	RAS-Related Protein RAB-15	14	19	1.357142857	0.736842105
SPU_008844	protein phosphatase 2 with ef hands; protein phosphatase ef hand calcium binding domain 2	26	18	0.692307692	1.444444444
SPU_026757	hypothetical EF-hand protein	10	18	1.8	0.555555556
SPU_016198	Proteasome 26S ATPase subunit 4; prosome	9	18	2	0.5
XP_780116.2	glyceraldehyde-3-phosphate dehydrogenase-like	18	18	1	1

SPU_019817	LRP2 binding protein	10	18	1.8	0.555555556
SPU_028826	kinesin family member 1A-like	10	18	1.8	0.555555556
XP_783106.2	similar to dynein heavy chain	16	18	1.125	0.888888889
SPU_016156	hypothetical LOC592629	1	18	18	0.055555556
SPU_005779	Sp-Rap1A	9	18	2	0.5
SPU_002937	proteasome (prosome, macropain) subunit alpha type 7	12	18	1.5	0.666666667
SPU_011029	Sp-RhoA/B/C; Sp-Rho1, RAS Homology A	7	18	2.571428571	0.388888889
SPU_017987	ADP-Ribosylation Factor-Like 6	15	18	1.2	0.833333333
SPU_009194	WD repeat-containing protein 65	25	18	0.72	1.388888889
SPU_003894	beta tubulin 5	15	18	1.2	0.833333333
XP_001186396.1	similar to LOC496205 protein	14	17	1.214285714	0.823529412
SPU_001247	proteasome (prosome, macropain) 26S subunit, non-ATPase, 12	15	17	1.133333333	0.882352941
SPU_028599	dynein, axonemal, heavy chain 11	12	17	1.416666667	0.705882353
SPU_010802	leucine-rich repeat-containing protein 51	21	17	0.80952381	1.235294118
SPU_019139	annexin A7	16	17	1.0625	0.941176471
SPU_013202	Intraflagellar transport 172, Wimple, Selective LIM-binding factor	17	17	1	1
SPU_003046	similar to Rtdr1-prov protein	10	17	1.7	0.588235294
SPU_011316	hypothetical protein-1972	6	17	2.833333333	0.352941176
SPU_007504	calcium transporter 2_1; XCAT2 protein-1	17	17	1	1
SPU_025771	Rho GDP disassociation inhibitor	7	17	2.428571429	0.411764706
SPU_026428	PPM serine threonine phosphatase	13	17	1.307692308	0.764705882
SPU_021830	hypothetical protein-2578; peptidase C14, caspase catalytic subunit p20	16	17	1.0625	0.941176471
SPU_011145	Polymerase (RNA) III (DNA directed) polypeptide E	31	17	0.548387097	1.823529412
SPU_009561	WD repeat domain 78-1; dynein intermediate chain-like	19	17	0.894736842	1.117647059
SPU_010511	protein phosphatase 3	12	17	1.416666667	0.705882353
SPU_028660	centrin	7	16	2.285714286	0.4375
SPU_017692	armadillo repeat containing 3	15	16	1.066666667	0.9375
XP_001182731.1	hypothetical protein	10	16	1.6	0.625
SPU_012002	tetratricopeptide repeat domain 21B	21	16	0.761904762	1.3125
SPU_000552	ADP-Ribosylation Factor 1	4	16	4	0.25
SPU_020508	coiled-coil domain containing 108-2	11	16	1.454545455	0.6875
SPU_003847	Proteasome (Prosome, macropain) 26S subunit, ATPase 3	15	16	1.066666667	0.9375
SPU_025435	proteasome (prosome, macropain) 26S subunit, non-ATPase 1	5	16	3.2	0.3125
SPU_023020	telomerase-associated protein 1-like-2	9	16	1.777777778	0.5625
SPU_026963	hypothetical protein-2878	24	16	0.666666667	1.5

SPU_002712	hypothetical protein	22	16	0.727272727	1.375
SPU_022726	similar to ribosomal protein L1	10	16	1.6	0.625
SPU_009006	hypothetical protein-3069	14	16	1.142857143	0.875
SPU_018505	GbetaA, gnb, Gbeta	10	15	1.5	0.666666667
SPU_007058	WD repeat domain 61	10	15	1.5	0.666666667
SPU_028593	ATP-dependent 26S proteasome regulatory subunit	10	15	1.5	0.666666667
XP_797065.2	hypothetical protein	6	15	2.5	0.4
SPU_025307	adenosine kinase	13	15	1.153846154	0.866666667
SPU_013414	Gi, G alpha i, Gnah	9	15	1.666666667	0.6
SPU_010203	HLC-32	0	15	-	-
SPU_025370	Tctex1 domain-containing protein 2	10	15	1.5	0.666666667
SPU_005316	similar to Wiskott-Aldrich syndrome-like	17	15	0.882352941	1.133333333
SPU_026944	Arf1-Like 1, ADP-Ribosylation Factor 1 Like 1	9	15	1.666666667	0.6
SPU_026255	IQ motif and ubiquitin domain containing	26	15	0.576923077	1.733333333
SPU_019233	proteasome (prosome, macropain) 26S subunit, non-ATPase, 14	9	15	1.666666667	0.6
SPU_022537	14-3-3 proteins	18	15	0.833333333	1.2
SPU_012605	casein kinase II alpha subunit	6	15	2.5	0.4
SPU_007485	Gs, G-alpha s, Gnas	9	15	1.666666667	0.6
SPU_017778	hypothetical protein	13	15	1.153846154	0.866666667
XP_001176985.1	hypothetical protein	2	15	7.5	0.133333333
SPU_023334	proliferating cell nuclear antigen	11	15	1.363636364	0.733333333
SPU_020607	gelsolin (amyloidosis, Finnish type)	19	14	0.736842105	1.357142857
SPU_025426	hypothetical protein-1147	9	14	1.555555556	0.642857143
SPU_006443	acid phosphatase 1	12	14	1.166666667	0.857142857
XP_001176541.1	hypothetical protein	11	14	1.272727273	0.785714286
SPU_017032	pyrophosphatase	14	14	1	1
SPU_020730	similar to thioredoxin family Trp26	2	14	7	0.142857143
SPU_025555	ADP-Ribosylation Factor 6	5	14	2.8	0.357142857
SPU_007700	human chromosome 6 open reading frame 103	10	14	1.4	0.714285714
SPU_012606	coiled-coil domain containing 113	19	14	0.736842105	1.357142857
SPU_000178	Epsilon isoform of regulatory subunit B56, protein phosphatase 2A	5	14	2.8	0.357142857
SPU_013628	coiled-coil domain containing 108-1	11	14	1.272727273	0.785714286
SPU_009255	coiled-coil domain containing 135; human chromosome 16 open reading frame 50-like	20	14	0.7	1.428571429
SPU_004882	human chromosome 2 open reading frame 77-like	26	14	0.538461538	1.857142857
SPU_003329	Choline transporter-like protein 2 (Solute carrier family 44 member 2)	8	13	1.625	0.615384615

XP_782050.2	growth arrest-specific protein 8	23	13	0.565217391	1.769230769
SPU_007743	hypothetical protein	19	13	0.684210526	1.461538462
SPU_003162	Arf1-Like 2, ADP-Ribosylation Factor 1-Like 2	3	13	4.333333333	0.230769231
SPU_024912	CapZ	11	13	1.181818182	0.846153846
SPU_006645	GDP dissociation inhibitor 1 - duplicate	15	13	0.866666667	1.153846154
SPU_023889	beta-arrestin 1, beta arr1, arrb1, ArrK, krz, kurtz, arr-1	9	13	1.444444444	0.692307692
SPU_009169	hypothetical protein	6	13	2.166666667	0.461538462
XP_780818.2	WD repeat-containing protein 63	13	13	1	1
XP_001184178.1	similar to LOC553519 protein	11	13	1.181818182	0.846153846
SPU_010221	RasK, Kirsten rat sarcoma viral oncogene homolog	9	13	1.444444444	0.692307692
SPU_020747	axonemal dynein heavy chain 7	15	13	0.866666667	1.153846154
SPU_002460	hydrocephalus-inducing protein	30	13	0.433333333	2.307692308
SPU_005791	IQ motif containing K	2	13	6.5	0.153846154
SPU_003223	intraflagellar transport 81 homolog, carnitine deficiency-associated gene expressed in ventricle 1	17	13	0.764705882	1.307692308
SPU_010337		12	13	1.083333333	0.923076923
SPU_014564	Erythrocyte band 7 integral membrane protein (Stomatin) (Protein 7.2b)	15	13	0.866666667	1.153846154
SPU_024766	hypothetical protein	24	13	0.541666667	1.846153846
SPU_005322	human chromosome X open reading frame 30-like	9	13	1.444444444	0.692307692
SPU_025175	tubulin, alpha 3	12	13	1.083333333	0.923076923
SPU_024152	reverse transcriptase-like-61	9	13	1.444444444	0.692307692
SPU_010897	SNX26, Sorting Nexin 26, TCGAP	5	13	2.6	0.384615385
SPU_014083	coiled-coil domain containing 19	14	12	0.857142857	1.166666667
SPU_001621	grk, bark2, bark, ADRBK	14	12	0.857142857	1.166666667
SPU_008471	outer arm dynein DLC3	14	12	0.857142857	1.166666667
SPU_000503	RAS-Related Protein RAB-11, Sp-RAB11B	11	12	1.090909091	0.916666667
SPU_021592	CPC1, Central Pair Complex 1	12	12	1	1
SPU_013480	NACHT and WD repeat domain-containing protein 1	15	12	0.8	1.25
XP_001183168.1	EF-hand calcium-binding domain-containing protein 6	19	12	0.631578947	1.583333333
IXP_796614.2	similar to tubulin, beta, 2	7	12	1.714285714	0.583333333
SPU_027060	RAS-Related Protein RAB-5, Sp-RAB5B	12	12	1	1
SPU_005868	hypothetical protein LOC200403	17	12	0.705882353	1.416666667
SPU_022172	Cytosolic nonspecific dipeptidase (Glutamate carboxypeptidase-like protein 1) (CNDP dipeptidase 2)	7	12	1.714285714	0.583333333
SPU_026768	hypothetical protein	11	12	1.090909091	0.916666667
SPU_011119	Glucose-6-phosphate isomerase (GPI) (Phosphoglucose isomerase) (PGI)	16	12	0.75	1.333333333
SPU_002035	adenylate kinase 8-like	9	12	1.333333333	0.75

SPU_022187	tubulin, alpha 7	5	12	2.4	0.41666667
XP_001182481.1	hypothetical protein	7	11	1.571428571	0.636363636
SPU_026539	dynein, axonemal, heavy chain 10	8	11	1.375	0.727272727
SPU_006139	hypothetical protein-469; patatin family phospholipase (bacterial)-like	10	11	1.1	0.909090909
SPU_019232		1	11	11	0.090909091
SPU_018584	hypothetical protein-2392; coiled-coil domain containing 74B-like	1	11	11	0.090909091
SPU_009652	aminopeptidase	7	11	1.571428571	0.636363636
SPU_005308	human chromosome 2 open reading frame 63-like	15	11	0.733333333	1.363636364
SPU_008434	Arachidonate 5-lipoxygenase (5-lipoxygenase) (5-LO)	7	11	1.571428571	0.636363636
SPU_016441	Transketolase (TK)	21	11	0.523809524	1.909090909
SPU_027362	Thimet oligopeptidase 1	9	11	1.222222222	0.818181818
SPU_003324	26S proteasome non-ATPase regulatory subunit 4	9	11	1.222222222	0.818181818
SPU_021760	Intraflagellar transport 172, Wimple, Selective LIM-binding factor	11	11	1	1
SPU_009370	human chromosome 3 open reading frame 15-1	18	11	0.611111111	1.636363636
SPU_014566	Erythrocyte band 7 integral membrane protein (Stomatin) (Protein 7.2b)	9	11	1.222222222	0.818181818
SPU_012330	IQ motif containing D	25	11	0.44	2.272727273
SPU_010829	Translational elongation factor 2	18	11	0.611111111	1.636363636
SPU_007117	MORN repeat containing 3	15	11	0.733333333	1.363636364
SPU_000976	proteasome 26S non-ATPase subunit 7	4	11	2.75	0.363636364
SPU_028684	apolipoprotein B	0	11	-	-
SPU_020812	tubulin, alpha 1C	2	11	5.5	0.181818182
SPU_020159	IFT140, Intraflagellar Transport Protein 140	9	11	1.222222222	0.818181818
SPU_004604	Gallus gallus Obg-like ATPase 1	6	11	1.833333333	0.545454545
SPU_017471	proteasome (prosome, macropain) subunit, alpha type 3-1	13	11	0.846153846	1.181818182
XP_802079.1	outer dense fiber protein 3	24	11	0.458333333	2.181818182
SPU_026146	human chromosome 1 open reading frame 177-like	33	11	0.333333333	3
SPU_024507	Skp-1, s-phase kinase-associated protein 1, Cyclin A/CDK2-associated protein p19	7	11	1.571428571	0.636363636
SPU_022939	similar to Caltractin (Centrin)	4	11	2.75	0.363636364
SPU_004585	hypothetical LOC578897	1	11	11	0.090909091
SPU_018101	Rho family orphan 1	7	10	1.428571429	0.7
SPU_003629	hypothetical protein-1464; human chromosome 14 open reading frame 166B-like	5	10	2	0.5
XP_783801.2	uncharacterized protein C20orf26-like	4	10	2.5	0.4
XP_001196943.1	coiled-coil domain-containing protein 147	10	10	1	1
SPU_020695	MORN repeat containing 3	12	10	0.833333333	1.2
SPU_009027	RAS-Related Protein RAB-35	8	10	1.25	0.8

SPU_009992	hypothetical protein	10	10	1	1
SPU_018018	human chromosome 4 open reading frame 47	12	10	0.8333333333	1.2
XP_001183154.1	phospholipid scramblase 2-like	7	10	1.428571429	0.7
SPU_003280	similar to malignant T cell amplified sequence 1	14	10	0.714285714	1.4
SPU_015478	translin-associated factor X interacting protein 1-1	5	10	2	0.5
SPU_027281	Triosephosphate isomerase (TIM) (Triose-phosphate isomerase)	9	10	1.111111111	0.9
SPU_013006	hydrocephalus inducing	28	10	0.357142857	2.8
SPU_022196	hypothetical protein-2602; ankyrin-like	14	10	0.714285714	1.4
SPU_025818	proteasome (prosome, macropain) 26S subunit, non-ATPase, 2-1	13	10	0.769230769	1.3
SPU_000965	hypothetical LOC585129	1	10	10	0.1
SPU_011106	Annexin A4	12	10	0.8333333333	1.2
SPU_000759	proteasome 26S non-ATPase subunit 13 isoform 2	8	10	1.25	0.8
SPU_007014	P-glycoprotein-3	6	10	1.666666667	0.6
SPU_015605	Ras-Related Protein RAB-23-LIKE	15	10	0.666666667	1.5
SPU_012228	Arp2/3	8	10	1.25	0.8
SPU_021029	human chromosome 6 open reading frame 183	5	10	2	0.5
SPU_000056	TPR repeat-containing protein c10orf93	10	10	1	1
SPU_005719	human chromosome 1 open reading frame 125	5	10	2	0.5
SPU_002638	Sp-Rap2C	4	10	2.5	0.4
SPU_010656	NCAG1	4	10	2.5	0.4
SPU_021056	Nucleoside diphosphate kinase NBR-A (NDK NBR-A) (NDP kinase NBR-A)	4	10	2.5	0.4
SPU_007516	myotropin	7	9	1.285714286	0.777777778
SPU_015691	Inositol monophosphatase 1	2	9	4.5	0.222222222
SPU_004349	hypothetical protein	9	9	1	1
SPU_015356	BTB (POZ) domain containing 16; germ cell-less homolog 1 (Drosophila)-like	13	9	0.692307692	1.444444444
SPU_009400	KIFC5	6	9	1.5	0.666666667
SPU_023461	calpain-3 isoform c	9	9	1	1
SPU_025703	grk, bark, ADRBK	8	9	1.125	0.888888889
SPU_010943	singed; actin bundling protein	19	9	0.473684211	2.111111111
SPU_022332	thiopurine S-methyltransferase	4	9	2.25	0.444444444
XP_001181546.1	RIKEN cDNA 4930404H21 gene	4	9	2.25	0.444444444
SPU_009263	glycogen synthase kinase 3 beta	26	9	0.346153846	2.888888889
XP_786996.2	proteasome subunit alpha type-4	8	9	1.125	0.888888889
XP_001175851.1	similar to protein phosphatase 1	7	9	1.285714286	0.777777778
XP_793130.2	similar to Adenylate kinase	8	9	1.125	0.888888889

XP_001197072.1	similar to Na/Ca exchanger	2	9	4.5	0.22222222
SPU_016847	mediator of cell motility 1	7	9	1.285714286	0.77777778
SPU_000145	putative apoptosis-inducing factor, mitochondrion associated 2	12	9	0.75	1.33333333
SPU_023605	FAP80, IFT122A, Intraflagellar Transport Protein 122A	34	9	0.264705882	3.77777778
SPU_023931	proteasome 26S non-ATPase subunit 1	8	9	1.125	0.88888889
SPU_017502	Arp2/3 complex	5	9	1.8	0.55555556
SPU_016161	similar to WD repeat domain 52	17	9	0.529411765	1.88888889
SPU_028912	proteasome subunit p58; proteasome (prosome, macropain) 26S subunit, non-ATPase	7	9	1.285714286	0.77777778
SPU_017072	RAS-Related Protein RAB-8, Sp-RAB8A	5	9	1.8	0.55555556
SPU_010492	human chromosome 14 open reading frame 45	17	9	0.529411765	1.88888889
SPU_025420	human chromosome 10 open reading frame 92-like	12	9	0.75	1.33333333
SPU_008243	human chromosome 10 open reading frame 79	12	9	0.75	1.33333333
XP_001193778.1	hypothetical protein	7	9	1.285714286	0.77777778
SPU_030233	DNAH14, DHC5B, Sp-DNAH14, axonemal dynein	3	9	3	0.33333333
SPU_017815	WD repeat domain 52	2	9	4.5	0.22222222
XP_001200629.1	hypothetical protein	4	9	2.25	0.44444444
SPU_024596	dynein, axonemal, heavy chain 8-like-1	3	9	3	0.33333333
SPU_019788	ribosomal protein L27	0	9	-	-
SPU_002939	neurofilament heavy polypeptide	12	9	0.75	1.33333333
SPU_006879	tubulin beta-2C	8	9	1.125	0.88888889
SPU_026177	integrator complex subunit 6	10	9	0.9	1.11111111
SPU_008000	ODA-DC3	4	8	2	0.5
SPU_026866	KIAA1529 protein-like-3	9	8	0.88888889	1.125
SPU_024961	hypothetical protein-2760	8	-	-	-
SPU_017347	GDP-mannose 4,6 dehydratase (GDP-D-mannose dehydratase) (GMD)	10	8	0.8	1.25
SPU_014463	IQ motif containing H; protein kinase NYD-SP5	7	8	1.142857143	0.875
SPU_007884	adenylate kinase 8-like	10	8	0.8	1.25
SPU_011581	hypothetical protein-72	6	8	1.33333333	0.75
SPU_010977	4930451C15Rik protein	0	8	-	-
SPU_000513	Sp-urchin dual oxidase	2	8	4	0.25
SPU_005509	kinesin family member 3A [Homo sapiens]	5	8	1.6	0.625
SPU_011353	kinesin family member 13A [Homo sapiens]	7	8	1.142857143	0.875
SPU_008114	hypothetical protein	7	8	1.142857143	0.875
SPU_019491	hypothetical protein	10	8	0.8	1.25
SPU_020833	nuclear transport factor 2	7	8	1.142857143	0.875

XP_001182314.1	radial spoke head 10	14	8	0.571428571	1.75
SPU_018598	UBE2N	11	8	0.727272727	1.375
SPU_016045	cAMP-dependent protein kinase A catalytic subunit	7	8	1.142857143	0.875
SPU_021809	Forkhead-associated domain-containing protein 1	14	8	0.571428571	1.75
SPU_012611	Neurotensin endopeptidase, Mitochondrial oligopeptidase M, Microsomal endopeptidase	3	8	2.666666667	0.375
SPU_026433	human chromosome 10 open reading frame 123-like	16	8	0.5	2
SPU_015907	similar to Wiskott-Aldrich syndrome-like	7	8	1.142857143	0.875
XP_001190661.1	serine/threonine protein kinase	2	8	4	0.25
SPU_009254	hypothetical protein	9	8	0.888888889	1.125
SPU_011989	coiled-coil domain containing 19	4	8	2	0.5
SPU_013387	human chromosome 6 open reading frame 103-like; calpain family cysteine protease domain-containing	14	8	0.571428571	1.75
SPU_000446	protein ADRM1 (adhesion-regulating molecule 1), putative ARM-1 protein	2	8	4	0.25
SPU_025472	ubiquitin-activating enzyme E1-like 2	5	8	1.6	0.625
SPU_027825	hypothetical protein-1215	9	8	0.888888889	1.125
SPU_001411	hypothetical protein-1325; RAB9A, member RAS oncogene family-like	5	8	1.6	0.625
SPU_021350	long transient receptor potential channel 3	8	8	1	1
XP_001192985.1	dynein light chain 1 (LRR-DLC), axonemal	3	8	2.666666667	0.375
SPU_010580	ubiquitin-conjugating enzyme	4	8	2	0.5
SPU_026858	ropporin	6	8	1.333333333	0.75
SPU_014869	Thioredoxin peroxidase 2, Thioredoxin-dependant peroxide reductase 2	3	8	2.666666667	0.375
SPU_008543	Alcohol dehydrogenase [NADP+] (Aldo-keto reductase family 1, member A1) (aldehyde reductase)	6	7	1.166666667	0.857142857
XP_781655.2	hydrocephalus-inducing protein	6	7	1.166666667	0.857142857
XP_001186505.1	GDP-dissociation inhibitor	11	7	0.636363636	1.571428571
XP_001177076.1	similar to Proteasome (prosome, macropain) subunit, beta type, 1	2	7	3.5	0.285714286
SPU_009022	spermatogenesis associated 4	3	7	2.333333333	0.428571429
SPU_021034	coiled-coil domain containing 37	9	7	0.777777778	1.285714286
SPU_025962	annexin A7-2	7	7	1	1
XP_001197593.1	proteasome subunit alpha type-7	2	7	3.5	0.285714286
SPU_026993	hippocalcin-like 1	8	7	0.875	1.142857143
SPU_025490	similar to RIKEN cDNA 4930415O20	7	7	1	1
SPU_017631	hypothetical protein-2348	7	7	1	1
SPU_016763	casein kinase II beta isoform 1	8	7	0.875	1.142857143
SPU_016555	fibrillin-2-like	12	7	0.583333333	1.714285714
SPU_013538	testis development protein NYD-SP29	5	7	1.4	0.714285714
SPU_006716	hypothetical protein-491	2	7	3.5	0.285714286

SPU_026571	KIAA1992 protein; tetratricopeptide repeat domain 21B	20	7	0.35	2.857142857
SPU_022266	calmoddulin	5	7	1.4	0.714285714
SPU_004813		0	7	-	-
SPU_014567	Erythrocyte band 7 integral membrane protein (Stomatin) (Protein7.2b)	10	7	0.7	1.428571429
SPU_015240	HEAT repeat containing 4-2	5	7	1.4	0.714285714
SPU_018636	arachidonate 5-lipoxygenase-8	5	7	1.4	0.714285714
SPU_013770	Adenosylhomocysteinase 1 (S-adenosyl-L-homocysteine hydrolase 1) (ADOHCYASE 1)	21	7	0.333333333	3
gi 115668824 ref XP_0 similar to calcium transporter 2		5	7	1.4	0.714285714
SPU_023066		0	7	-	-
SPU_013856	ubiquitin specific protease 14	12	7	0.583333333	1.714285714
SPU_000508	GbetaA, gnb, Gbeta	2	7	3.5	0.285714286
SPU_014344	ADP_ribosyl_GH superfamily	14	7	0.5	2
SPU_030225	DNAH3, DHC7B, axonemal dynein	4	7	1.75	0.571428571
SPU_000060	ankyrin repeat domain-containing protein 42	4	7	1.75	0.571428571
SPU_010738		0	7	-	-
SPU_006261	Adenine phosphoribosyltransferase (APRT)	3	7	2.333333333	0.428571429
SPU_025198	myc-binding protein-associated protein; MYCBP associated protein	16	7	0.4375	2.285714286
SPU_023221	Tctex2-related dynein light chain	7	7	1	1
SPU_016106	ankyrin superfamily	1	7	7	0.142857143
SPU_026331	human chromosome 1 open reading frame 125-like	15	7	0.466666667	2.142857143
SPU_007145	hypothetical protein-507; ubiquitin-protein ligase (Tom1)-like	5	7	1.4	0.714285714
XP_790497.2	leucine-rich repeat-containing protein 71	10	7	0.7	1.428571429
XP_001197263.1	similar to major yolk protein precursor	0	7	-	-
SPU_024936	tubulin, beta, 2	5	7	1.4	0.714285714
SPU_013076	uncharacterized protein C1orf194	3	7	2.333333333	0.428571429
SPU_005542	ankyrin2,3/unc44-278	7	7	1	1
SPU_018822	hypothetical protein LOC757406	0	6	-	-
SPU_015312	Rab23 Like, RAS-Related Protein RAB-23-LIKE	8	6	0.75	1.333333333
SPU_007550		0	6	-	-
SPU_018376	hypothetical LOC581148	0	6	-	-
SPU_005804	hypothetical protein-1603; coiled-coil domain containing 27-like	9	6	0.666666667	1.5
SPU_009781	NACHT and WD repeat domain containing 1-1	2	6	3	0.333333333
SPU_013287	calcium and integrin binding protein CIB	2	6	3	0.333333333
SPU_019300	N-ethylmaleimide sensitive fusion protein attachment protein alpha, alpha-SNAP	6	6	1	1
SPU_015508	unnamed protein product	8	6	0.75	1.333333333

SPU_000663	Dual specificity protein phosphatase 24	14	6	0.428571429	2.333333333
SPU_008443	P-glycoprotein-3	6	6	1	1
SPU_028917	Glycerol-3-phosphate dehydrogenase [NAD+], cytoplasmic (GPD-C) (GPDH-C)	3	6	2	0.5
SPU_008799	dynein light chain Type 1	10	6	0.6	1.666666667
SPU_011239	Intraflagellar transport 80 homolog (WD-repeat protein 56) [Homo sapiens]	17	6	0.352941176	2.833333333
SPU_017466	malignant T cell amplified sequence 1	8	6	0.75	1.333333333
SPU_027227	Intraflagellar transport 20	11	6	0.545454545	1.833333333
SPU_017225	similar to rhopty protein	12	6	0.5	2
SPU_004076	hypothetical protein	5	6	1.2	0.833333333
SPU_002507	Ras-associated protein Rap1	3	6	2	0.5
SPU_002164	122C, DUF590	3	6	2	0.5
XP_001180380.1	NACHT and WD repeat domain-containing protein 1	5	6	1.2	0.833333333
SPU_017612	phosphodiesterase 6D, retinal rod rhodopsin-sensitive cGMP 3',5'-cyclic phosphodiesterase subunit delta	2	6	3	0.333333333
SPU_001788	Serine/threonine protein phosphatase PP1-beta catalytic subunit (PP-1B)	5	6	1.2	0.833333333
XP_001195864.1	similar to LOC414565 protein	0	6	-	-
SPU_002694	glutathione S-transferase class-alpha	7	6	0.857142857	1.166666667
SPU_006321	telomerase-associated protein 1-like-7	4	6	1.5	0.666666667
XP_001192237.1	dynein, axonemal, heavy chain 5	2	6	3	0.333333333
XP_001185449.1	GDP-mannose 4,6 dehydratase	5	6	1.2	0.833333333
SPU_022072	Histone H4	0	6	-	-
SPU_010637	WD repeat domain 35; flagellar associated protein (Chlamydomonas)-like	26	6	0.230769231	4.333333333
SPU_000253	Ras-associated protein Rap1-LIKE 1	1	6	6	0.166666667
SPU_011157	RAS-Related Protein RAB-14	7	6	0.857142857	1.166666667
SPU_008319	hypothetical protein LOC561722	3	6	2	0.5
SPU_022268	ankyrin repeat domain 5	6	6	1	1
SPU_024958	hypothetical protein-222	4	6	1.5	0.666666667
XP_001181406.1	proteasomal ubiquitin receptor ADRM1-like	1	6	6	0.166666667
SPU_012542	Calcium binding protein 39 (Mo25 protein)	12	6	0.5	2
XP_001187936.1	ATP-binding cassette transporter subfamily A	6	6	1	1
SPU_004874	hypothetical protein-433	1	6	6	0.166666667
SPU_002459	similar to MGC68877 protein	5	6	1.2	0.833333333
SPU_012471	Dihydrofolate reductase	6	6	1	1
SPU_012112	Rab5 Like, RAS-Related Protein RAB-5 Like	6	6	1	1
SPU_016429	DLEC1 protein; deleted in lung and esophageal cancer 1	8	6	0.75	1.333333333
SPU_002490	6-phosphogluconolactonase (6PGL)	5	6	1.2	0.833333333

SPU_007129	membrane-type 1 matrix metalloproteinase cytoplasmic tail binding protein-1 like	6	6	1	1
SPU_005469	N-acetylneuraminc acid phosphate synthase	4	6	1.5	0.66666667
SPU_017462	aspartate aminotransferase 1; glutamic-oxaloacetic transaminase 1, soluble	18	6	0.333333333	3
XP_001181395.1	similar to arginine kinase	3	6	2	0.5
SPU_005437	UPF0732 protein v1g81173-like	3	6	2	0.5
SPU_010436	similar to LOC365476 protein	24	6	0.25	4
SPU_021651	Intraflagellar transport 172, Wimple, Selective LIM-binding factor	12	6	0.5	2
SPU_027840	dynein heavy chain 8, axonemal	7	6	0.857142857	1.16666667
XP_001179561.1	similar to ATP-binding cassette transporter subfamily A	3	6	2	0.5
SPU_016790	Sp-Rac1/2/3	4	6	1.5	0.66666667
SPU_002101	KIAA1529-like	6	6	1	1
SPU_003506	hydrocephalus inducing homolog (mouse)-3	4	6	1.5	0.66666667
XP_790174.2	uncharacterized protein KIAA1751 homolog	8	6	0.75	1.33333333
SPU_022529	thioredoxin peroxidase, Thiol-specific antioxidant protein	1	6	6	0.16666667
SPU_010886	dynein, axonemal, heavy chain 7A	6	6	1	1
SPU_018965	uncharacterized protein LOC580808	3	6	2	0.5
SPU_015797	hypp-115; neuron navigator 2-like; neuron navigator 3-like	3	6	2	0.5
SPU_018240	3-oxo-5-alpha-steroid 4-dehydrogenase 1 (Steroid 5-alpha-reductase 1) (SR type 1) (S5AR)	7	6	0.857142857	1.16666667
SPU_009464	hypothetical protein-47; centromere-binding protein-like	7	6	0.857142857	1.16666667
SPU_010396	tubulin, beta 4	15	6	0.4	2.5
SPU_007820	histone H3	0	5	-	-
XP_780182.2	protein phosphatase with EF-hand	2	5	2.5	0.4
SPU_005032	calmodulin	9	5	0.555555556	1.8
XP_001176581.1	similar to MGC69420 protein	0	5	-	-
SPU_028506	puromycin-sensitive aminopeptidase	3	5	1.66666667	0.6
SPU_025585	TIP120 protein	4	5	1.25	0.8
SPU_019558	Arl13b, ADP-Ribosylation Factor-Like 2 Like 1	7	5	0.714285714	1.4
SPU_006767	Sp-Sar1b, Sp-Sara2, Sar1a gene homolog 2	0	5	-	-
SPU_024343	histone	0	5	-	-
SPU_001818	Ras-like protein enriched in brain 2	4	5	1.25	0.8
SPU_020184	reverse transcriptase-like-49	2	5	2.5	0.4
SPU_020097	human chromosome 1 open reading frame 173-like	15	5	0.333333333	3
SPU_013016	N-myc downstream regulated gene 1	4	5	1.25	0.8
SPU_020140	programmed cell death 6 interacting protein	8	5	0.625	1.6
SPU_020452	Glucose regulated protein	3	5	1.66666667	0.6

SPU_006852	Thymidylate synthase (TS) (TSase)	5	5	1	1
SPU_001062	Skp1/Elongin C	11	5	0.454545455	2.2
NP_999710.2	histone H2B	0	5	-	-
SPU_009451	spermatogenesis associated 6-like	2	5	2.5	0.4
SPU_003731	Glyoxylate reductase/hydroxypyruvate reductase	2	5	2.5	0.4
SPU_028894	retinitis pigmentosa (autosomal dominant); retinitis pigmentosa RP1 protein	8	5	0.625	1.6
SPU_020435	hexokinase I	6	5	0.833333333	1.2
SPU_011920	transcription elongation factor B (SIII)	4	5	1.25	0.8
SPU_008574	hypothetical protein-1794; patatin (bacterial)-like	8	5	0.625	1.6
SPU_018233	tetratricopeptide repeat domain 26	6	5	0.833333333	1.2
SPU_027647	ATP-binding cassette, sub-family B (MDR/TAP), member 1B-3	1	5	5	0.2
SPU_019136	uncharacterized protein LOC752384	6	5	0.833333333	1.2
SPU_011446	Bardet-Biedl syndrome 1 protein	6	5	0.833333333	1.2
SPU_007332	ankyrin2,3/unc44-like-58	9	5	0.555555556	1.8
SPU_015573	ATP-binding cassette transporter 1	1	5	5	0.2
SPU_016327	Peptidase_M49	7	5	0.714285714	1.4
SPU_026062	similar to RIKEN cDNA 3100002J23 gene	1	5	5	0.2
SPU_028358	Aldo keto reductase, AKR fragment	0	5	-	-
SPU_021207	Phosphodiesterase 8A, isoform 1	0	5	-	-
SPU_008490	human chromosome 1 open reading frame 222-like	7	5	0.714285714	1.4
XP_796198.2	similar to LOC365476 protein	16	5	0.3125	3.2
SPU_012795	hypothetical protein-2050; human chromosome 6 open reading frame 103-like	5	5	1	1
SPU_020429	RAS-Related Protein RAB-28	5	5	1	1
SPU_009878	CaM kinase-like 3	2	5	2.5	0.4
SPU_015669	hypothetical protein-797; cathepsin-like	7	5	0.714285714	1.4
SPU_007155	Glyceraldehyde-3-phosphate dehydrogenase (GAPDH)	9	5	0.555555556	1.8
XP_785052.2	coiled-coil domain-containing protein 147	7	5	0.714285714	1.4
SPU_027631	End Binding Protein 1	2	5	2.5	0.4
SPU_028434	dynein heavy chain 14	1	5	5	0.2
SPU_007319	cytochrome b5 domain containing 1	5	5	1	1
SPU_026843	echinonectin-43	2	5	2.5	0.4
SPU_014715	Gelsolin	4	5	1.25	0.8
SPU_027893	IQ motif containing G	7	5	0.714285714	1.4
SPU_005869	hypothetical protein-465	6	5	0.833333333	1.2
SPU_010531	tubulin alpha-1C	0	5	-	-

SPU_010118	MAPK14, p38 alpha	2	5	2.5	0.4
XP_001177415.1	similar to HLC-32	0	5	-	-
SPU_020282	Intraflagellar transport 88, tetratricopeptide repeat domain 10 (TTC10), TG737, Polaris	8	5	0.625	1.6
SPU_014107	sperm flagellar 2-1	10	5	0.5	2
SPU_014562	Erythrocyte band 7 integral membrane protein (Stomatin) (Protein 7.2b)	8	5	0.625	1.6
SPU_000795	Tctex1 outer arm dynein light chain	6	5	0.833333333	1.2
SPU_004764	arachidonate 12-lipoxygenase, 12R type-like	2	5	2.5	0.4
SPU_006392	RAS-Related Protein RAB-33	7	5	0.714285714	1.4
SPU_005922	hypothetical protein-1616; telomerase-associated protein 1-like	2	5	2.5	0.4
XP_001181510.1	ubiquitin-conjugating enzyme E2 variant 2	3	5	1.666666667	0.6
SPU_007977	ketanin p60 subunit A-like 2	3	5	1.666666667	0.6
SPU_020621	axonemal dynein heavy chain DNAH5	3	5	1.666666667	0.6
SPU_000003	hypothetical protein-1239	6	5	0.833333333	1.2
SPU_015431	ankyrin2,3/unc44-like-108	6	5	0.833333333	1.2
SPU_026704	human chromosome X open reading frame 30-like-1	8	5	0.625	1.6
SPU_003378	zf-C2H2	1	5	5	0.2
SPU_001176	zinc finger protein 862-2	5	5	1	1
SPU_004774	hypothetical protein-1543	1	5	5	0.2
SPU_023380	SEC14-like protein 2 (Alpha-tocopherol associated protein) (TAP) (hTAP)	8	5	0.625	1.6
SPU_009119	pol polyprotein like-252	7	5	0.714285714	1.4
SPU_012282	actin	1	4	4	0.25
SPU_004242	Argininosuccinate synthase (Citrulline--aspartate ligase)	6	4	0.666666667	1.5
SPU_025823	uncharacterized protein LOC100892708	1	4	4	0.25
SPU_001513	thioredoxin-like 1, various isoforms	3	4	1.333333333	0.75
SPU_028375	golgi phosphoprotein 3	1	4	4	0.25
XP_001183497.1	LRP2-binding protein	3	4	1.333333333	0.75
SPU_024014	similar to hypothetical protein LOC28989	10	4	0.4	2.5
SPU_024773	all-trans retinol dehydrogenase	1	4	4	0.25
SPU_014790	protein phosphatase 1, regulatory subunit 7; yeast sds22 homolog	6	4	0.666666667	1.5
SPU_002304	von Willebrand factor A domain-containing protein 3A	5	4	0.8	1.25
SPU_013929	RAS-Related Protein RAB-10	3	4	1.333333333	0.75
XP_001178733.1	hypothetical protein	2	4	2	0.5
SPU_026430	proteasome (prosome, macropain) subunit, alpha type, 2(psma2	0	4	-	-
SPU_011107	annixin	3	4	1.333333333	0.75
SPU_026381	polycystic kidney and hepatic disease 1-like 1	5	4	0.8	1.25

SPU_009066	S-methyl-5-thiadenosine phosphorylase (5'-methylthiadenosine phosphorylase)	11	4	0.363636364	2.75
SPU_004856	acetyl-Coenzyme A acetyltransferase 3	0	4	-	-
SPU_013172	adhesion receptor	4	4	1	1
SPU_021944	KIAA1095 protein-like; PDZ domain containing ring finger 3-like; TNF receptor-associated factor 6-like	0	4	-	-
SPU_008266	Heat shock protein beta-11	2	4	2	0.5
SPU_028887	cystatin-A2-like	1	4	4	0.25
XP_797673.1	leucine rich repeat containing 48	0	4	-	-
SPU_021236	Rab-like protein 4, RAYL	3	4	1.333333333	0.75
SPU_011785	uncoordinated locomotion-89, kinesin-like motor protein	5	4	0.8	1.25
SPU_007821	similar to LOC495986 protein	1	4	4	0.25
XP_779975.2	YKT6 v-SNARE protein	6	4	0.666666667	1.5
SPU_018479	Cell Division Cycle 42-LIKE	1	4	4	0.25
XP_001186225.1	hypothetical protein	3	4	1.333333333	0.75
SPU_012828	Ubiquitin-conjugating enzyme E2 L3	3	4	1.333333333	0.75
XP_001193460.1	dynein, cytoplasmic, light polypeptide 2A	5	4	0.8	1.25
XP_787940.2	voltage-dependent T-type calcium channel alpha-1	6	4	0.666666667	1.5
SPU_023692	ribosomal protein L18a	0	4	-	-
SPU_005519	ADP-Ribosylation Factor-Like1	4	4	1	1
SPU_010799	cyclin-dependent kinase-like 1, cell division cycle 2-related	0	4	-	-
SPU_015915	PF6 central apparatus protein	5	4	0.8	1.25
SPU_021306	similar to hypothetical protein LOC152940	2	4	2	0.5
SPU_006503	hippocalcin-like 1	3	4	1.333333333	0.75
XP_001179206.1	MORN repeat-containing protein 5	3	4	1.333333333	0.75
SPU_027579	RIB43A-like with coiled-coils protein 2	4	4	1	1
SPU_003898	Gq, G alpha q, Gnaq	4	4	1	1
SPU_009549	syndecan-binding protein prov protein (syntenin)	0	4	-	-
XP_001192105.1	hypothetical protein	0	4	-	-
SPU_017701	NACHT and WD repeat domain containing 1	17	4	0.235294118	4.25
SPU_019393	small fragment nuclease	0	4	-	-
SPU_004561	phosphoglutamase 1	1	4	4	0.25
SPU_012817	Phosphoglycerate kinase 1 (Primer recognition protein 2) (PRP 2)	9	4	0.444444444	2.25
SPU_020719	human chromosome 1 open reading frame 201	2	4	2	0.5
SPU_008872	coiled-coil domain containing 96	8	4	0.5	2
SPU_000742	Uev1a	3	4	1.333333333	0.75
SPU_017173	dynein, axonemal, heavy chain 9-like	7	4	0.571428571	1.75

XP_001179205.1	kinesin-like protein KIF17-like	5	4	0.8	1.25
SPU_028068	KCNMA1	4	4	1	1
SPU_015709	DCN1, defective in cullin neddylation 1, domain containing 1	2	4	2	0.5
SPU_009964	Protein phosphatase 2B regulatory subunit 1, Protein phosphatase 3 regulatory subunit B alpha isoform 1	9	4	0.444444444	2.25
SPU_004558	uncharacterized protein LOC755292	8	4	0.5	2
SPU_017972	Sp-Ral1, Ras like protein A	3	4	1.333333333	0.75
SPU_006445	PAF acetylhydrolase 29 kDa subunit	2	4	2	0.5
SPU_028357	WD repeat domain 1; actin interacting protein 1 [Xenopus laevis]	6	4	0.666666667	1.5
SPU_013756	peptidylprolyl isomerase B; peptidyl-prolyl cis-trans isomerase B	0	4	-	-
SPU_007813	hypothetical protein-527	0	4	-	-
XP_001192126.1	intraflagellar transport protein 140	5	4	0.8	1.25
SPU_021203	aminotransferase (mosquito)-like	3	4	1.333333333	0.75
SPU_028665	usherin	0	4	-	-
SPU_000707	S1 RNA binding domain 1	3	4	1.333333333	0.75
SPU_019591	Tektin1-2	11	4	0.363636364	2.75
SPU_012149	Glutathione S-transferase alpha-4	4	4	1	1
SPU_010980	arachidonate 5-lipoxygenase-6	24	4	0.166666667	6
SPU_020363	endo-beta-N-acetylglucosaminidase; cytosolic endo-beta-N-acetylglucosaminidase	5	4	0.8	1.25
SPU_003119	alpha isoform of regulatory subunit B55, protein phosphatase 2	2	4	2	0.5
XP_001177943.1	ADP-ribosylation factor-like 8B	1	4	4	0.25
SPU_017444	ADP-ribosylarginine hydrolase-2	1	4	4	0.25
SPU_017469	ATP-binding cassette, sub-family E (OABP)	0	4	-	-
XP_791435.2	adenylate kinase 8-like	4	4	1	1
SPU_025822	hypothetical protein-2803	1	4	4	0.25
SPU_012923	human chromosome 10 open reading frame 93	7	4	0.571428571	1.75
SPU_006037	Glycine N-methyltransferase (Folate-binding protein)	0	4	-	-
SPU_024670	proteasome (prosome, macropain) 26S subunit, ATPase 2, 26S protease regulatory subunit 7, Ms1	9	4	0.444444444	2.25
SPU_017819	human chromosome 14 open reading frame 50	1	4	4	0.25
SPU_004750	acyl-CoA synthetase bubblegum family member 1	3	4	1.333333333	0.75
SPU_015400	ankyrin2,3/unc44-308	0	4	-	-
SPU_008008	similar to mal5	1	4	4	0.25
SPU_025682	ring finger and SPRY domain containing 1 like	5	4	0.8	1.25
SPU_017780	leucine rich repeat containing 67	1	4	4	0.25
SPU_028057	dynein, axonemal, heavy chain 17-like	3	4	1.333333333	0.75
SPU_022153	CKI alpha, casein kinase I alpha	0	4	-	-

SPU_025320	UTP20, small subunit (SSU) processome component, homolog (yeast) like-2	3	4	1.333333333	0.75
XP_001186628.1	hypothetical protein	0	4	-	-
XP_783211.2	ankyrin repeat domain-containing protein 50	1	4	4	0.25
SPU_010266	amiloride-sensitive cation channel 2, neuronal	5	4	0.8	1.25
SPU_008067	uncharacterized protein LOC763602	1	4	4	0.25
SPU_009483	CyIIb	5	4	0.8	1.25
SPU_017363	DNA replication helicase 2 homolog (yeast)	2	4	2	0.5
XP_798615.2	uncharacterized protein LOC587715	8	3	0.375	2.66666667
SPU_008645	platelet-activating factor acetylhydrolase 1-like	0	3	-	-
XP_001178110.1	hypothetical protein	0	3	-	-
SPU_009009	coiled-coil domain containing 108	2	3	1.5	0.66666667
SPU_019387	RAS-Related Protein RAB-32	3	3	1	1
SPU_003074	leucine rich repeat containing 69	5	3	0.6	1.66666667
SPU_002998	Hypoxanthine-guanine phosphoribosyltransferase (HGPRT) (HGPRTase)	3	3	1	1
SPU_013838	electron-transfer-flavoprotein, alpha polypeptide	0	3	-	-
SPU_028857	Carbonyl reductase 3	4	3	0.75	1.33333333
SPU_022924	Glyoxylate reductase/hydroxypyruvate reductase	2	3	1.5	0.66666667
SPU_001218	uncharacterized protein LOC574562	2	3	1.5	0.66666667
SPU_027507	uncharacterized protein LOC580256	5	3	0.6	1.66666667
NP_999742.1	metallothionein-A	2	3	1.5	0.66666667
SPU_022991	Rab21 Like, RAS-Related Protein RAB-21 LIKE	2	3	1.5	0.66666667
XP_794667.2	cAMP-dependent protein kinase catalytic subunit-like 2	2	3	1.5	0.66666667
XP_001203167.1	tetratricopeptide repeat domain 26	1	3	3	0.33333333
SPU_024431	lambda-crystallin	6	3	0.5	2
SPU_010876	SpPKC1, cPKC, conventional PKC, protein kinase C	3	3	1	1
SPU_023430	arachidonate 5-lipoxygenase-9	2	3	1.5	0.66666667
SPU_024413	Plant cadmium resistance 3-like	0	3	-	-
SPU_006679	N-acetyltransferase 11	1	3	3	0.33333333
SPU_001909	LanC lantibiotic synthetase component C-like 3	2	3	1.5	0.66666667
SPU_002189	ArfGAP superfamily, PH-like superfamily	7	3	0.428571429	2.33333333
SPU_005978	Mannose-6-phosphate isomerase (Phosphomannose isomerase) (PMI) (Phosphohexomutase)	5	3	0.6	1.66666667
SPU_025413	c-Myc-binding protein	5	3	0.6	1.66666667
SPU_018047	proteasome subunit alpha type 7	4	3	0.75	1.33333333
SPU_000411	tubulin beta-2C	1	3	3	0.33333333
SPU_021702	ribosomal protein L11 - duplicate	0	3	-	-

XP_001177275.1	gelsolin	7	3	0.428571429	2.333333333
SPU_000091	fimbrin, isoform A	1	3	3	0.333333333
SPU_007250	WD repeat domain 19-1; WD repeat membrane protein	5	3	0.6	1.666666667
XP_793431.2	Tetratricopeptide repeat domain 21B	4	3	0.75	1.333333333
XP_001180090.1	glutamate-cysteine ligase modifier subunit	2	3	1.5	0.666666667
SPU_002227	protein pitchfork-like	3	3	1	1
SPU_018981	ARL11-Like 2, ADP-Ribosylation Factor-Like 11 LIKE 2	4	3	0.75	1.333333333
XP_001182996.1	flocculin-like protein	0	3	-	-
SPU_010443	ankyrin and armadillo repeat containing	11	3	0.272727273	3.666666667
SPU_018316	similar to 11R-lipoxygenase	4	3	0.75	1.333333333
SPU_019590	intraflagellar transport 52 homolog (Chlamydomonas)-1	10	3	0.3	3.333333333
SPU_004938	similar to Prohibitin-2	0	3	-	-
SPU_009686	B-cell receptor associated protein (LOC575755)	1	3	3	0.333333333
SPU_018717	actin-related protein 2 isoform a	10	3	0.3	3.333333333
SPU_011022	discs large	0	3	-	-
SPU_018369	Arp2/3 complex	1	3	3	0.333333333
SPU_005605	human chromosome 12 open reading frame 63-like	8	3	0.375	2.666666667
SPU_012598	PREDICTED: similar to WD repeat domain 56 [Strongylocentrotus purpuratus]	8	3	0.375	2.666666667
SPU_005282	human chromosome 14 open reading frame 166B	15	3	0.2	5
XP_001199021.1	uncharacterized protein LOC763141	5	3	0.6	1.666666667
SPU_007441	similar to MGC139263 protein	1	3	3	0.333333333
SPU_014399	Carbonyl reductase [NADPH] 1 (NADPH-dependent carbonyl reductase 1)	1	3	3	0.333333333
SPU_002678	primary ciliary dyskinesia protein 1	2	3	1.5	0.666666667
SPU_003409	human chromosome 19 open reading frame 45-like	0	3	-	-
SPU_016277	ATP-binding cassette sub-family A member 3 (ATP-binding cassette transporter 3)	0	3	-	-
SPU_014770	telomerase-associated protein 1	4	3	0.75	1.333333333
SPU_019927	TNF receptor-associated factor 3 interacting protein 1	5	3	0.6	1.666666667
SPU_018575	TNF receptor-associated factor 3 interacting 1	1	3	3	0.333333333
SPU_010691	DEAD (Asp-Glu-Ala-Asp) box polypeptide 3, Y-linked	1	3	3	0.333333333
SPU_026895	uncharacterized protein LOC587261	2	3	1.5	0.666666667
SPU_022648	ubiquitin-conjugating enzyme E2G 1	2	3	1.5	0.666666667
NP_999644.1	calmodulin-binding carboxy-terminal kinesin	1	3	3	0.333333333
SPU_002491	6-phosphogluconolactonase (6PGL)	4	3	0.75	1.333333333
SPU_023560	kinesin family member 1B [Homo sapiens], kinesin family member 1Bbeta isoform 1 [Homo sapiens]	4	3	0.75	1.333333333
XP_795619.2	Translationally-controlled tumor protein homolog	4	3	0.75	1.333333333

SPU_012909	eukaryotic translation initiation factor 6	6	3	0.5	2
XP_788383.2	oublecortin domain-containing protein 5	3	3	1	1
SPU_007655	Cyclin-dependent protein kinase 2, Cell division protein kinase 2, EC 2.7.1.37	4	3	0.75	1.333333333
XP_001191065.1	uncharacterized protein LOC764814	5	3	0.6	1.666666667
SPU_010631	arp 3	3	3	1	1
SPU_002855	hypothetical protein	4	3	0.75	1.333333333
SPU_007036	vacuolar protein sorting 35 homolog (S. cerevisiae)	4	3	0.75	1.333333333
SPU_012023	hypothetical protein-2013	4	3	0.75	1.333333333
SPU_027527	Hatpase	0	3	-	-
SPU_011700	nasal embryonic LHRH factor	6	3	0.5	2
SPU_004893	alanyl-tRNA synthetase	10	3	0.3	3.333333333
SPU_005840	telomerase-associated protein 1-like-5	3	3	1	1
SPU_002909	Glutamate--cysteine ligase regulatory subunit (Gamma-glutamylcysteine synthetase)	0	3	-	-
SPU_020991	uncharacterized protein LOC587107	4	3	0.75	1.333333333
SPU_012488	Dihydropteridine reductase (DHPR) (Quinoid dihydropteridine reductase)	3	3	1	1
SPU_002761	hypothetical protein-1412	0	3	-	-
SPU_023557	axonemal dynein heavy chain 6	5	3	0.6	1.666666667
SPU_011031	Rho related BTB domain containing protein 3	1	3	3	0.333333333
SPU_004107	Sp-Sarm-related 12	1	3	3	0.333333333
SPU_004780	thioredoxin reductase 3-like; thioredoxin and glutathione reductase-like	0	3	-	-
XP_783551.2	hypothetical protein	3	3	1	1
SPU_019223	hypothetical protein	2	3	1.5	0.666666667
SPU_006810	Na/Ca exchanger (Na(+)/Ca(2+)-exchange protein)	0	3	-	-
SPU_023959	hypothetical protein-2698	5	3	0.6	1.666666667
SPU_014778	prion protein interacting protein	3	3	1	1
XP_796283.1	cytosolic malate dehydrogenase	2	3	1.5	0.666666667
SPU_021227	dynein, axonemal, heavy chain 8	2	3	1.5	0.666666667
XP_001175845.1	uncharacterized protein ZK1073.1-like	4	3	0.75	1.333333333
SPU_001302	similar to oxysterol-binding protein	3	3	1	1
SPU_016258	coiled-coil domain containing 40-2	3	3	1	1
SPU_009608	hypothetical protein-52; nephrin-like	0	3	-	-
SPU_012877	KIF27, KIF7	1	3	3	0.333333333
SPU_028685	adhesion protein	1	3	3	0.333333333
SPU_003110	eukaryotic translation initiation factor 5A	0	3	-	-
SPU_012472	alpha-amylase (EC 3.2.1.1) precursor	0	3	-	-

SPU_010283	hypothetical protein	0	3	-	-
SPU_026644	transcription factor Sp-GCF1	4	3	0.75	1.333333333
SPU_019812	dynein, axonemal, heavy chain 2-like	0	2	-	-
SPU_014584	D-3-phosphoglycerate dehydrogenase (3-PGDH)	3	2	0.666666667	1.5
XP_001186669.1	EF-hand domain-containing family member B	3	2	0.666666667	1.5
SPU_000146	Karyopherin (Importin) beta 1	3	2	0.666666667	1.5
SPU_008678	protein kinase C delta type	4	2	0.5	2
SPU_024642	hypothetical protein	6	2	0.333333333	3
XP_001186151.1	Fructose-1,6-bisphosphatase 1	4	2	0.5	2
SPU_003652	family with sequence similarity 49, member B	4	2	0.5	2
SPU_009131	Pyridoxine-5'-phosphate oxidase (Pyridoxamine-phosphate oxidase)	8	2	0.25	4
SPU_020095	similar to glutathione S-transferase Ia	3	2	0.666666667	1.5
SPU_008652	phosphoserine aminotransferase 1	3	2	0.666666667	1.5
SPU_003109	Peptidyl prolyl isomerase H	3	2	0.666666667	1.5
SPU_013608	Park7	4	2	0.5	2
XP_001176548.1	14-3-3 protein homolog isoform 2	7	2	0.285714286	3.5
XP_001187144.1	histone-lysine N-methyltransferase PRDM9-like	4	2	0.5	2
SPU_002319	similar to cytochrome P450 2R1	4	2	0.5	2
XP_001193634.1	similar to CG5588-PC	4	2	0.5	2
SPU_007643	hypothetical protein-1739	3	2	0.666666667	1.5
SPU_006306	galectin 8	3	2	0.666666667	1.5
SPU_024250	similar to gelsolin	3	2	0.666666667	1.5
SPU_001767	Amine oxidase [flavin-containing] A (Monoamine oxidase type A)(MAO-A)	4	2	0.5	2
XP_001181010.1	hypothetical protein	3	2	0.666666667	1.5
SPU_017300	KIAA1529 protein-like-2	7	2	0.285714286	3.5
SPU_017283	tetratricopeptide repeat domain 6	6	2	0.333333333	3
XP_786484.2	TRP superfamily	3	2	0.666666667	1.5
SPU_000784	A6	5	2	0.4	2.5
SPU_009446	Asparaginyl-tRNA synthetase	4	2	0.5	2
SPU_006556	monoamine oxidase A	6	2	0.333333333	3
SPU_004498	DLC-like	3	2	0.666666667	1.5
XP_001179657.1	Cytochrome b5 domain-containing protein 1	6	2	0.333333333	3
SPU_023743	spermatogenesis associated protein 17	4	2	0.5	2
SPU_024215	similar to calponin	3	2	0.666666667	1.5
SPU_000147	dynein, axonemal, heavy chain 5	6	2	0.333333333	3

SPU_018582	dynein 2 light intermediate chain	12	2	0.166666667	6
SPU_022845	Hydroxypyruvate isomerase homolog	3	2	0.666666667	1.5
SPU_002210	CDC2, Cell Division Cycle 2, EC 2.7.1.37	5	2	0.4	2.5
SPU_019768	isochorismatase domain containing 1	3	2	0.666666667	1.5
SPU_013820	Beta enolase (2-phospho-D-glycerate hydro-lyase) (Muscle-specific enolase)	5	2	0.4	2.5
SPU_015249	ubiquitin domain containing 2; dendritic cell-derived ubiquitin-like protein	4	2	0.5	2
SPU_012290	deleted in lung and esophageal cancer protein 1-like	5	2	0.4	2.5
XP_001186213.1	annexin A7-like	3	2	0.666666667	1.5
SPU_025440	similar to adenylate kinase 3	7	2	0.285714286	3.5
SPU_009510	hypothetical protein-1853	4	2	0.5	2
XP_795420.1	uncharacterized protein C9orf9	3	2	0.666666667	1.5
SPU_022476	Transaldolase	4	2	0.5	2
SPU_006395	hypothetical protein	3	2	0.666666667	1.5
SPU_005062	E3 ubiquitin-protein ligase TRIM37	3	2	0.666666667	1.5
SPU_007387	putative homeodomain transcription factor 2-like	3	2	0.666666667	1.5
SPU_014776	WD repeat domain 78; dynein, axonemal, intermediate chain 1-like	4	2	0.5	2
SPU_006906	human chromosome 9 open reading frame 117	9	2	0.222222222	4.5
SPU_012101	hypothetical protein-668	5	2	0.4	2.5
SPU_022417	hypothetical protein-1045	6	2	0.333333333	3
SPU_003296	Sp-SNF7/cytidine_deaminase	4	2	0.5	2
XP_001193456.1	UPF0443 protein C11orf75 homolog	3	2	0.666666667	1.5
SPU_000737	Macoilin transmembrane protein domain containing	4	2	0.5	2
SPU_013237	spectrin repeat containing, nuclear envelope 1	3	2	0.666666667	1.5
SPU_013804	atrophin-1 related protein, arginine glutamic acid dipeptide repeats	3	2	0.666666667	1.5
SPU_012388	Sp-IGv-containing1	4	2	0.5	2
SPU_011041	Cystine/glutamate transporter (Amino acid transport system xc-) (xCT)	6	2	0.333333333	3
SPU_027859	Erythrocyte band 7 integral membrane protein (Stomatin) (Protein 7.2b)	3	1	0.333333333	3
SPU_027041	glyceraldehydephosphate dehydrogenase	4	1	0.25	4
SPU_013930	Intraflagellar transport 172, Wimple, Selective LIM-binding factor	3	1	0.333333333	3
SPU_014771	hypothetical protein	3	1	0.333333333	3
SPU_008601	hypothetical protein-1798; NACHT nucleoside triphosphatase (bacterial)-like	4	1	0.25	4
NP_999692.1	actin, cytoskeletal 3B	3	1	0.333333333	3
SPU_017494	human chromosome 10 open reading frame 67-like	4	1	0.25	4
SPU_001085	Ribose-5-phosphate isomerase (Phosphoriboisomerase)	4	1	0.25	4
SPU_000074	testis-specific gene A14 protein, centrosomal protein of 41 kDa	6	1	0.166666667	6

NP_001032234.1	actin 2	3	1	0.333333333	3
SPU_009880	hypothetical protein-1877; G protein-coupled receptor	4	1	0.25	4
SPU_001762	hypothetical protein-338; leucine-rich repeats and IQ motif containing 3-like	4	1	0.25	4
SPU_025011	hypothetical protein-1134	8	1	0.125	8
SPU_014312	Phosphomannomutase 2 (PMM 2)	3	1	0.333333333	3
SPU_007775	Guanidinoacetate N-methyltransferase	4	1	0.25	4
SPU_004485	prolyl endopeptidase (Prep)	4	1	0.25	4
SPU_002609	hypothetical protein	3	1	0.333333333	3
SPU_020609	Fumarylacetoacetate (Fumarylacetoacetate hydrolase) (Beta-diketonase) (FAA)	3	1	0.333333333	3
SPU_010970	hypothetical protein	15	1	0.066666667	15
SPU_010981	arachidonate 5-lipoxygenase-4	14	1	0.071428571	14
SPU_025893	OTTHUMP00000016025	5	1	0.2	5
XP_794016.2	aspartate aminotransferase 1-like	3	1	0.333333333	3
SPU_017584	human chromosome 12 open reading frame 63-like	3	1	0.333333333	3
SPU_001001	hypothetical protein-320	3	1	0.333333333	3
SPU_006747	family with sequence similarity 154, member B	10	1	0.1	10
SPU_019742	calpain 9; calcium-dependent cysteine proteinase	5	1	0.2	5
XP_788355.2	monoamine oxidase	4	1	0.25	4
SPU_011299	Macrophage migration inhibitory facto	3	1	0.333333333	3
SPU_021463	WD repeat domain 19-2; intraflagellar transport protein 144 [Chlamydomonas reinhardtii]	8	1	0.125	8
SPU_018337	intraflagellar transport 74 homolog (Chlamydomonas)	4	1	0.25	4
SPU_022333	thiopurine methyltransferase	3	1	0.333333333	3
XP_001177258.1	peptidyl-prolyl cis-trans isomerase-like 4	3	1	0.333333333	3
SPU_015038	similar to LOC496288 protein	3	1	0.333333333	3
SPU_002011	doublecortin domain containing 2	10	1	0.1	10
SPU_000082	ATP-dependent DNA helicase PIF1, PIF1/RRM3, PIF1 5'-to-3' DNA helicase homolog	3	1	0.333333333	3
XP_001185605.1	uncharacterized protein C7orf72-like	6	1	0.166666667	6
SPU_003732	hypothetical protein-3094	4	1	0.25	4
SPU_011586	aminotransferase class V-1	24	0	-	-
SPU_013999	ankyrin; ankyrin 1-2, eukaryotic	7	0	-	-
SPU_022860	ankyrin 1-3, erythrocytic	8	0	-	-
NP_999633.1	77 kDa echinoderm microtubule-associated protein	5	0	-	-
SPU_026386	alcohol dehydrogenase class 3	6	0	-	-
SPU_001025	hypothetical protein-321	8	0	-	-
SPU_014343	Iron-responsive element binding protein 1 (IRE-BP 1) (Iron regulatory protein 1) (IRP1)	5	0	-	-

SPU_000974	coronin	5	0	-	-
SPU_028435	hypothetical protein-2955	5	0	-	-
SPU_006911	77 kDa echinoderm microtubule-associated protein	5	0	-	-
SPU_022935	unknown ST protein kinase	5	0	-	-
SPU_004248	clusterin associated protein 1	4	0	-	-
SPU_028633	Glutathione transferase omega 1 (GSTO 1-1)	4	0	-	-
SPU_024052	similar to Serotonin/octopamine receptor family protein 7	3	0	-	-
SPU_027911	similar to formin homology 2	5	0	-	-
SPU_017475	calpain 3/8	3	0	-	-
SPU_013705	coiled-coil domain containing 87	3	0	-	-
SPU_023371	regulator of G-protein signaling 22-like-1	3	0	-	-
XP_001194049.1	ubiquitin-conjugating enzyme E2 variant 2	3	0	-	-
SPU_026711	proteasome (prosome, macropain) subunit, alpha type 3; proteasome alpha 3 subunit	4	0	-	-
SPU_005580	leucine-rich repeat and WD repeat-containing protein KIAA1239	3	0	-	-
XP_001188734.1	electron-transfer-flavoprotein, beta	4	0	-	-
SPU_006891	aminotransferase, class V	3	0	-	-
SPU_007788	human chromosome 6 open reading frame 185-like	3	0	-	-
SPU_005295	Ras association (RalGDS/AF-6) and pleckstrin homology domains 1-like	3	0	-	-
SPU_026035	leucine rich repeat containing 34-1	4	0	-	-
SPU_023892	tetratricopeptide repeat protein 40	3	0	-	-
SPU_002097	hypothetical protein-1369	3	0	-	-
SPU_011585	hypothetical protein-652; aminotransferase, class V (bacterial)-like	3	0	-	-
SPU_018491	dynein, cytoplasmic 2, heavy chain 1	3	0	-	-
SPU_011305	apolipoprotein A-I binding protein precursor	3	0	-	-
SPU_025241	casein kinase I alpha subunit	3	0	-	-
SPU_026810	E3 UFM1-protein ligase 1-like	3	0	-	-
SPU_002376	betaine-homocysteine methyltransferase 2	3	0	-	-
SPU_022514	hypothetical protein-186	3	0	-	-
SPU_015849	hypothetical protein	3	0	-	-
SPU_011109	hypothetical protein-1960; G-protein coupled receptor-like	3	0	-	-
SPU_020801	threonyl-tRNA synthetase	3	0	-	-
SPU_005294	hypothetical protein-1576	3	0	-	-
SPU_002343	hypothetical protein	3	0	-	-

Proteins with peptide counts of more than 2 in either normal or Zn-treated embryos are listed.

Table 2. Proteins specific or more abundant in cilia of Zn-treated embryos.

Gene ID	Molecular weight	pI	Description	peptide counts in normal embryo (N)	peptide counts in Zn-treated embryo (Z)	Z/N
SPU_028683	614986.8	8.47	vitellogenin	-	94	-
SPU_002788	50116.2	4.73	tubulin beta-2C chain	-	70	-
SPU_016269	19702.9	8.65	similar to glutathione S-transferase theta 1	-	49	-
SPU_013301	154019	7.04	vitellogenin	-	43	-
SPU_021662	25318.5	7.03	similar to glutathione S-transferase theta 1	-	42	-
XP_001197604.1	40442.7	5.62	hypothetical protein	-	29	-
SPU_027236	30397.8	6.32	voltage-dependent anion-selective channel protein 2	-	23	-
SPU_010203	38476	7.78	yolk granule protein; fasciclin-like	-	15	-
SPU_028684	202977.8	6.12	vitellogenin	-	11	-
SPU_019788	16057.9	10.73	ribosomal protein L27	-	9	-
SPU_024961	57228.2	8.69	hypothetical protein-2760 (AnkAT-1)	-	8	-
SPU_010977	31009.9	9.07	similar to 4930451C15Rik protein	-	8	-
SPU_004813	32740	9.86	ADP/ATP translocase 2	-	7	-
SPU_023066	36279.3	6.13	chromosome 11 open reading frame 54 protein	-	7	-
SPU_010738	19376.1	5	vitellogenin	-	7	-
XP_001197263.1	100016.3	7.79	similar to major yolk protein precursor	-	7	-
SPU_018822	293267.6	5.37	hypothetical protein LOC757406	-	6	-
SPU_007550	47116.7	8.77	enta-EF hand domain containing 1-1	-	6	-
SPU_018376	10991.9	7.74	hypothetical LOC581148, transcript variant 2	-	6	-
XP_001195864.1	32139.5	8.55	similar to LOC414565 protein	-	6	-
SPU_022072	11369.3	11.2	histone H4	-	6	-
SPU_007820	15402	11.27	histone H3.2	-	5	-
XP_001176581.1	19620.9	8.93	similar to MGC69420 protein	-	5	-
SPU_006767	22189.7	5.96	Sp-Sar1b (Ras superfamily, ARF family)	-	5	-
SPU_024343	13600.8	10.72	similar to histone H2B-1	-	5	-
NP_999710.2	13615.1	10.43	histone H2B	-	5	-
SPU_028358	15058.4	6.95	Aldo keto reductase, AKR fragment	-	5	-
SPU_021207	40091.5	6.39	Phosphodiesterase 8A, isoform 1	-	5	-

SPU_010531	51611	4.98	similar to alpha-tubulin 1C	-	5	-
XP_001177415.1	38534.2	9.16	yolk granule protein; fasciclin-like	-	5	-
SPU_016270	20652	7.08	similar to glutathione S-transferase theta 1	1	27	27
SPU_016156	29227.9	9.35	hypothetical LOC592629	1	18	18
SPU_006495	25100	5.99	similar to glutathione S-transferase theta 1	5	62	12.4
SPU_019232	10257	6.02	similar to MGC80929 protein	1	11	11
SPU_018584	36837	9.68	coiled-coil domain containing 74B-like	1	11	11
SPU_004585	32549	5.64	hypothetical LOC578897	1	11	11
SPU_000965	25947.4	8.74	hypothetical LOC585129	1	10	10
XP_001190137.1	15858	5.79	similar to proteasome-like protein, partial	2	19	9.5
SPU_013919	27343.4	5.49	fibronectin type III and ankyrin repeat domains 1	2	19	9.5
XP_001176985.1	22241.8	5.31	hypothetical protein	2	15	7.5
SPU_023486	395128.1	4.3	fibrocystin L	8	59	7.4
SPU_020730	23740.2	5.19	similar to thioredoxin family Trp26	2	14	7
SPU_016106	60510	6.3	several ankyrin repeat protein transcript variant 2	1	7	7
SPU_005791	41687.1	6.1	IQ motif containing K	2	13	6.5
SPU_000253	31918	8.73	Ras-associated protein Rap1-LIKE 1	1	6	6
XP_001181406.1	42417.5	5.3	similar to putative ARM-1 protein	1	6	6
SPU_004874	84229.3	9.12	hypothetical protein-433	1	6	6
SPU_022529	28978.3	5.77	thioredoxin peroxidase	1	6	6
SPU_000595	50448.4	9.28	elongation factor 1A	4	22	5.5
SPU_020812	46293.3	4.96	tubulin, alpha 1C	2	11	5.5
SPU_027647	40643.2	4.89	ATP-binding cassette, sub-family B	1	5	5
SPU_015573	77710.8	5.93	ATP-binding cassette transporter 1	1	5	5
SPU_026062	16406.4	6.84	similar to RIKEN cDNA 3100002J23 gene	1	5	5
SPU_028434	370512.4	8.17	similar to dynein heavy chain 14, axonemal	1	5	5
SPU_003378	79189.9	9.03	zinc finger protein PLAG1	1	5	5
SPU_004774	52312.6	8.64	hypothetical protein-1543	1	5	5

Proteins with peptide counts from mass spectrometry more than 4 and Z/N more than 5 are listed.

Table 3. Proteins specific or more abundant in cilia from normal embryos.

Gene ID	Molecular weight	pI	Description	peptide counts in normal embryo	peptide counts in Zn-treated embryo	N/Z
SPU_011586	62619.5	7.98	aminotransferase class V-1	24	-	-
SPU_022860	136675.3	6.85	ankyrin 1-3	8	-	-
SPU_001025	69496.8	9.56	hypothetical protein-321	8	-	-
SPU_013999	61453.2	8.55	ankyrin 1-2	7	-	-
SPU_026386	40267.2	6.71	alcohol dehydrogenase class 3	6	-	-
NP_999633.1	75453.5	6.36	77 kDa echinoderm microtubule-associated protein	5	-	-
SPU_014343	96739.4	5.58	Iron-responsive element binding protein 1	5	-	-
SPU_000974	53865.5	6.54	coronin	5	-	-
SPU_028435	34187	10.17	hypothetical protein-2955	5	-	-
SPU_006911	75632.7	6.36	77kDa-microtubule-associated protein	5	-	-
SPU_022935	39144.1	9.28	unknown Ser/The protein kinase	5	-	-
SPU_027911	16443.7	5.46	FH1/FH2 domain-containing protein 3-like	5	-	-
SPU_004248	48274.1	4.45	clusterin associated protein 1	4	-	-
SPU_028633	28321.2	5.65	Glutathione transferase omega 1 (GSTO 1-1)	4	-	-
SPU_026711	27642.4	5.61	proteasome subunit, alpha type 3	4	-	-
XP_001188734.1	6557.6	9.36	similar to ENSANGP00000021736, partial	4	-	-
SPU_026035	39968.6	5.39	leucine rich repeat containing 34-1	4	-	-
SPU_010970	22267.1	9.54	hypothetical protein isoform 1	15	1	15
SPU_010981	77300.6	5.37	arachidonate 5-lipoxygenase-4	14	1	14
SPU_006747	59730.7	9.58	family with sequence similarity 154, member B	10	1	10
SPU_002011	96337.4	5.22	doublecortin domain containing 2	10	1	10
SPU_025011	103635.9	4.86	hypothetical protein-1134	8	1	8
SPU_021463	59717.3	6.53	IFT 144 (Chlamydomonas reinhardtii)	8	1	8
SPU_010980	47817.1	5.41	arachidonate 5-lipoxygenase-6	24	4	6
SPU_018582	29056.2	9.03	cytoplasmic dynein 2 light intermediate chain 1	12	2	6
SPU_000074	36013.9	8.75	41 kDa centrosomal protein	6	1	6
XP_001185605.1	19993.4	8.93	hypothetical protein, partial	6	1	6
SPU_005282	66085.2	8.05	human chromosome 14 open reading frame 166B	15	3	5
SPU_025893	67824.3	9.75	similar to OTTHUMP00000016025	5	1	5
SPU_019742	37610.6	8.08	calpain 9; calcium-dependent cysteine proteinase	5	1	5

Proteins with peptide counts from mass spectrometry more than 4 and N/Z more than 5 are listed.

Table 4. Axonemal proteins and the proteins for ciliogenesis found in cilia from normal or Zn-treated embryos.

	Protein	Gene ID			N	Z	Z/N
Outer Arm Dynein							
DNAH5 (sea urchin alpha)		SPU_003660	SPU_030226	SPU_000147	1122	1250	1.1
		SPU_024529	SPU_020621				
DNAH8 (sea urchin alpha)		SPU_024596	SPU_002110	XP_783106.2	123	135	1.1
		SPU_027840					
DNAH9 (sea urchin beta)		SPU_030230	SPU_003404	SPU_017173	1166	1206	1.0
		SPU_024245					
DNAH11 (sea urchin beta)		SPU_028599	SPU_028057		15	21	1.4
IC1 (TNDK-IC)		SPU_007092			99	105	1.1
IC2 (Chlamy IC69)		SPU_019506			221	186	0.84
IC3 (Chlamy IC78)		SPU_026533	SPU_005973	SPU_009561	200	181	0.91
		SPU_014776					
LC1 (Tctex2)		SPU_013200	SPU_023221		27	34	1.3
LC2 (LRR)		SPU_018854	XP_001192985.1		27	51	1.9
		SPU_006844	SPU_000795	SPU_007633			
LC3 (Tctex1)		SPU_008471			67	93	1.4
LC4		SPU_008799	SPU_004377		18	35	1.9
LC5 (roadblock)		SPU_008699			16	24	1.5
LC6		SPU_024498	SPU_025272		93	137	1.5
ODA-DC2		SPU_004762			130	111	0.85
ODA binding protein (Ap58)		SPU_015625			215	165	0.77
Inner Arm Dynein							
DNAH1		SPU_000013	SPU_030223		492	540	1.1
DNAH2		SPU_030224			586	718	1.2
		SPU_026539	SPU_012417	SPU_030225			
DNAH3		SPU_004622			349	412	1.2
DNAH6		SPU_030227			316	320	1.0
DNAH7		SPU_030228	SPU_020747	SPU_010886	582	641	1.1
DNAH10		SPU_030231			465	467	1.0
DNAH12		SPU_030232	SPU_003564		382	428	1.1

DNAH14	SPU_030233	SPU_028434	4	14	3.5	
DNAH15	SPU_030234		366	409	1.1	
IC140	SPU_012809	SPU_013538	SPU_006699	211	215	1.0
Actin	SPU_009481		247	368	1.5	
p33	SPU_015320		106	109	1.0	
centrin	SPU_024357	SPU_028660	23	42	1.8	
Radial Spoke						
RSP1	SPU_025942		94	105	1.1	
RSP3	SPU_014801	SPU_012045	179	216	1.2	
RSP4/6	NP_999761.1		19	23	1.2	
RSP9	SPU_005442		161	305	1.9	
RSP10	XP_001182314.1		14	8	0.57	
HSP40	SPU_026705		106	138	1.3	
MORN40/meichroacidin	SPU_010316		21	26	1.2	
CMUB116 (<i>Ciona</i>)	SPU_020748	SPU_026255	38	37	0.97	
calmodulin	SPU_008000		4	8	2.0	
Central Apparatus						
PF6 (Spag17)	SPU_015915	SPU_000735	SPU_013103	100	98	0.98
PF16 (Spag6)	SPU_025787		177	277	1.6	
PF20 (Spag16)	SPU_003263		110	124	1.1	
hydin	SPU_019525	SPU_002460	SPU_013006	131	81	0.62
CPC1 (centralpair complex 1)	SPU_021592		12	12	1.0	
kinesin, KIF9	SPU_010081		37	32	0.86	
Other axonemal proteins						
tektin-1	SPU_013841		192	200	1.0	
tektin-2	SPU_020728		249	225	0.90	
tektin-3	SPU_023618		213	266	1.2	
tektin-4	SPU_019591	SPU_008777	239	239	1.0	
RIB43A protein 2	SPU_027579		4	4	1.0	
ODF3 (shippo 1)	SPU_005728	XP_802079.1	50	45	0.90	
PACRG	SPU_004619		264	383	1.5	
PF2 (Dynein Regulatory Complex)	SPU_003865		72	71	0.99	

	coiled-coil domain containing 147 (FAP189/58)	SPU_027352	XP_785052.2	137	103	0.75	
ciliogenesis							
	DYNC2H1	SPU_030235		60	50	0.83	
	dynein 2 light intermediate chain	SPU_018582		12	2	0.17	
	dynein light chain 1, cytoplasmic	SPU_018567		29	25	0.86	
	Kinesin KIF3B	SPU_022982		27	22	0.81	
	Intraflagellar transport 20	SPU_027227		11	6	0.55	
	intraflagellar transport 52	SPU_019590		10	3	0.30	
	intraflagellar transport 74	SPU_018337		4	1	0.25	
	Intraflagellar transport 80	SPU_011239		17	6	0.35	
	intraflagellar transport 81	SPU_003223		17	13	0.76	
	intraflagellar transport 88	SPU_020282		8	5	0.63	
	intraflagellar transport 122A	SPU_023605		34	9	0.26	
	intraflagellar transport 139	SPU_002620		39	39	1.0	
	intraflagellar transport 140	SPU_021918	SPU_020159	XP_001192126.1	38	50	1.3
	intraflagellar transport 144				8	1	0.13
	intraflagellar transport 172	SPU_013202	SPU_021651	SPU_021760	40	34	0.85
	Bardet-Biedl syndrome 1 protein	SPU_011446			6	5	0.83
	ketanin p60 subunit A-like 2	SPU_007977			3	5	1.7

Axonemal components other than tubulins are listed.

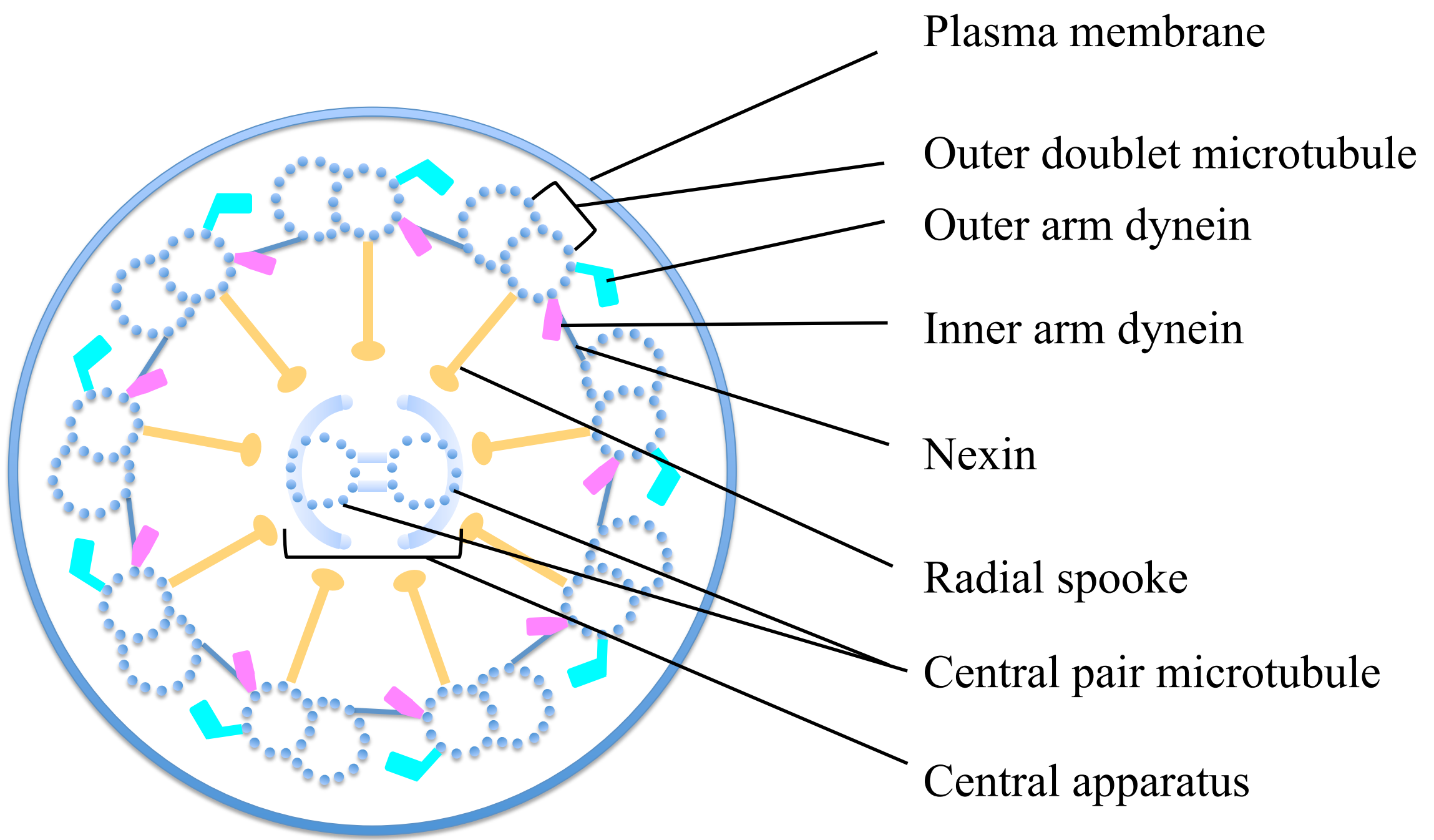


Fig. 1 Schematic drawing of the structure of cilia and flagella.

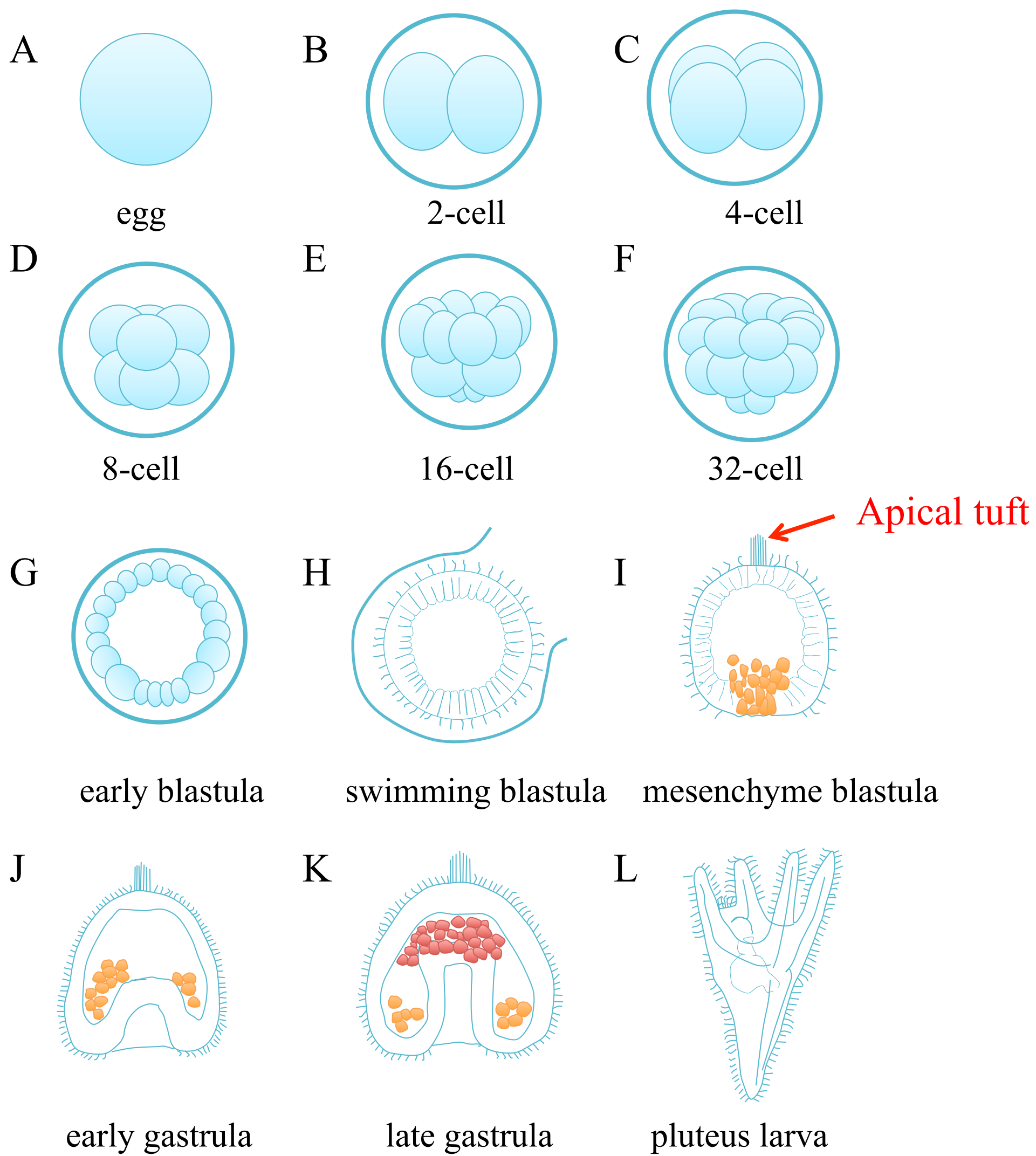


Fig. 2 Schematic representation of sea urchin embryonic development (based on Pruli  re et al., 2011).

Cilia are formed in individual ectodermal cell from blastula stage just before hatching and become highly motile in the swimming blastula stage (H). Apical tuft become clear on the animal plate from mesenchyme blastula stage (red arrow in I). The cells drawn in orange or red represent primary or secondary mesenchyme cells, respectively.

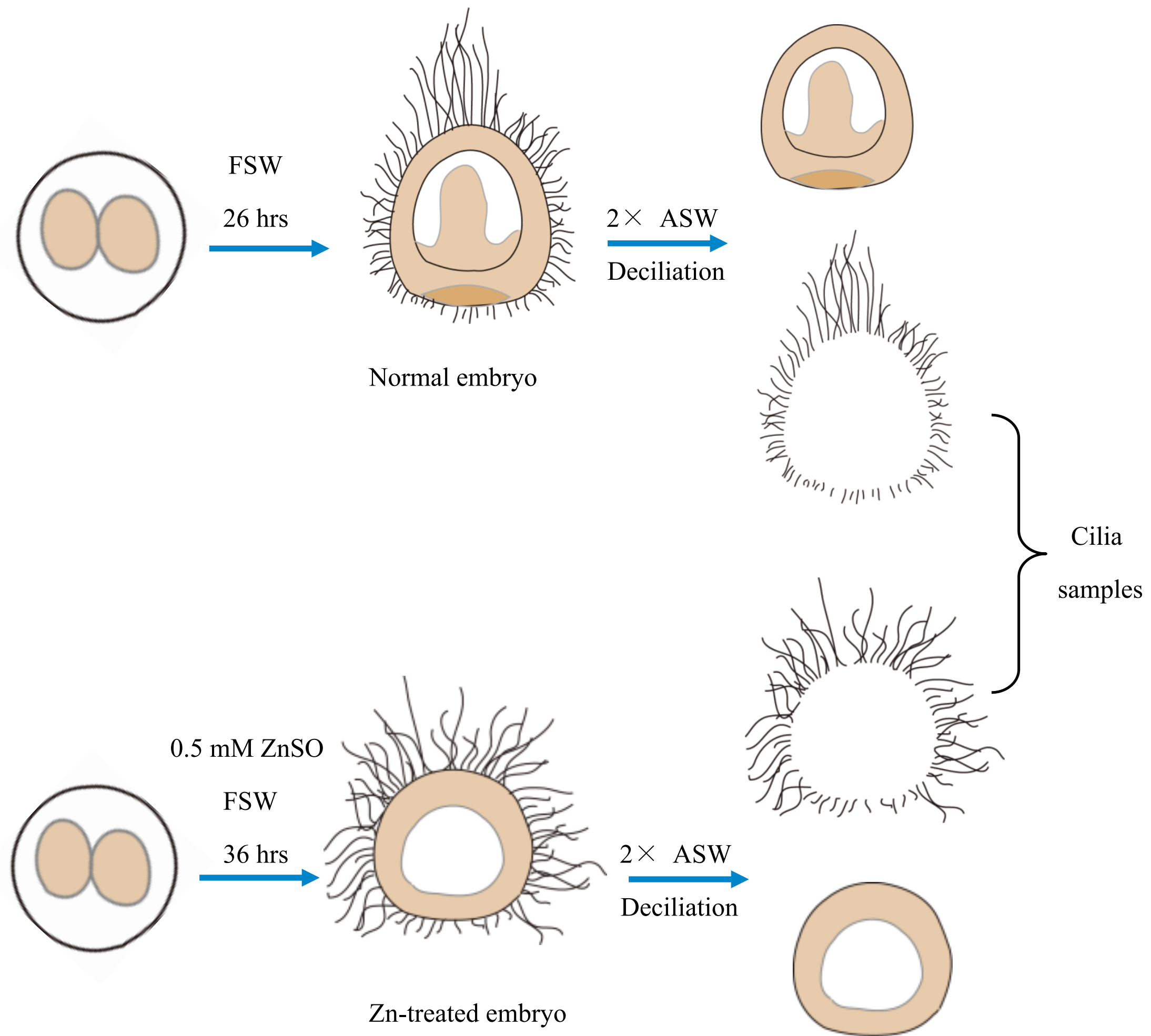


Fig. 3 Procedure for the isolation of cilia from normal and Zn-treated embryo.

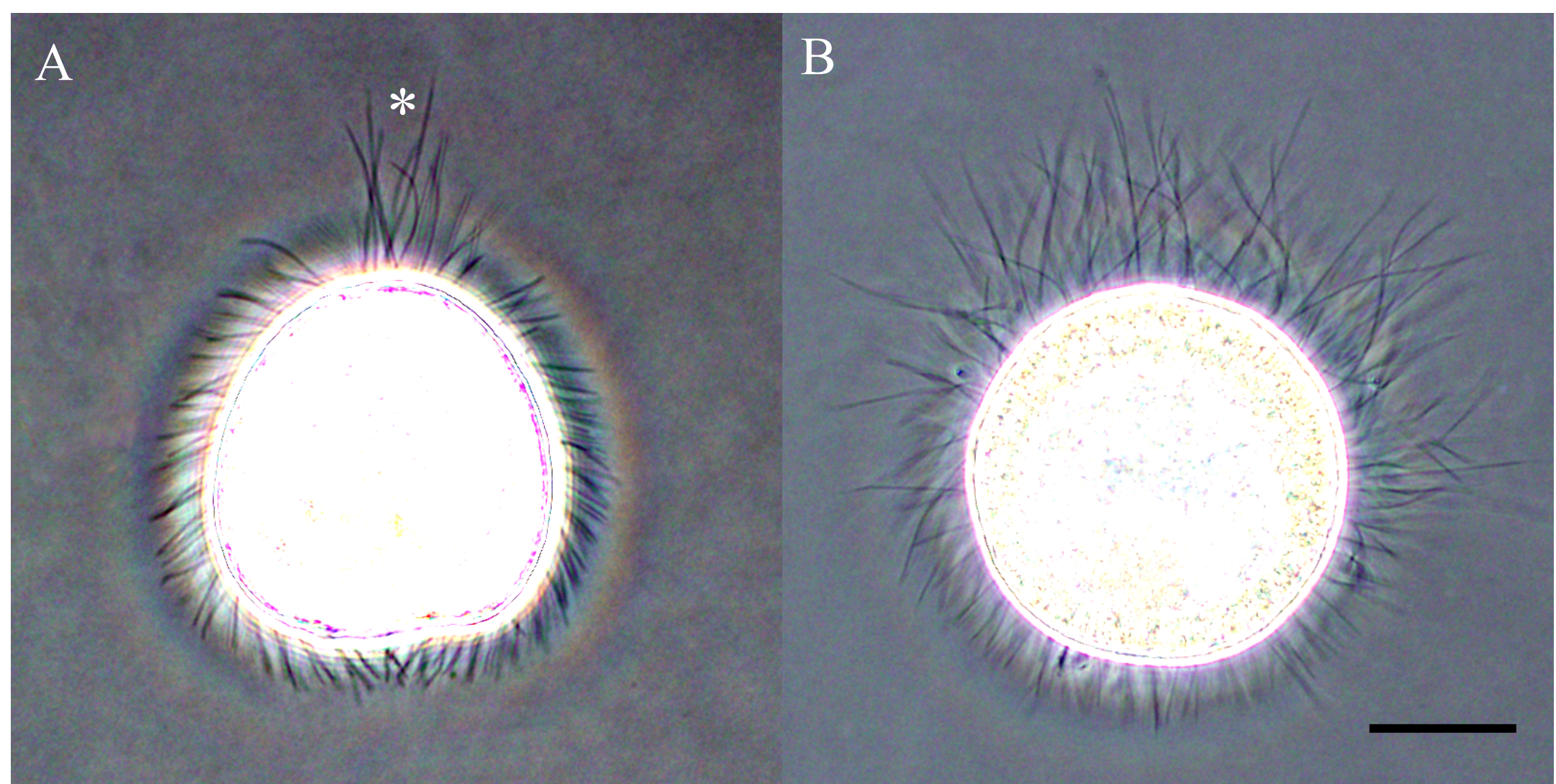


Fig. 4 Normal and zinc-treated sea urchin embryos.

Phase contrast microscopic images of normal (A) and Zn-treated (B) embryos. The asterisk indicates the apical tuft. Zn-treated embryos are animalized and bear long and less-motile cilia that appear apical tuft. Bar: 50 μ m.

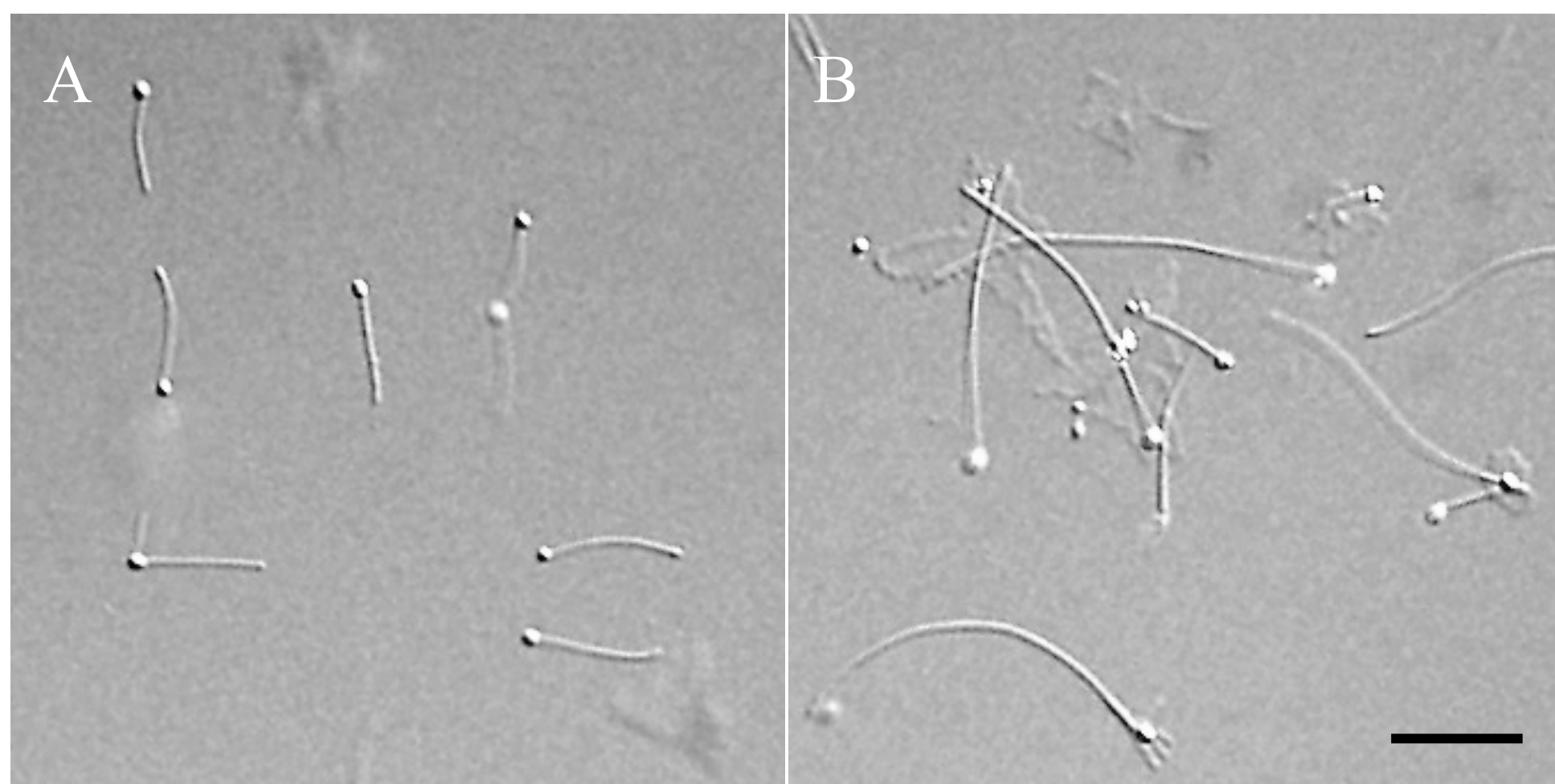


Fig. 5 Isolated normal and Zn-treated embryo cilia.

Different interference contrast images of isolated cilia from normal (A) and Zn-treated (B) embryos. Cilia were obtained by deciliation with high salt seawater. Note that cilia from Zn-treated are as long as apical tuft.
Bar: 20 μ m.

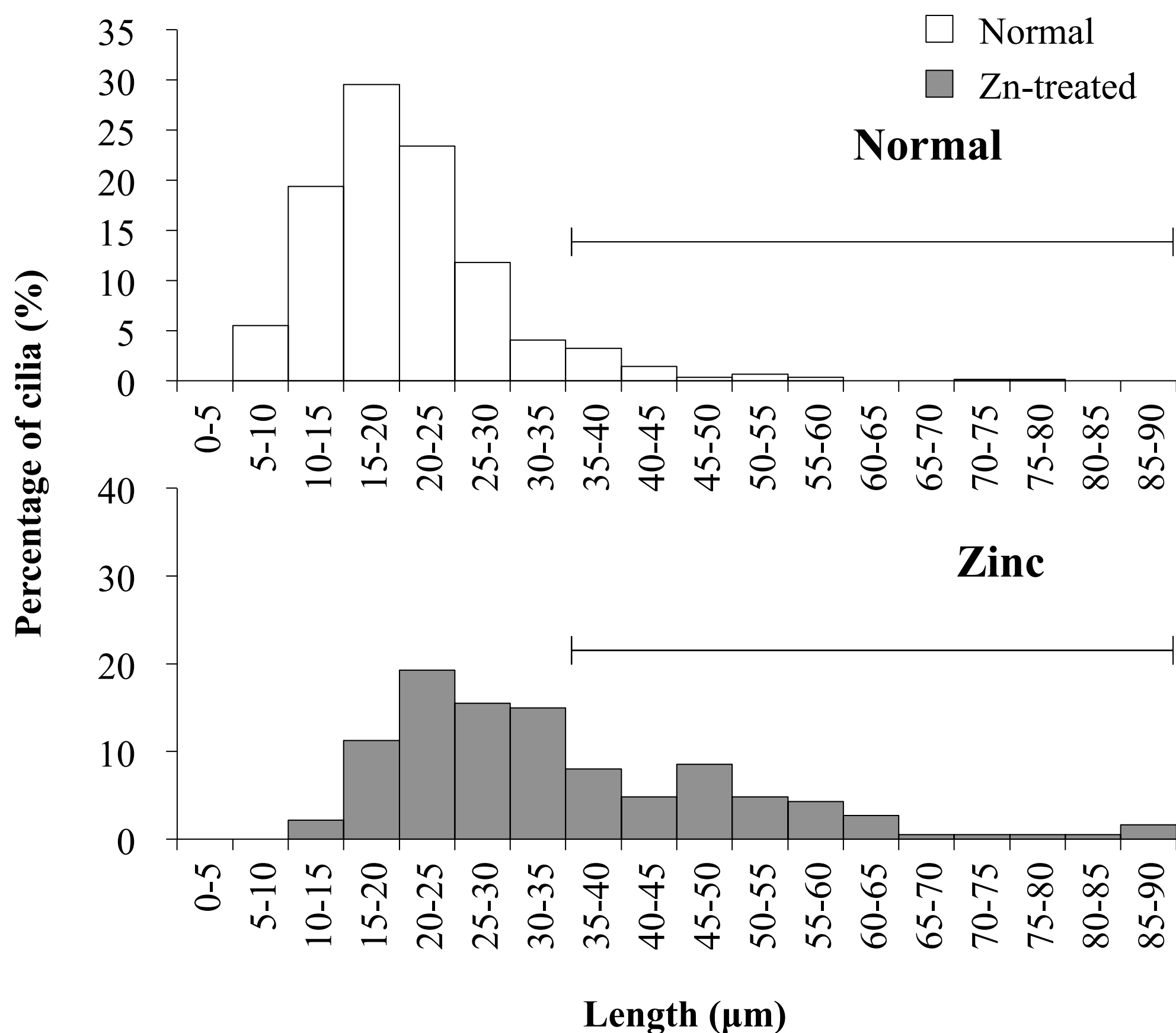
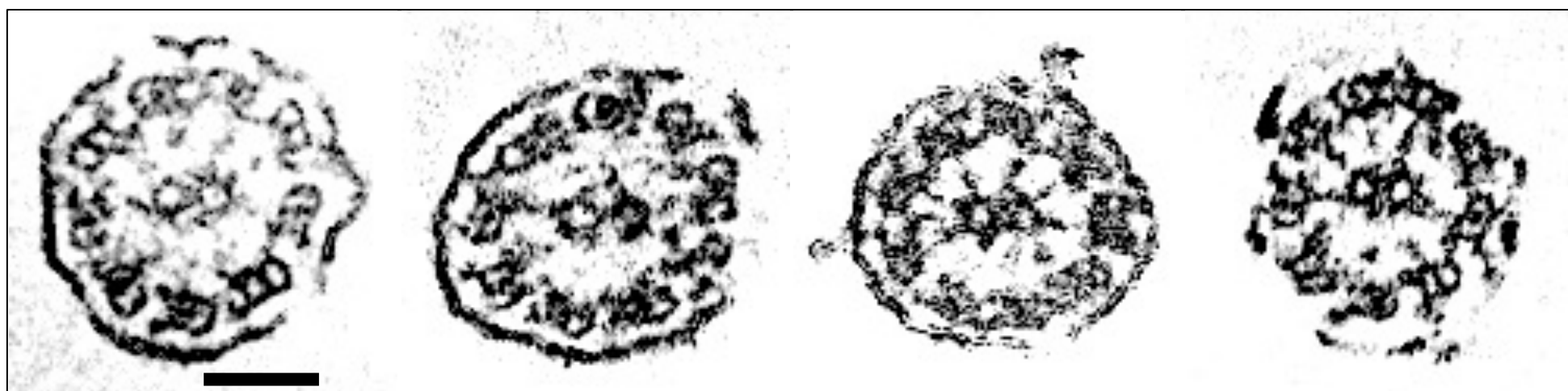


Fig. 6 Distribution of the length of cilia isolated from embryos.

Open bar and closed bar show percentage of ciliary length in normal and Zn-treated embryos, respectively. The horizontal bar represents the range of apical tuft cilia directly measured from normal embryos before deciliation.

Normal



Zn-treated

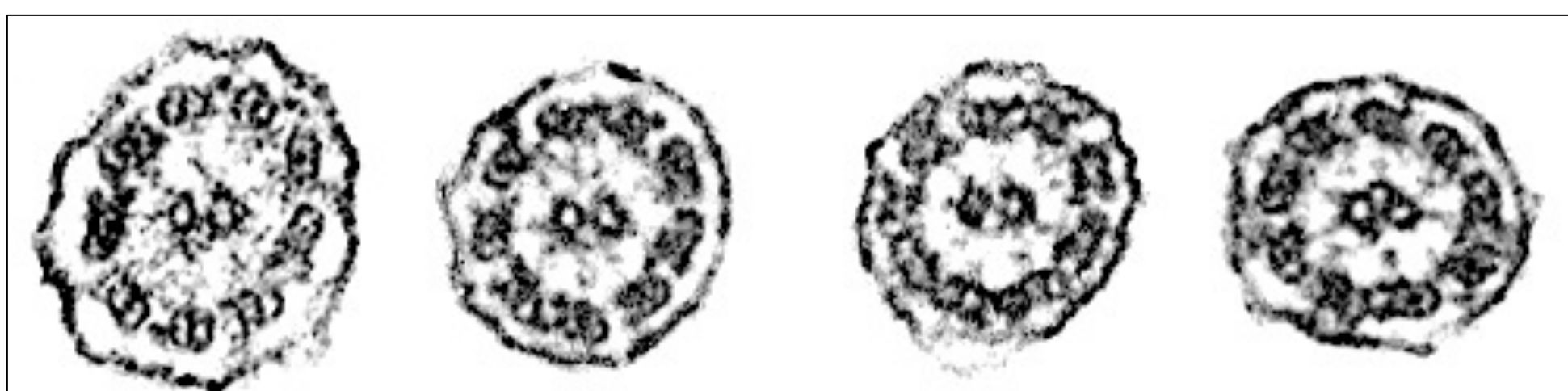


Fig. 7 Observation of thin-sectioned cilia by transmission electron microscopy.

Typical images of cilia from normal (top) and Zn-treated (bottom) embryos are shown. Bar, 100 nm.

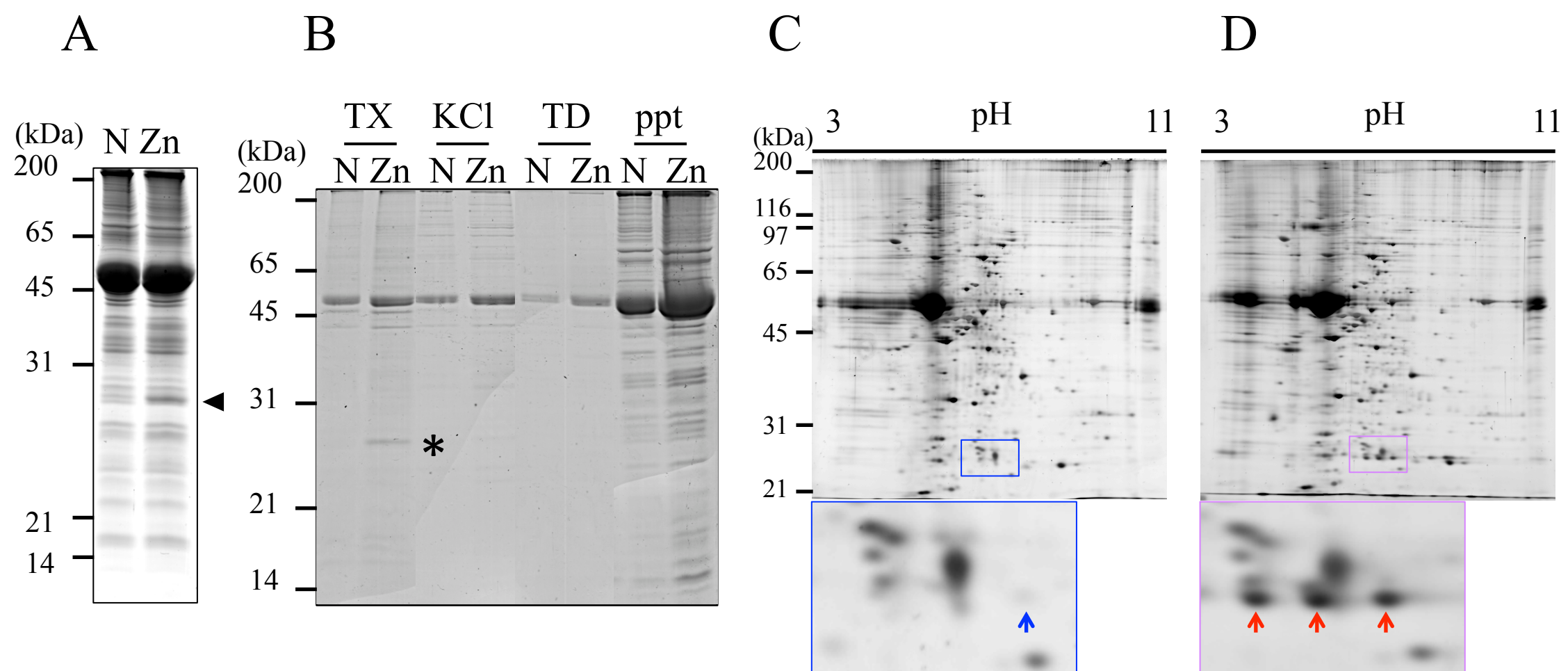
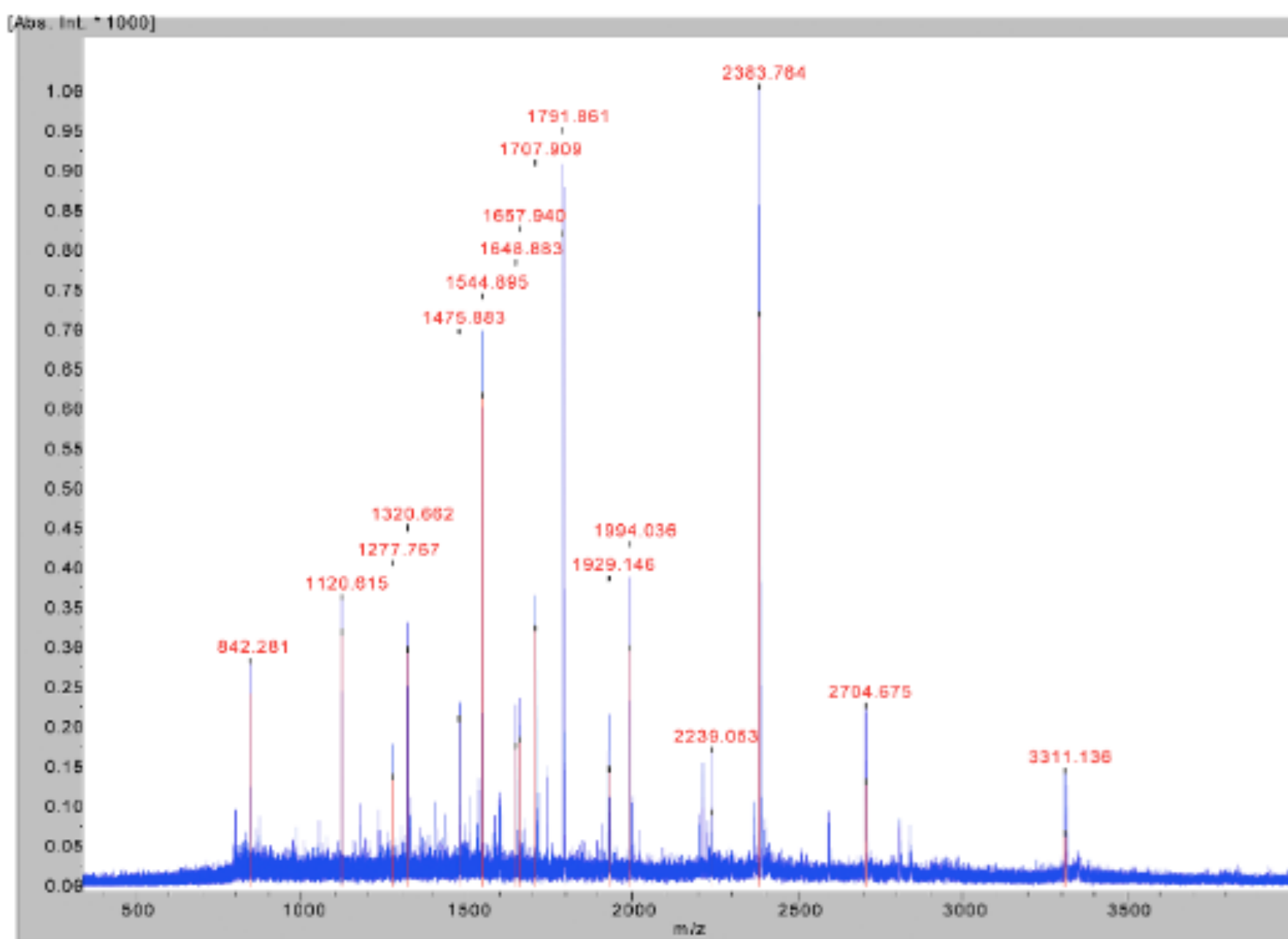


Fig. 8 Comparison of ciliary proteins between normal and Zn-treated embryos.

A: SDS-PAGE of ciliary proteins (~20 µg) from normal (N) and Zn-treated (Zn) embryos. The arrowhead shows ~25-kDa protein specifically present in cilia from Zn-treated embryos. B: Successive extraction of cilia isolated from normal (N) and Zn-treated (Zn) embryos. Cilia were successively extracted with a buffer containing 0.1% Triton X-100 (TX), a high salt buffer (KCl) and then a low salt buffer (TD). “ppt” represents the axonemal residues. The ~25-kDa protein (asterisk) shows present in TX fraction. C, D: 2DE patterns of ciliary proteins from normal and Zn-treated embryos. Horizontal numbers represent pH ranges for isoelectric focusing. The two lower panels show magnified images of the ~25-kDa regions. The red arrows or a blue arrow show spots of ~25-kDa proteins specifically present in cilia from Zn-treated embryos or commonly present in both cilia, respectively.

A



B

SPU_16269

1 M**TIQLYVDLR** SQPCRAVVMF LK**LTDIPHEL** QYIDIFAGEH KKPEFADKFP
51 LETLPGLKD**G DFYLGEMVAI** FRYLINKYAD KIKDNWYPKD MKSRAR**VNEY**
101 IAF**HHTGTRG** KCMALFVAEF AQFTVNGRDI FKDNPKMKG**Y MDRVVKACLQP**
151 AFDEIIVKLY DWRDSLAK

Fig. 9 Identification of GSTT by MALDI-TOF/MS.

A: Mass spectrum of tryptic fragments of ~25-kDa protein used for identification. B: The amino acid sequence of SPU_016269. The portions of peptides matching with peptide masses in A are indicated in red. From the Mascot analysis, the ~25-kDa protein was identified as GSTT. All of three spots from 2DE were hit with SPU_016269.

Hp_GSTT	1 MTIQLYVDLRSQPCRAVMFLKLTDIPHELYIDIFAGEHKKPEFADKFPLETLPGHQDG
Sp_GSTT	1 MTIELYVDLRSQPCRAVAIFLNLMGIPHELYIDIFAGEHKKPEFADNFPLETLPGLKDG ***:*****. : * . *****;*****:*****:*****;
Hp_GSTT	61 DFYLGEMVAIFRYLINKYADKIKDNWYPEDVKSARVNEYIAFHHTGTRGKCMALFVAEV
Sp_GSTT	61 DFYLGEMVAIFRYLTTKYADKIKDNWYPKDLKSRARVDEYIAFHHTGTRGKCMALFVAEV *****. *****:*****:*****:*****
Hp_GSTT	121 FAPVVDQEKVTEAENLKQGLEKIEQSFLKDNDLFGKEISIADIMAVCELAQFIVNGRD
Sp_GSTT	121 FAPVPDQEKKTEAENLKQGVDKIEQSFLKDNDLFGKEISIADIMAVCEFAQFTVNGRD **** * ;*****:*****:*****:*****:*****:*****:*****
Hp_GSTT	181 ILKDNPKMKGYMDRVKACLOPAFDETIVKLYGWRDSLAK
Sp_GSTT	181 ILKDNPKMKGYMDRVKACLOPAFDEISVKLCAWRDSHAK *****. *** . **** **

Fig. 10 Amino acid sequences and alignments of sea urchin GSTT.

Asterisks, colons, and dots indicate identical residues in all sequences in the alignment, conserved substitutions, and semi-conserved substitutions, respectively. Hp, *hemicentraotus pulcherrimus*; Sp, *Strongylocentrotus purpuratus*.

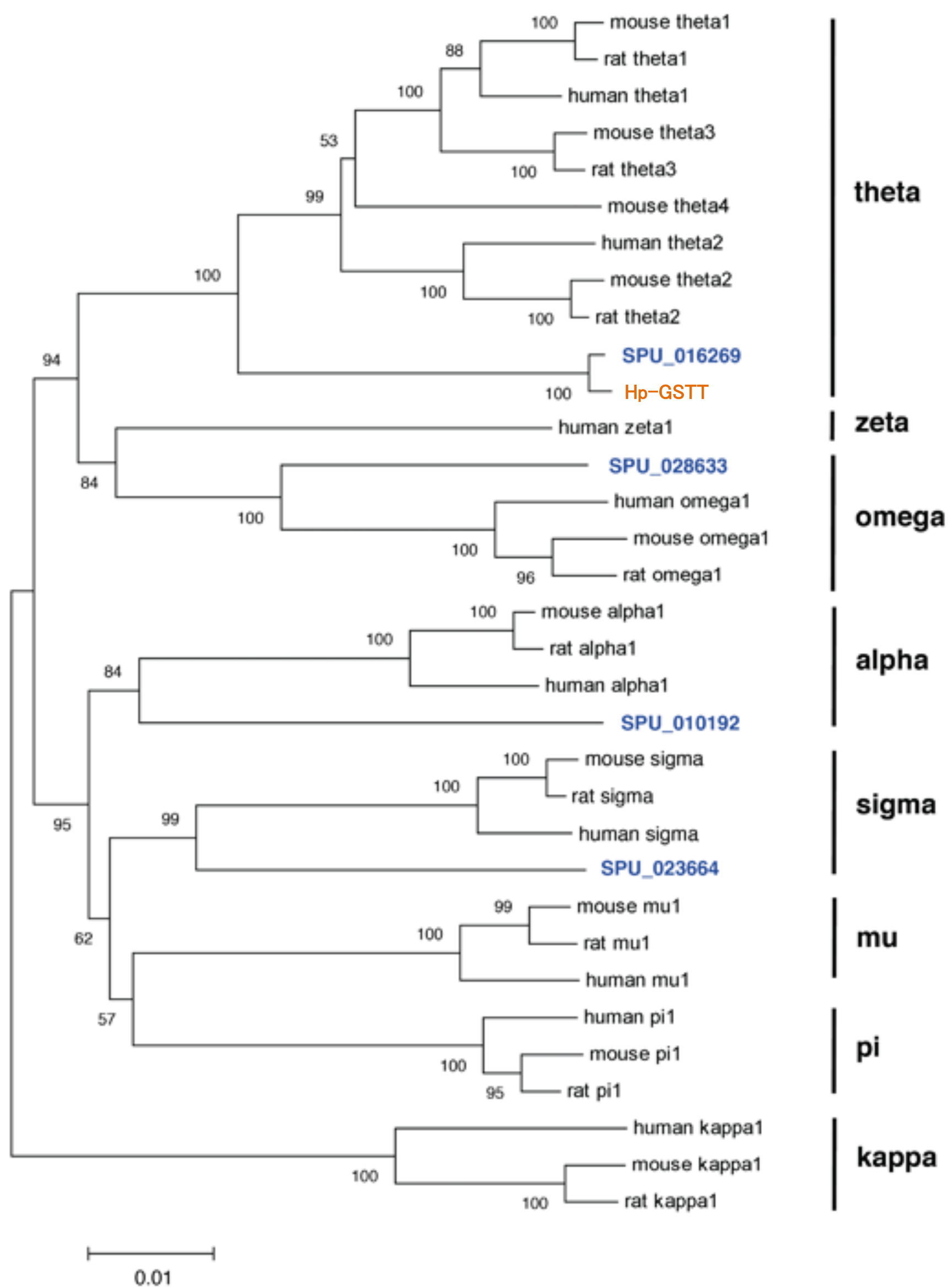


Fig. 11 Phylogenetic tree of GSTs.

The consensus phylogenetic tree was constructed by neighbor-joining method. Numbers at each node are the percentage bootstrap value of 1000 replicates. Accession numbers of protein sequences used are indicated in Materials and Methods. The analysis supports that ~25-kDa protein identified in apical tuft is classified into GSTT.

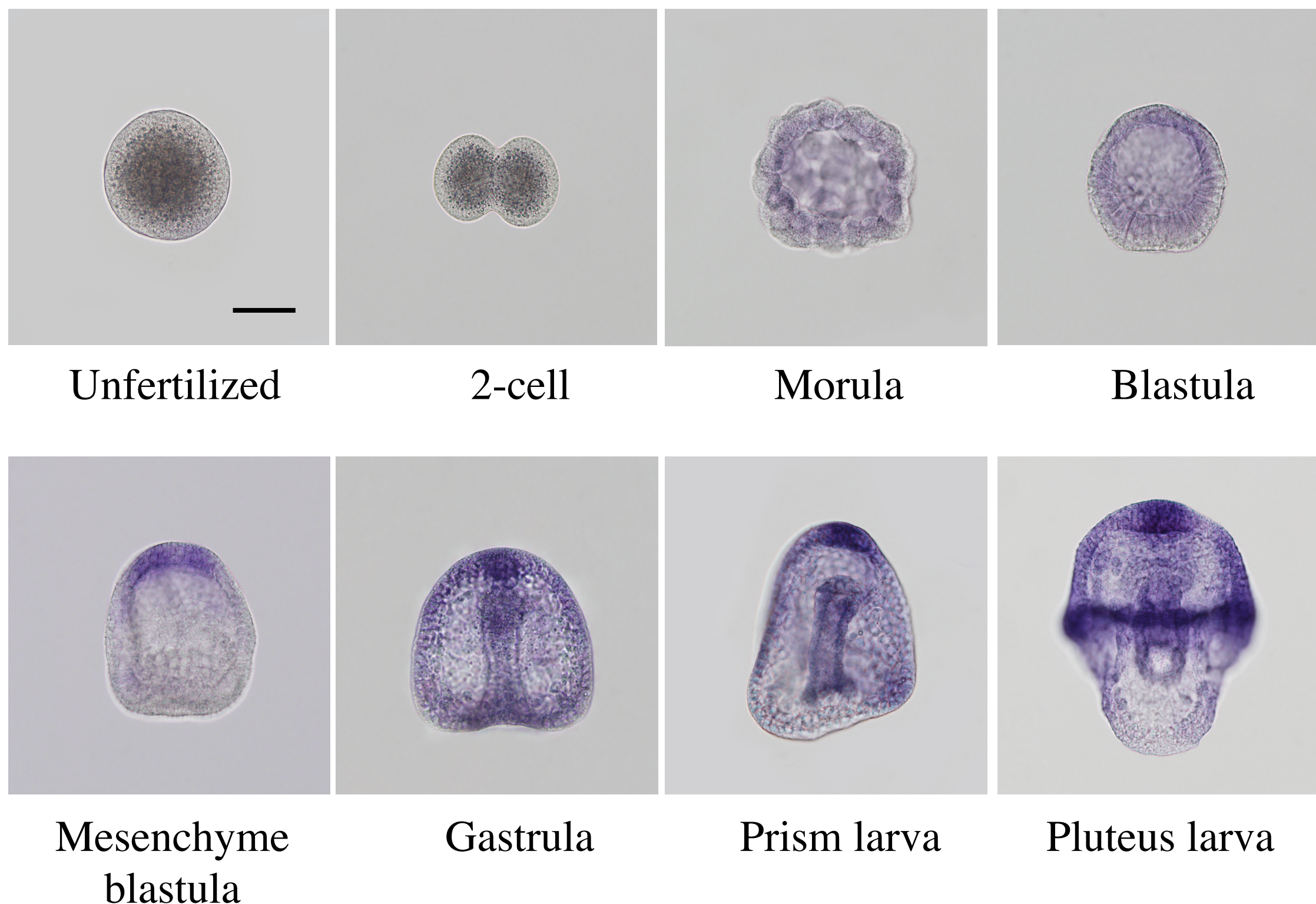


Fig. 12 Expression of GSTT gene during development of sea urchin embryo.

Expression patterns of GSTT in several stages of sea urchin embryos by *in situ* hybridization are shown. *GSTT* mRNA begins to be highly expressed in the animal plate of mesenchymal blastula and then in the ciliary band of pluteus larva. Bar: 50 μ m.

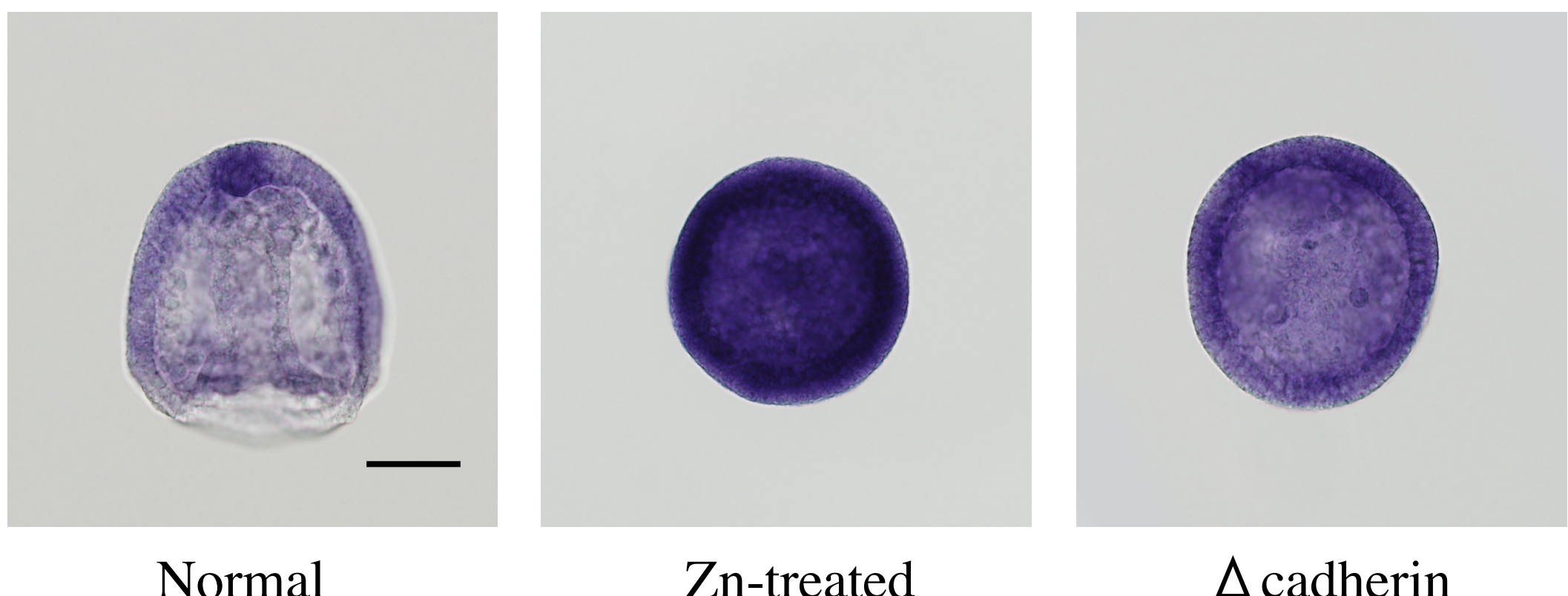


Fig. 13 *GSTT* mRNA is highly and entirely expressed over Zn-treated or cadherin-depleted embryos.

Expression patterns by *in situ* hybridization are shown for normal (left), Zn-treated (middle) and Δ cadherin (right) embryos. Bar: 50 μ m.

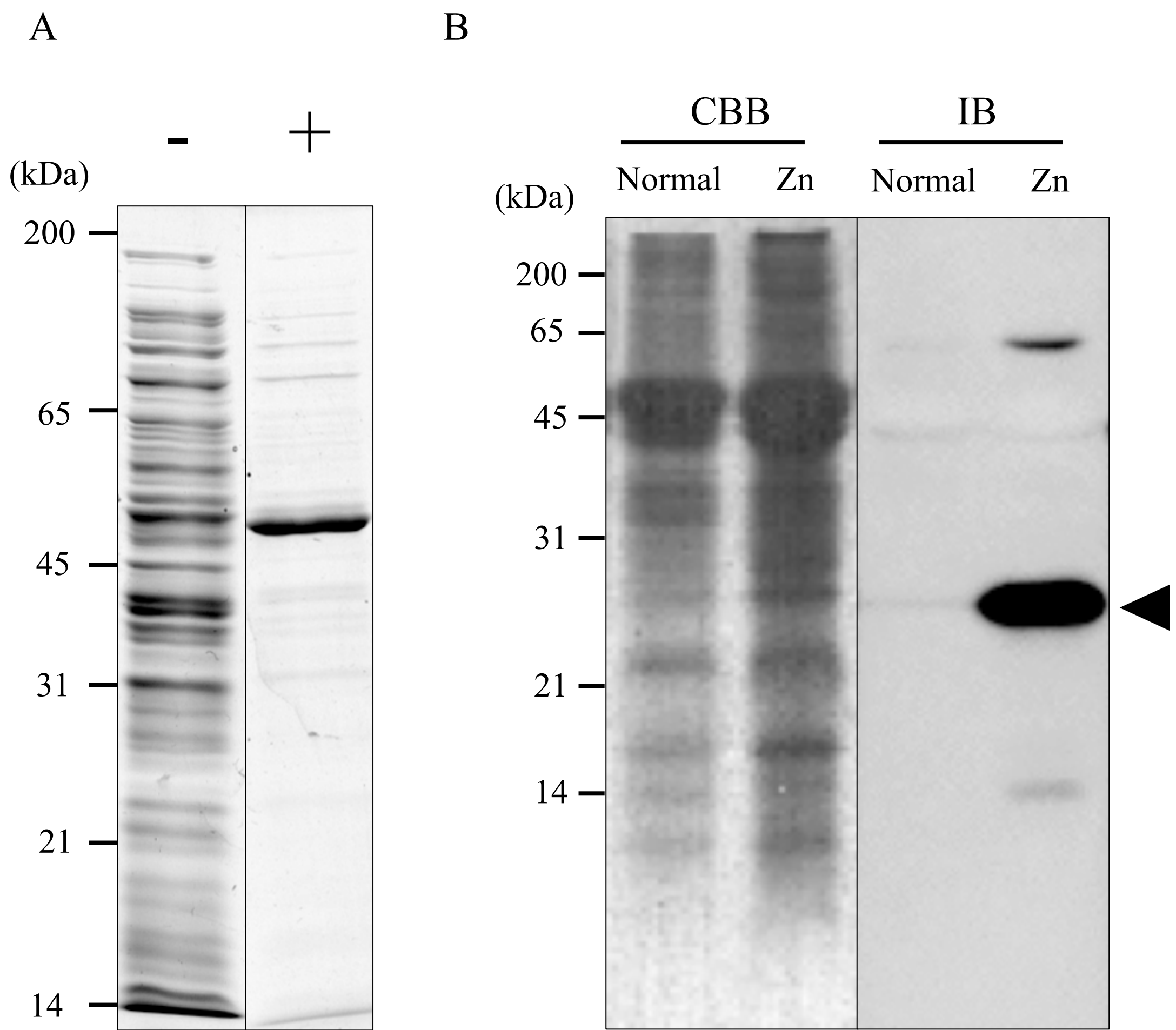


Fig. 14 Preparation of anti-GSTT antibody.

A: SDS-PAGE of *E. coli* whole lysate with (+) or without (-) induction by 1 mM IPTG. *E. coli* AD494 was transformed by pET32a-GSTT recombinant vector for production of thioredoxin-GSTT fusion protein. The fusion protein was purified by His-tag and immunized into mouse to get polyclonal antibodies. B: Immunoblots (IB) of ciliary proteins from normal and Zn-treated embryos (Zn) by anti-GSTT antibody. Strong signal is observed in ~25-kDa band (arrowhead) in Zn-treated embryos, whereas the signal is quite faint in normal embryos.

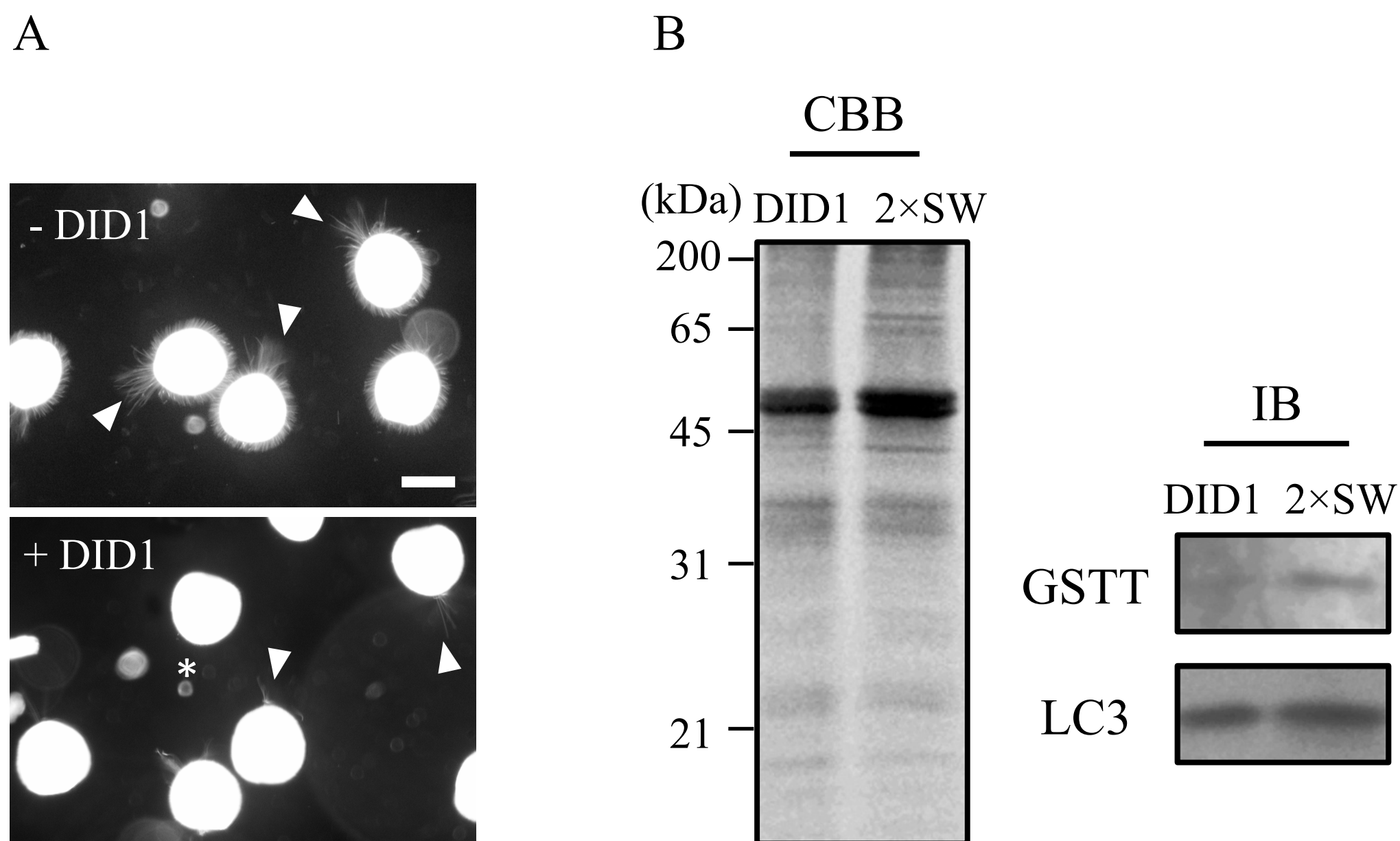


Fig. 15 Preparation of apical tuft by DID1-treatment.

A: Selective deciliation of lateral motile cilia by DID1. Dark field images of embryos without (-) or with (+) DID1 treatment are shown. After the treatment of 24-h embryos with DID1, lateral motile cilia and a part of apical tuft were detached. Arrowheads show apical tufts. Asterisks represent embryos of which apical tuft is detached. Bar, 100 μ m. B: Lateral motile cilia and a part of apical tuft were isolated by DID1 (“DID1”). The rest of apical tuft was isolated by 2 \times ASW (“2 \times SW”) without contamination of lateral motile cilia. Ciliary proteins were separated by SDS-PAGE, followed by immunoblotting with anti-GSTT antibody (IB). GSTT was significantly detected in 2 \times SW. An antibody against a light chain of outer arm dynein (LC3) was used as an internal control (Hozumi et al., 2006).

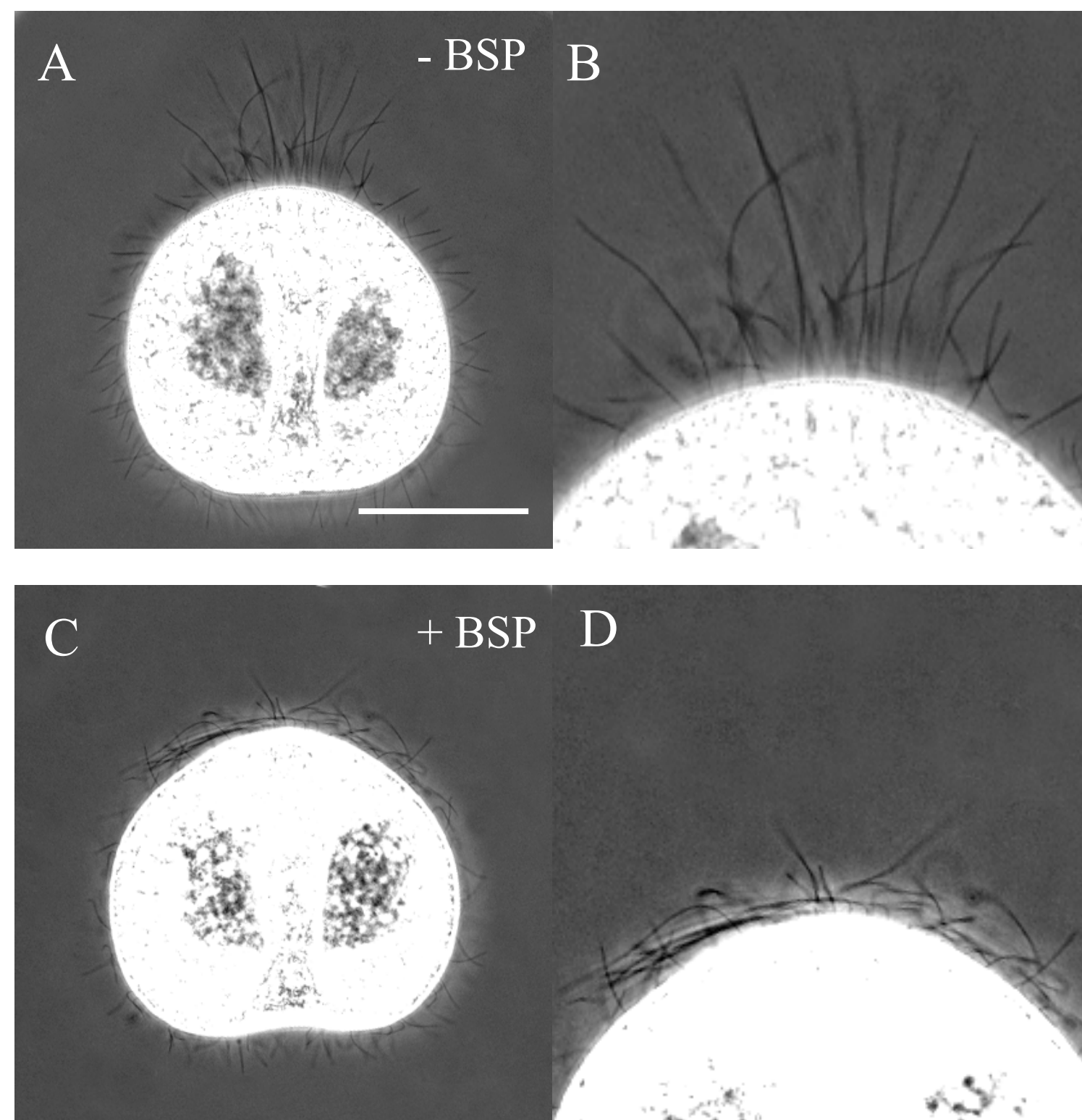


Fig. 16 Effect of a GST inhibitor BSP on the apical tuft.

Phase contrast images of normal embryo (A) and the embryo treated with 10 μ M BSP (C) are shown. B and D, magnified image of apical tuft regions of A and C, respectively. Note the bending of apical tuft cilia in the BSP-treated embryo. Bar: 50 μ m.

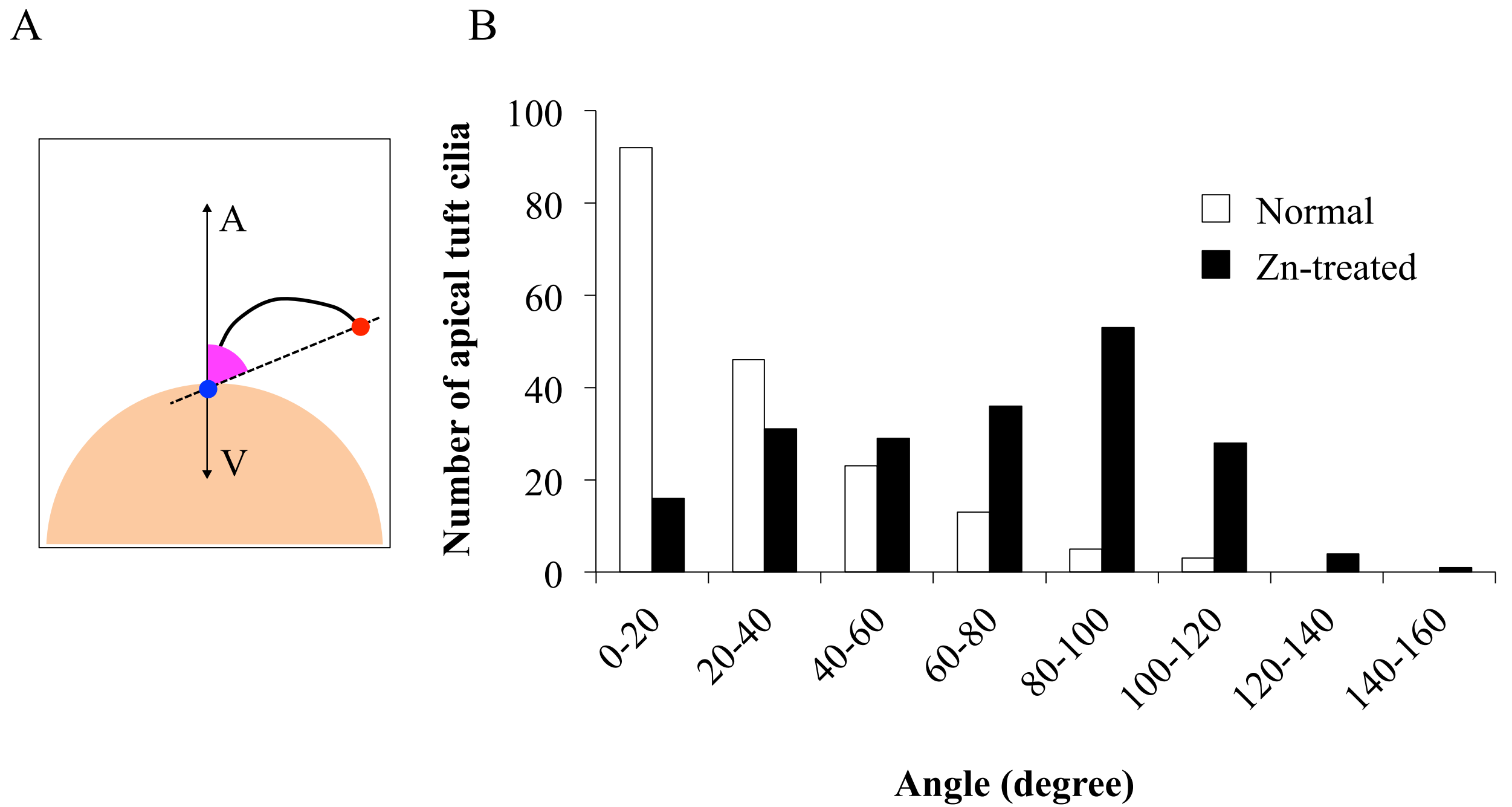
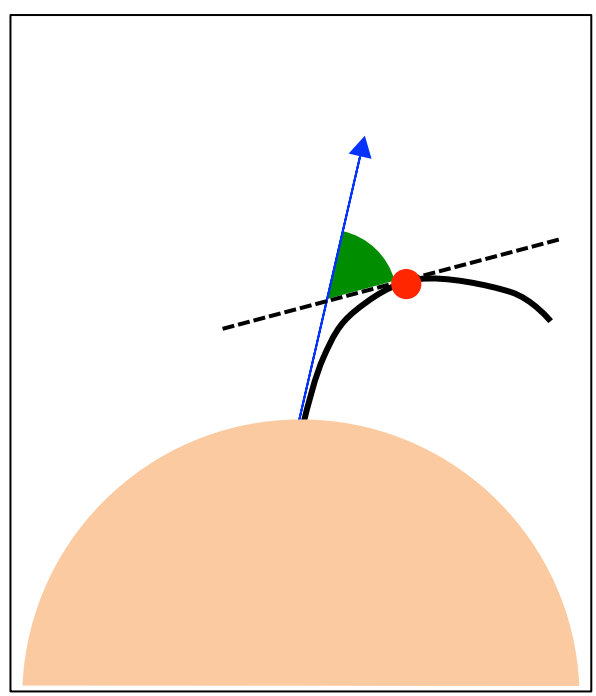


Fig. 17 Angles of the cilia of apical tuft relative to the animal-vegetal axis.

A: Schematic drawing of the angle(magenta) of the cilia of apical tuft relative to the animal-vegetal axis(A-V). B: Open and closed bar represents normal embryos and those treated with 10 μM BSP, respectively. The angle of each cilium was measured from recorded images.

A



B

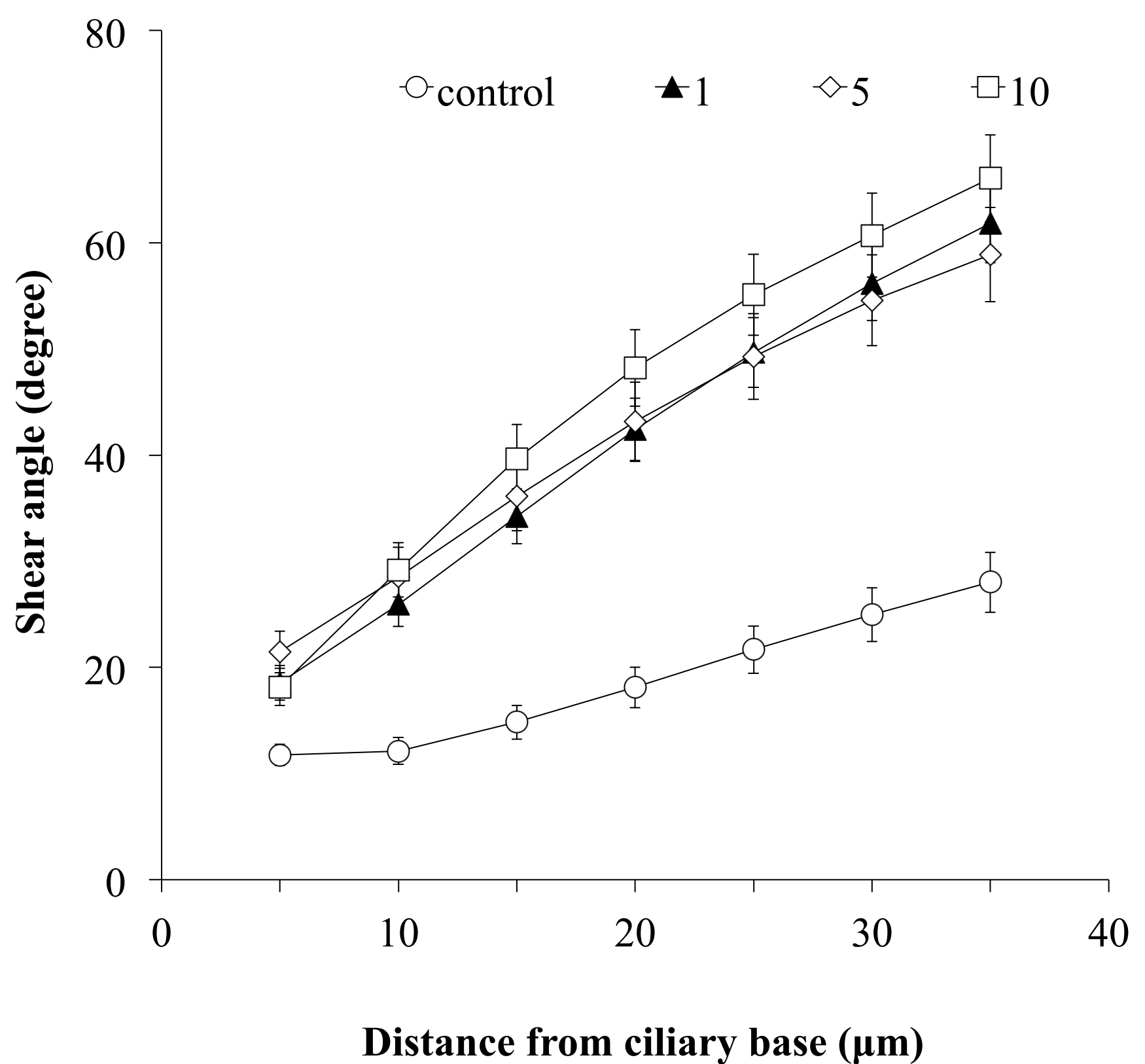


Fig. 18 Shear angles at various distances from the base of cilia.

A: Schematic drawing of the shear angle(green). B: Open circles, control (0 μM BSP); closed triangles, 1 μM BSP; open rhombuses, 5 μM BSP; open squares, 10 μM BSP. Bars represent standard error (SE) (n = 15).

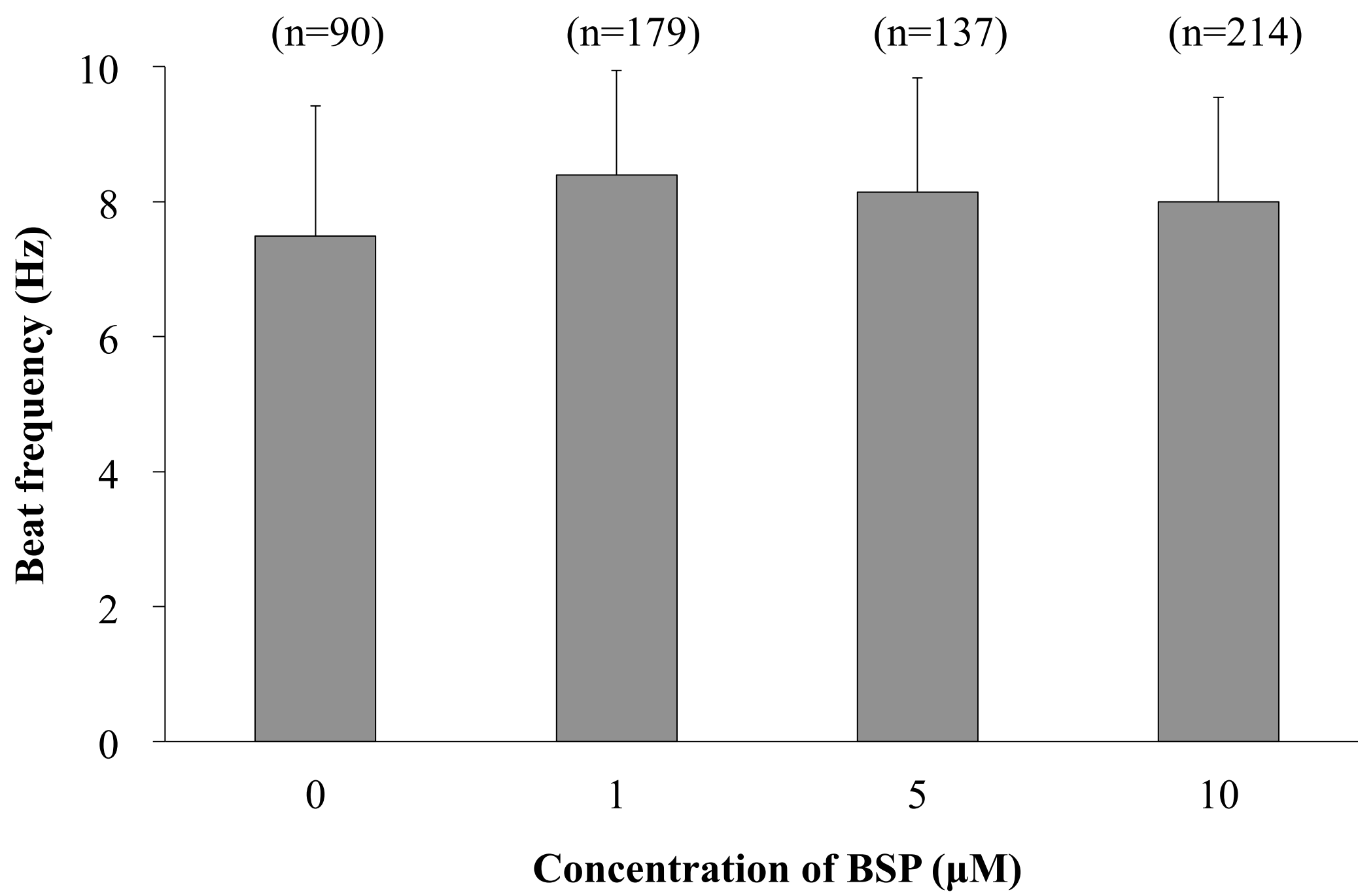


Fig. 19 Beat frequency of lateral cilia in embryos treated with several concentrations of BSP.

Embryos treated with 0 μM to 10 μM BSP were recorded and the beat frequency of each cilium was measured . Bars, SE ($n = 15$).

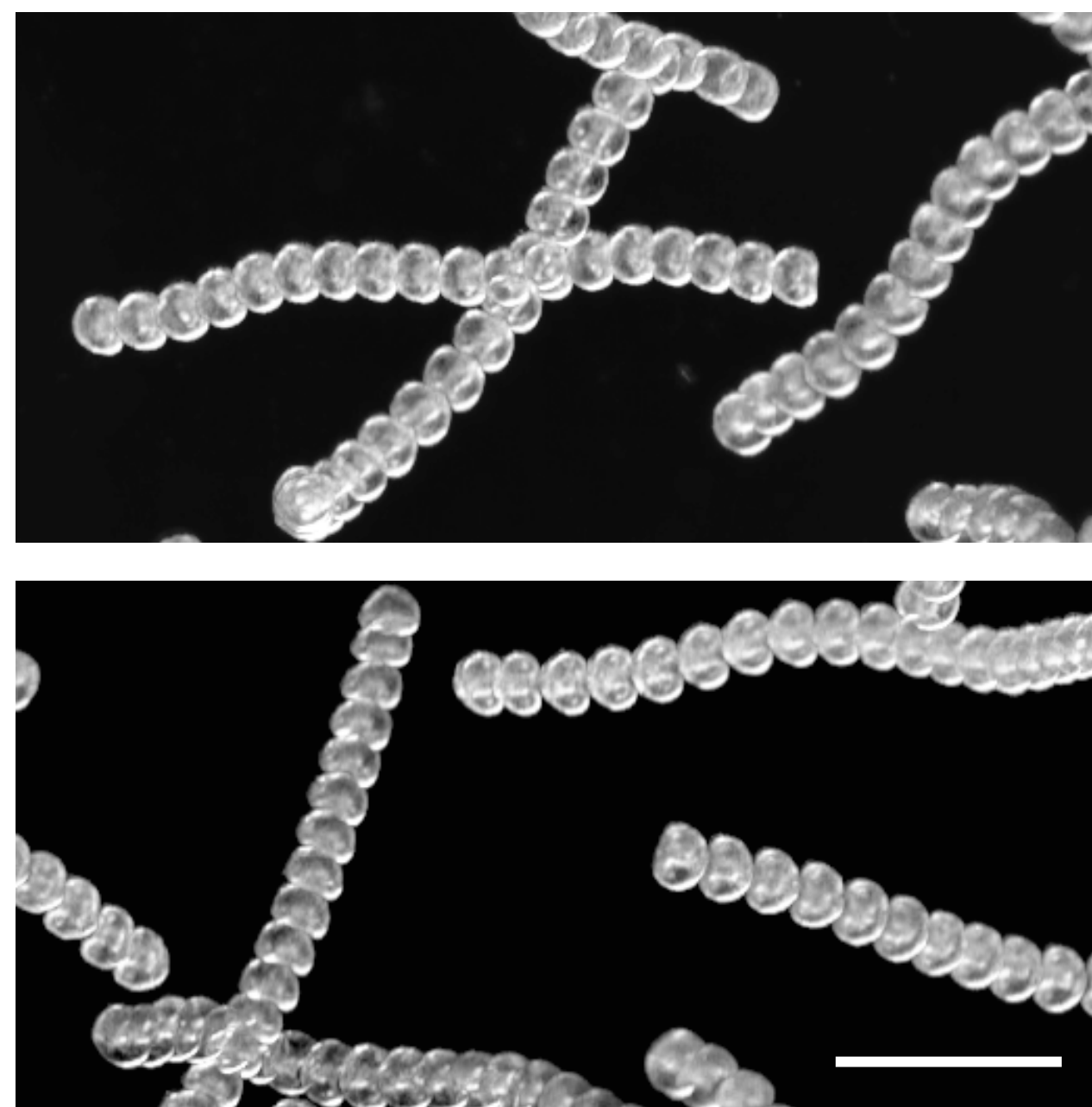


Fig. 20 Effects of BSP on the swimming behavior of embryos.
Multiple images of normal embryos (top) or those treated with 10 μM BSP (bottom) at 0.05-sec intervals are overdrawn by Bohboh software.
Bar: 500 μm .

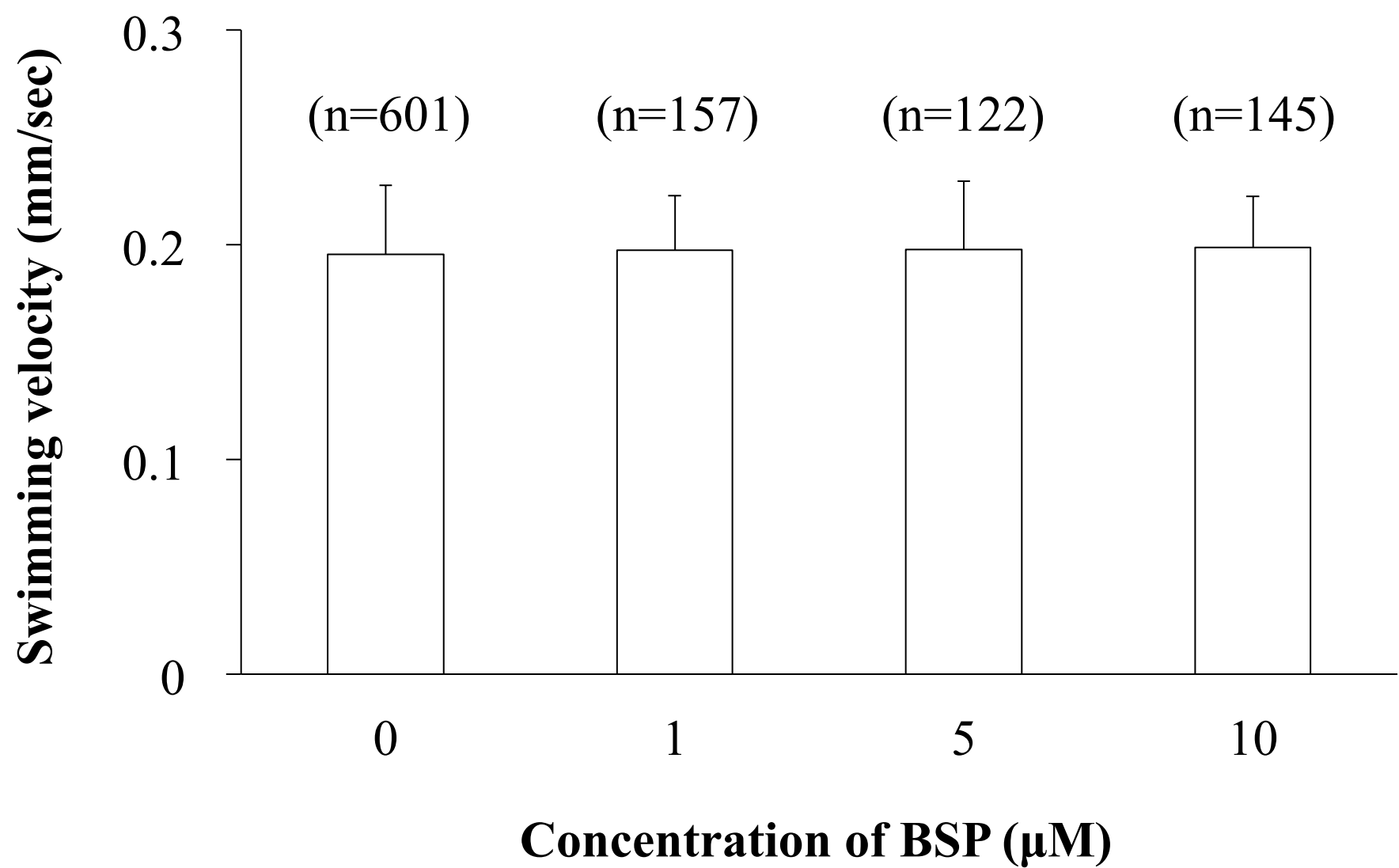


Fig. 21 Effect of BSP on the swimming velocity of embryos.
Trajectories of free-swimming embryos were recorded and the swimming velocity was measured. Bars, SE (n=3).

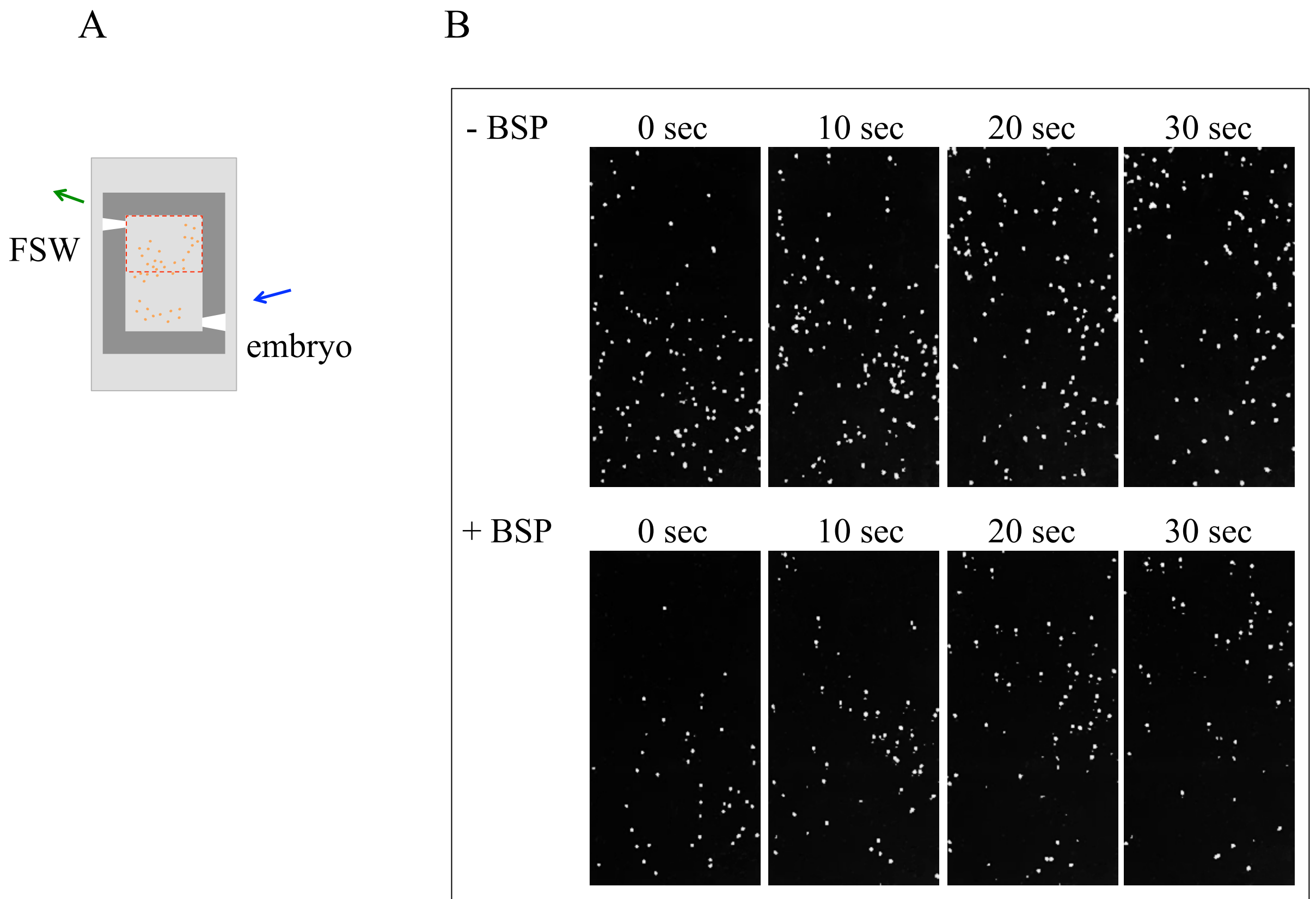


Fig. 22 Negative geotactic behavior of sea urchin embryos.

A: Schematic drawing of the chamber used in the experiments. Embryos were introduced to the chamber from the bottom (blue arrow), and excess FSW was removed from the top (green arrow). B: Sequential images of embryonic movements in a vertically placed chamber. Images from dark-field were processed to draw embryos stuck to the wall and background nonembryonic debris. Top, in the absence of BSP; bottom, in the presence of 10 μ M BSP.

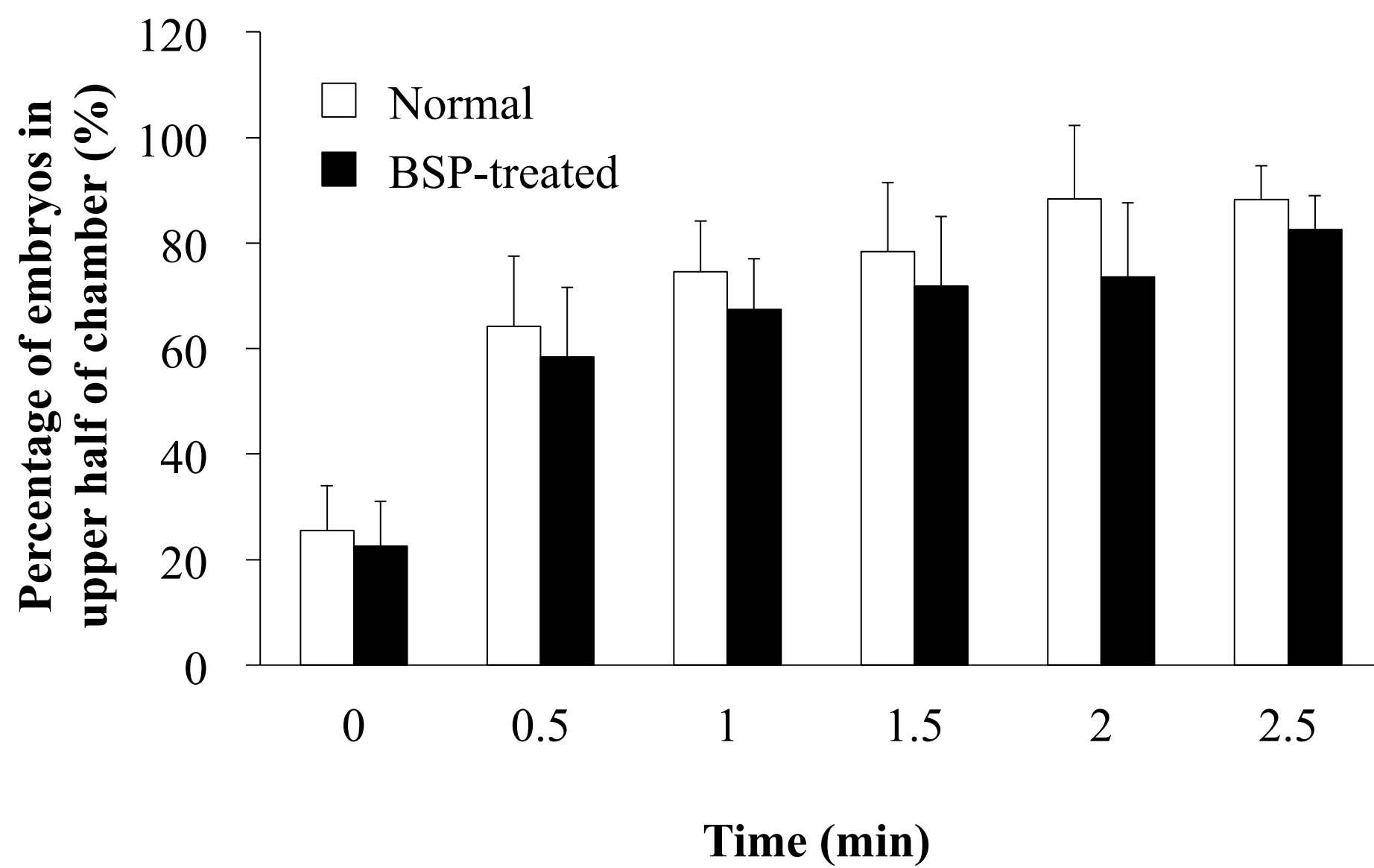


Fig. 23 Percentage of embryos that moved into the half top of the chamber against time(shown in red square in Fig. 22 A). Open and closed bar represents embryos in the absence and presence of 10 μ M BSP, respectively. Bars: SE ($n = 6$).

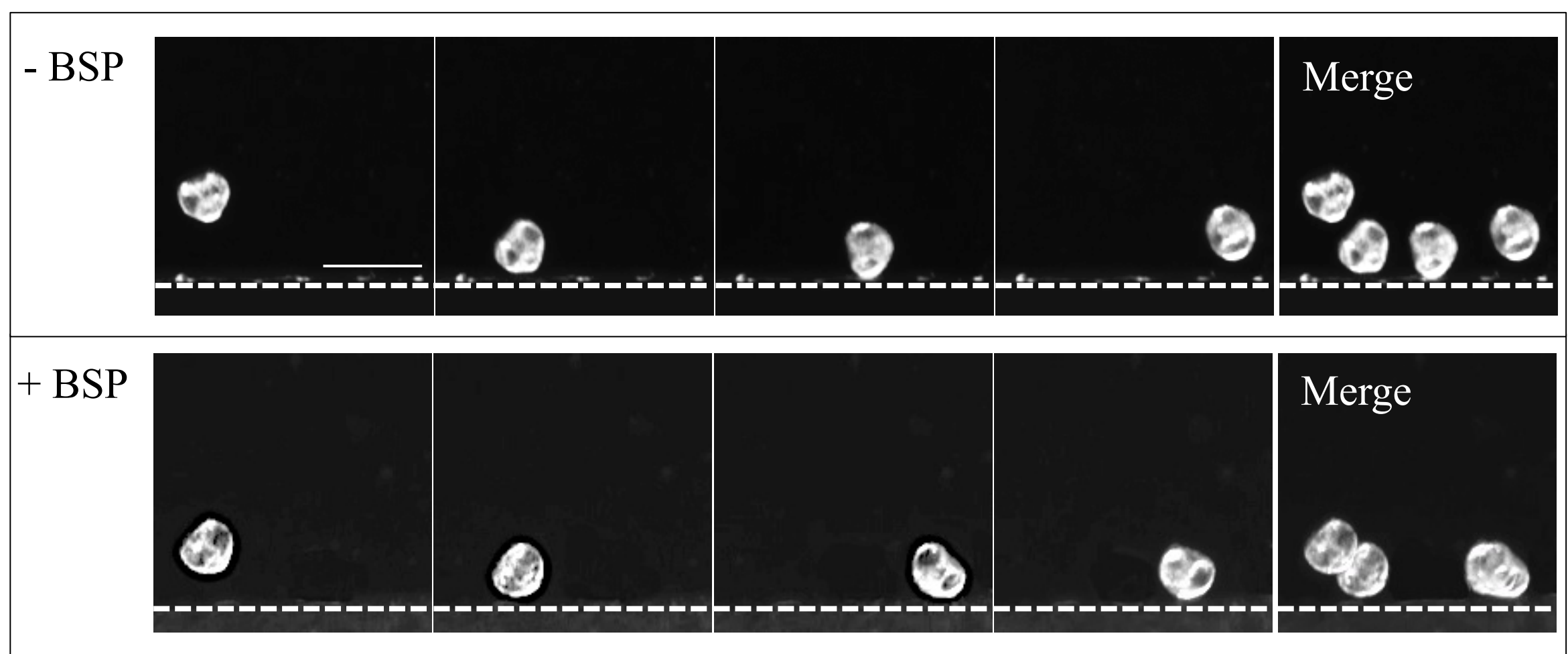


Fig. 24 Sequential images of embryos near the wall of the chamber, showing the inhibition of escaping response of the embryos by BSP.

The bottom dotted lines show the wall of the silicon chamber. The normal embryos changed their swimming direction after colliding with the chamber wall, whereas the BSP-treated embryos were unable to escape and became trapped at the wall. Right panels represent overdrawn images showing trajectories. Bar: 200 μ m

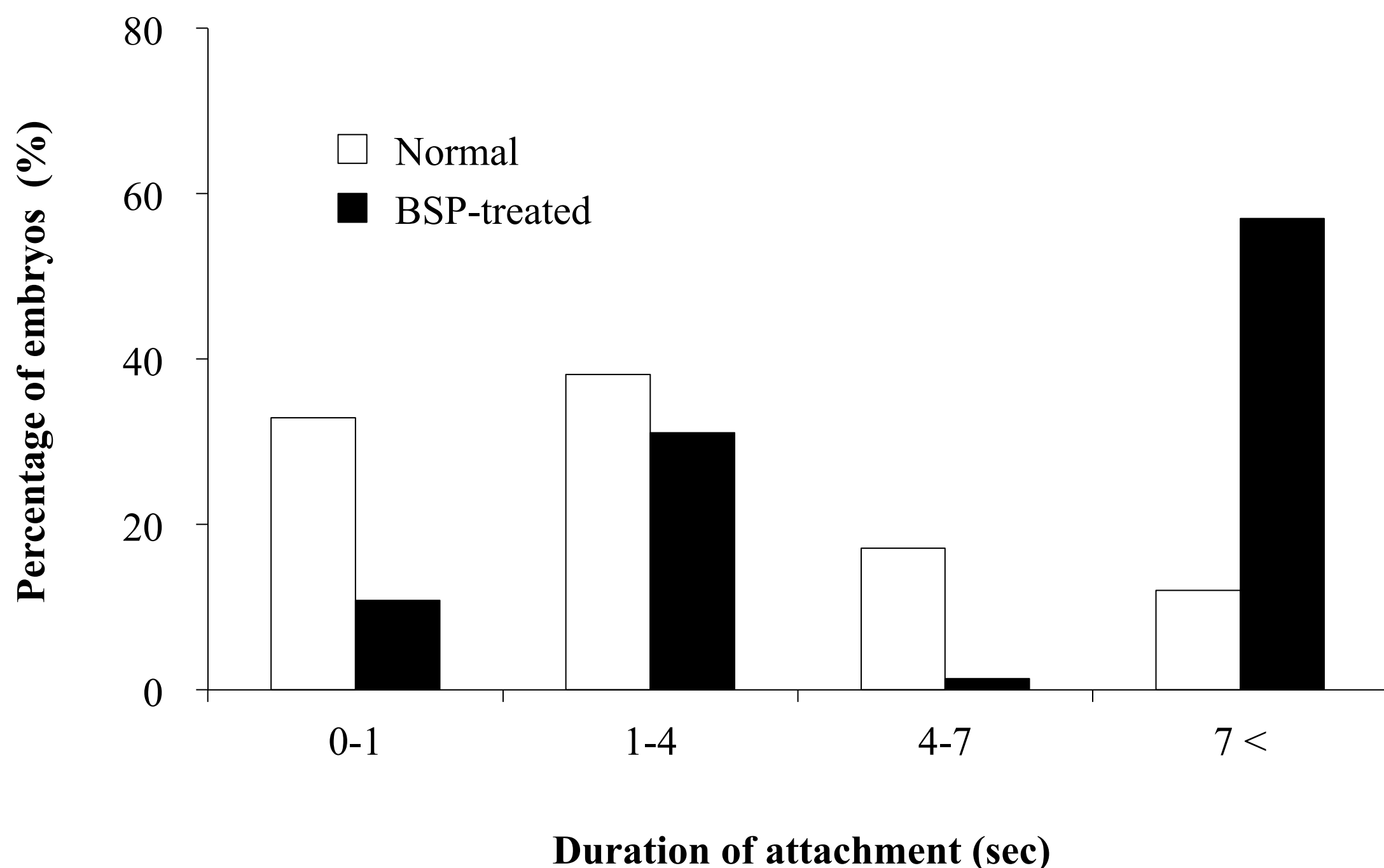


Fig. 25 Distribution of time required for escaping from the wall after collisions.

Open and closed bar is normal embryos and those treated with 10 μM BSP, respectively. Video images from 336 (-BSP) or 356 (+10 μM BSP) embryos were analyzed. The vertical axis represents the percentage of embryos with escaping time in the range of 0-1, 1-4, 4-7, and over 7 sec. BSP- treated embryos with escaping times over 7 sec include those trapped on the wall.

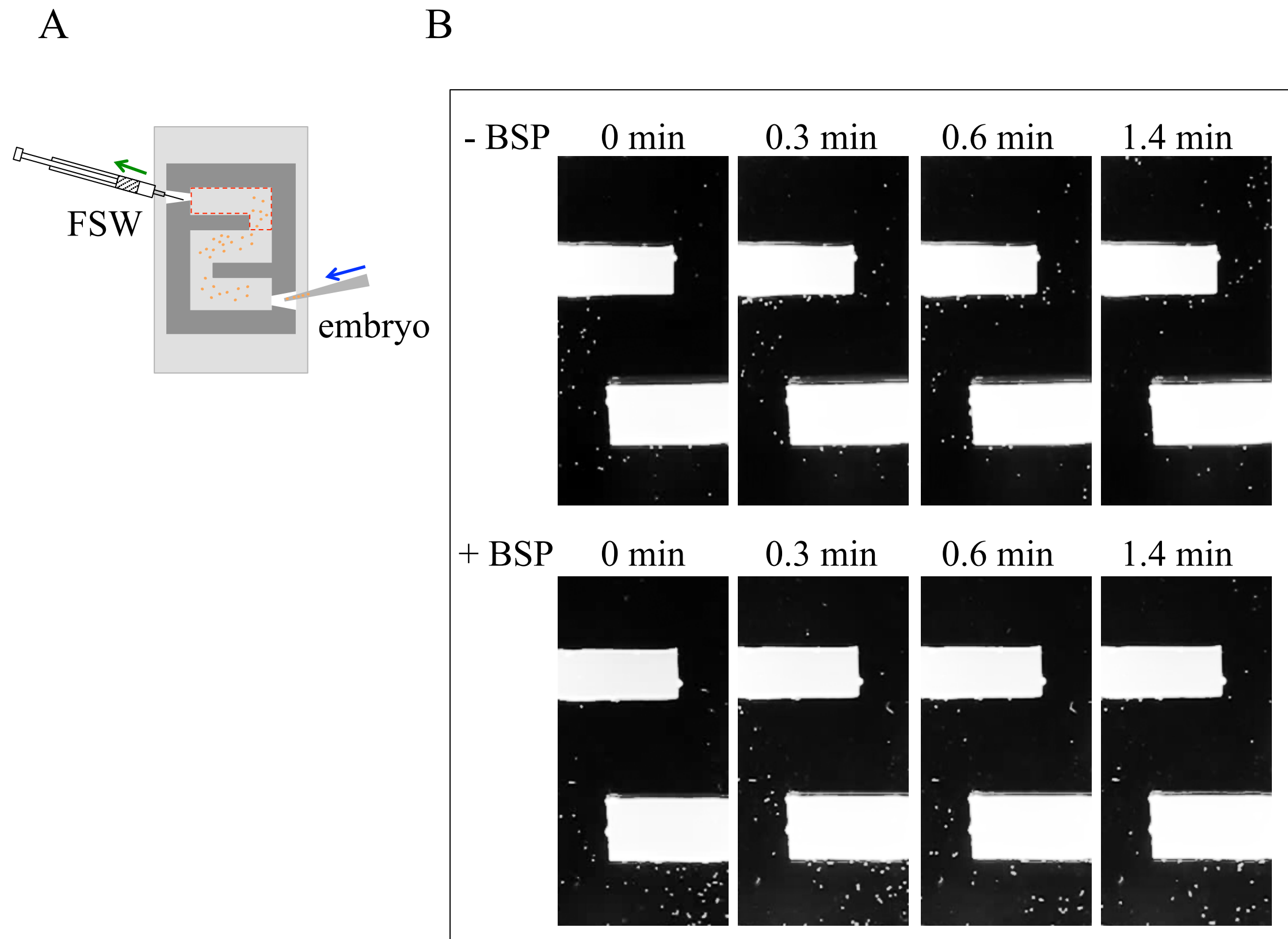


Fig. 26 Negative geotaxis in a micro-maze.

A: Schematic drawing of the micro-maze used in the experiments. Embryos were introduced to the chamber from the bottom (blue arrow), and excess FSW was removed from the top (green arrow). B: Sequential images of the distribution of normal (top) and BSP-treated embryos (bottom) in the micro-maze. Dark-field images were processed to draw the background non-embryonic debris. Note that many embryos were still stacked in the lower part of the maze at 1.4 min.

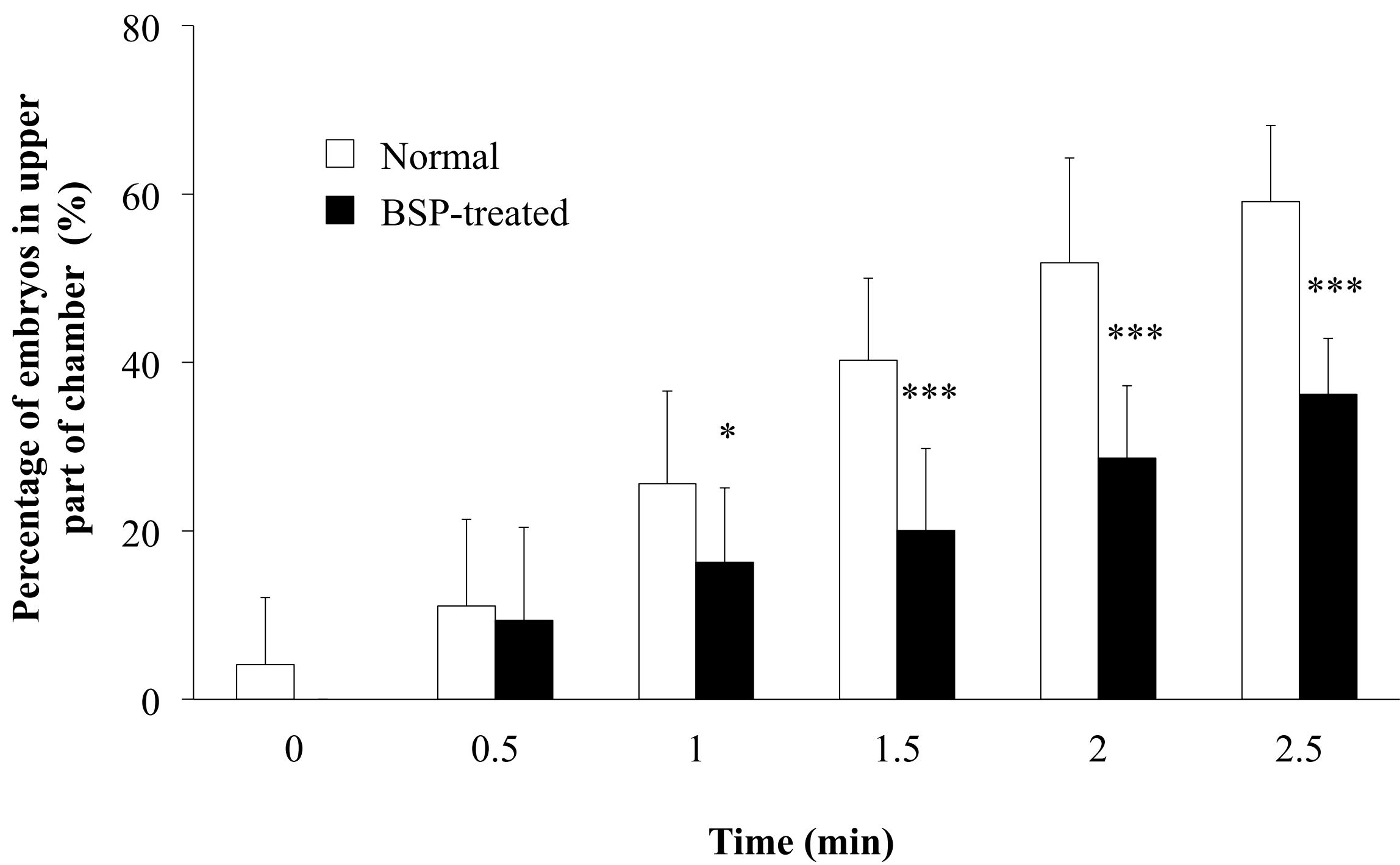


Fig. 27 Comparison of the efficiency for negative geotaxis in a micro-maze between normal and BSP-treated embryos.

The percentage of embryos that moved into the top compartment of the chamber (shown in red square in Fig. 26 A) was counted against time. Open and closed bars represent embryos in the absence and presence of 10 μ M BSP, respectively. Bars, SE ($n = 9$). * $P < 0.05$, ** $P < 0.001$.